



PHD COURSE in  
ENVIRONMENTAL AND ENERGY ENGINEERING SCIENCE

XXX CYCLE

Seismic deconvolution interferometry applied to the monitoring of dams  
structural integrity

Candidate:

Giulia Massolino

Coordinator:

Chiar.mo Prof. Alessandro Trovarelli  
University of Udine

Supervisor:

Chiar.mo Prof. Antonino Morassi  
University of Udine

Co-Supervisor:

Chiar.mo Prof. Stefano Grimaz  
University of Udine

Tutor:

Chiar.mo Prof. Stefano Parolai  
OGS – National Institute of Oceanography  
and Experimental Geophysics

YEAR 2018



## CONTENTS

Abstract .....	1
Acknowledgements .....	3
Acronyms list .....	10
Thesis structure .....	11
1. Introduction .....	13
1.1 Motivation .....	13
1.2 Objectives .....	16
1.3 Confidentiality agreement .....	19
2 Dam monitoring – framework and state of the art .....	20
2.1 Italian dams .....	24
2.2 Italian regulations about dams .....	27
2.3 Structural diagnosis .....	30
2.4 Aims .....	32
2.5 Geophysical and geomechanical testing .....	34
2.6 Dynamic monitoring .....	36
2.7 FEM updating and modal matching .....	38
2.8 Examples .....	39
2.8.1 Seismic monitoring .....	39
2.8.2 Seismic verification .....	41
2.8.3 Ambient Vibration Tests .....	43
2.8.4 Seismic Investigation for Characterization .....	44
3 Experimental structural analysis methods – framework and state of the art .....	46
3.1 Soil-structure interaction .....	46
3.2 Dynamic characterization of existing structures .....	49
3.3 Experimental methods for dynamic characterization of structures .....	53
3.4 Ambient vibration tests .....	58
3.5 Seismic Interferometry and Deconvolution .....	63
4 Case study: a Dam in Central Italy .....	70
4.1 Forced vibration tests .....	73

4.2	Ambient vibration tests before the earthquake .....	75
4.3	Ambient vibration tests after the earthquake .....	84
4.4	Seismic Monitoring .....	91
4.5	Deconvolution applied to earthquakes recordings .....	100
4.5.1	Recordings on the central transversal section .....	103
4.5.2	Recording at the side of the dam .....	112
4.6	Deconvolution applied to ambient vibration recordings.....	118
4.6.1	Ambient vibration test after the earthquake .....	118
4.6.2	Ambient vibration test before the earthquake .....	124
5	Discussion and comparison.....	126
5.1	Modal frequency and shapes comparison .....	126
5.2	Seismic deconvolution interferometry – applicability on dams 133	
5.3	Seismic deconvolution interferometry – results discussion .....	135
5.4	Use of ambient vibration tests for dam damage detection .	137
6.	Conclusion.....	139
	References.....	144

# Abstract

The aim of the thesis is to test the possibility of using a set of preliminary parameters to decide when and how to organize further detailed investigations to assess the structural integrity of dams. The parameters researched should be the outcome of a method that must be cost effective and therefore simplified. This work proposes to use the shear wave velocity and the structural damping obtained by interferometric analysis based on deconvolution of recorded seismic events or ambient vibrations. In this work, I discuss whether this method could be profitably used as a first explorative approach to dam dynamical characterization.

To verify the applicability of the deconvolution interferometry approach on dams, a concrete arch-gravity dam located in Central Italy is assessed as a case study, using different techniques. On the dam several survey campaigns were performed in different time periods: two dynamic forced vibrations tests were performed in the past (July 1988 and May 1993), on the basis of which a finite element model was developed. In 2015 an ambient vibration survey was performed; one year later the Central Italy earthquake of the 24<sup>th</sup> August 2016 hit the structure, causing non-structural damage. After the earthquake the Civil Defence Department repeated the ambient vibration tests on the dam and installed a permanent dynamic monitoring system, part of the Seismic Observatory for Structures (OSS – *Osservatorio Sismico delle Strutture*). The monitoring system recorded five seismic events in 2017, which are analysed in this thesis using deconvolution interferometry. The large amount of data recorded on this specific dam was used in order to compare the results obtained with the different techniques, working as a consistency check on the outcomes of the interferometric approach based on deconvolution.

The results obtained by the seismic deconvolution interferometry are promising. The shear wave velocity inside the structure, in the central section of the dam, was estimated to be around 900 m/s. This value of velocity could be expected, since shear wave velocity inside

regular buildings is usually around 300 m/s, but the investigated dam is much stiffer and does not present any empty spaces except the tunnels, which are negligible in comparison to the geometric dimensions of the dam. The consistency of this velocity value was also checked through the formula, valid for the shear beam model, which relates the fundamental frequency to the measured velocity, obtaining a value of frequency very close to the one determined by forced and ambient vibration tests, although the excessively simplification assumed to apply this formula. The damping factor was calculated too, using the attenuation of the recorded wavefield, resulted to be 3%.

The experimental tests on the dam were performed by several actors, in various time periods, with disparate instruments, different array configurations, for different purposes and – especially – with variations in reservoir water level. Hence, it was not easy to compare the results obtained. Considering the promising outcomes of this first explorative study, it would be interesting to apply the seismic deconvolution interferometry approach on a significant sample of existing dam, following a common *operational protocol* to perform the tests, in order to be able to easily compare the results.

In the framework of a multi-level approach to dam dynamical characterization, these parameters (frequency, shear wave velocity and structural damping), obtained through non-invasive cost-effective techniques, are able to provide useful preliminary information – although incomplete – in order to address further levels of investigation. Far from being exhaustively representative of the complex structural behaviour of the dam, these parameters could be used as a preliminary explorative indication on structural integrity condition, to address conventional ordinary and extraordinary monitoring methods.

# Acknowledgements

*My first thought goes to the late Professor Marco Mucciarelli, excellent scientist, brilliant communicator and passionate human being. Thanks to him I started this path and I treasure the precious memories of him.*

*My gratitude goes to Professor Stefano Parolai, who accepted to be my tutor, offering his inestimable contribution to this work.*

*Many thanks to Professors Grimaz and Professor Morassi for the definition of the structure of the work and of its framework.*

*My deepest thanks to the reviewers, Maria Rosaria Gallipoli and Dino Bindi, for their professionalism, willingness and suggestions in the revision of the work.*

*My sincere thankfulness to all the people who made this possible. Thanks to Ing. Marina Eusebio, Ing. Andriano De Sortis, Ing. Giovanni Marmo, for sharing data and suggestions. Thanks to the Civil Defence Department and the Italian Ministry of Infrastructures and Transportation for the authorization of presenting the results in this thesis. Thanks to the German Research Centre for Geosciences of Potsdam, for having hosted me, and especially to Bojana Petrovic for her precious help. Special thanks to Matteo Barnaba for his continuous support and his priceless help with computer programming. A thankful thought also to Michele Zuppichin for his help with physics.*

*Last but certainly not least, my gratitude goes to all the special people I had the luck to meet at the National Institute of Oceanography and Applied Geophysics for their scientific and human support during all the three years of my PhD. I'm genuinely thankful to: Alessandro Rebez, Laura Peruzza, Angela Saraò, Alessandro Vuan, Giuliana Rossi, Enrico Priolo, Roberto Romeo, Marco Santulin, Alberto Tamaro, Barbara Merson, Franca Petronio, Valentina Volpi, Lorenzo Facchin, Isabella Tomini, Fabrizio Zgur, Anna Riggio, Denis Sandron, Carla Barnaba, David Zuliani and Cristian Ponton.*

## TABLE OF FIGURES

Figure 1 – comparison between the payback ratios of the different power plants. Among them, it is possible to see how the hydropower with reservoir is the most efficient (ITCOLD 2012, a) .....	20
Figure 2 – territorial distribution of Italian large dams (Pascucci and Tamponi, 2013). It can be noticed how dams are well distributed on the entire Italian territory, also in seismic prone areas. ....	24
Figure 3 – history of construction and extraordinary maintenance intervention on Italian dams (ITCOLD, 2012) .....	25
Figure 4 – structural typologies of Italian dams (Fornari, 2013. The concrete gravity dam (last one, blue bar of the histogram) is the typology most present for Italian dams, reaching nearly 130 dams. Other common typologies are the arch and arch-gravity ones, the buttress, masonry gravity, earth filled dams. On all these typologies, it is possible to apply the seismic interferometry approach based on deconvolution described in the following chapters. ....	26
Figure 5 – velocity profile of the P-waves (left) and shear waves (right) for two sections of the dam, calculated through sonic cores (CS), cross-hole tests (CH) and laboratory analysis, on the Sella Pedicate dam, as reported in ITCOLD 2012 c. ....	42
Figure 6 – example of average amplitude Fourier spectra for a central buttress without (left) and with (right) running of hydro-mechanical equipment as reported in Abdulamit et al. (2017). ....	43
Figure 7 - An example of curved raytracing obtained for TS4 section (a) and P-wave tomographic model obtained for TS4 (b), TS10 (c) and TS14 (d) sections, as reported by Capizzi et al. (2016) .....	45
Figure 8 – Trifunac et al., 2001; forces involved in the soil-structure simplified model of a building: a damped oscillator, with one degree of freedom which represents the building and a stiff foundation with two degrees of freedom: horizontal translation and ground rotation. ....	47
Figure 9 – energy contribution of all the forces considered in the San Francisco earthquake; the energetic contribution of from the building to the soil can be a significant fraction of the initial energy (Trifunac et al., 2001) .....	48
Figure 10 – Scheme of the approach for the properties evaluation of existing buildings proposed by Stubbs et al. (2010) [SID stands for System Identification]. ....	52
Figure 11 – Example of S-Transform of an accelerometric recording with the upper bound of the frequency domain highlighted, as reported in the work of Ponzo et al. (2012). ....	60
Figure 12 – Figure from the work of Snieder and Şafak (2006): wave field obtained using the station located at the top floor as reference (on the left) and Impulse Response Function obtained using the bottom as reference station. ....	65
Figure 13 – geometry of the central transversal section of the dam .....	70
Figure 14 – modal shape identified through forced vibrations test: a) 1 <sup>st</sup> mode (around 5.1 Hz); b) 2 <sup>nd</sup> mode (around 6.8 Hz); c) 3 <sup>rd</sup> mode (around 9.1 Hz). The deformed shape of the first and third mode are symmetric, while the one of the second mode is anti-symmetric. ....	74
Figure 15 – Dam planimetry (a) and front view (b) with test sites locations.....	76
Figure 16 – a) HVSR on the bedrock reference (AR site); b) three component spectra diagram on the bedrock testing site (AR); c) H/V stability bedrock testing site (AR). ....	77
Figure 17 – Standard Spectral Ratios in the three components, for testing sites on the crest, related to the bedrock measure. Measuring points are reported in panel a); panel b), c) and d) relate to N-S, E-W and vertical directions respectively.....	79



Figure 18 - Standard Spectral Ratios in the three components (N-S, E-W and vertical), for testing site AC2 on the crest, related to the bedrock measure. ....	80
Figure 19 - Standard Spectral Ratios in the three components (N-S, E-W and vertical), for testing site AC3 on the crest, related to the bedrock measure. ....	80
Figure 20 - Standard Spectral Ratios in the three components (N-S, E-W and vertical), for testing site AC4 on the crest, related to the bedrock measure. ....	81
Figure 21- Standard Spectral Ratios in the three components (N-S, E-W and vertical), for testing site AC5 on the crest, related to the bedrock measure. ....	81
Figure 22- Standard Spectral Ratios in the three components (N-S, E-W and vertical), for testing site AC6 on the crest, related to the bedrock measure. ....	82
Figure 23 – sensors configuration for the ambient vibration tests performed in 2016, after the earthquake hit the structure. Each sensor was directed in the radial direction; before the analysis, data were rotated to be directed in the upstream-downstream direction, as the sensor at the centre of the crest.....	85
Figure 24 – Spectral density matrix in the frequency domain determined by ambient vibration tests after the earthquake; the blue line is the North-South direction, the red one the East-West and the green one the vertical direction. As can be noticed (and as could be expected), the main amplifications are on the North-South component, while the East-West component presents much lower amplifications and the vertical component almost no amplification. The only exception is the 6.9 frequency that shows amplification also on the vertical component, indicating a probable rocking motion. The power spectral density is also useful to see what is the range of frequencies of interest in the specific case. ....	88
Figure 25 - Modal shape identified by the ambient vibration tests after the earthquake. Black dots line represents the displacement from the undeformed shape (green line) per each sensor. Panel a) 1st Mode - 5.737 Hz ; Panel b) 2nd Mode - 6.87 Hz; Panel c) 3rd Mode - 8.896 Hz. It is evident how the downriver-right side of the dam show major deformability. This is actually the side of the dam that showed non-structural damage after the 2016 earthquake. ....	89
Figure 26 – position of the sensors of the permanent monitoring system: two in the tunnel immediately below the crest of the dam (G1) and one in the lower tunnel (G3).The sensor on the downriver-right side of the tunnel below the crest was installed with the North axis forming a 19.43° angle with the upstream-downstream direction. Hence, before the analysis data were rotated to be in the same direction as the central sensor. ....	92
Figure 27 – seismic event of magnitude 4 and 9 km distance: waveforms recorded at centre of the crest of the dam (panel a and b), at the downriver right side (panel c and d) and at the bottom of the dam (panel e and f). On the left side (panels a, c and e) there are the waveforms recorded in the North-South direction (upstream-downstream direction), while on the right side (panels b, d and f) those on the East-West direction (orthogonal to the previous). Please note that the scale is different per each panel. ....	94
Figure 28 – time - frequency analysis using the S-Transform (using the code written by Stockwell published in Stockwell et al., 1996) of the M3.9 event at 14 km distance .....	95
Figure 29 – time - frequency analysis using the S-Transform (using the code written by Stockwell published in Stockwell et al., 1996) of the M3.5 event at 4.9 km distance .....	96
Figure 30 – time - frequency analysis using the S-Transform (using the code written by Stockwell published in Stockwell et al., 1996) of the M 3.8 event at 5 km distance .....	97
Figure 31 – time - frequency analysis using the S-Transform (using the code written by Stockwell published in Stockwell et al., 1996) of the M 3.6 event at 4.2 km distance .....	98
Figure 32 – time - frequency analysis using the S-Transform (using the code written by Stockwell published in Stockwell et al., 1996) of the M 4 event at 9.3 km distance .....	99
Figure 33 – FFT spectra recorded on the top tunnel (panels a and b) and on the bottom tunnel (panels c and d) for the North-South and North-West directions (left panels and right panels respectively), for the seismic	

event of magnitude 4 at 9 km distance (log log graph). Please note that the scale is different per each panel. ....	101
Figure 34 – transfer function calculated as the average of the ratio between the spectra at the tunnel below the crest and the one at the bottom tunnel of the dam per each event recorded, in the North –South and East – West directions (left side and right side respectively). Recordings at the centre (panels a and b) and at the downriver side (panels c and d) of the tunnel below the crest. The dashed lines indicates the frequency of the first three vibrational modes. Please note that the scale on the y axes is different per each panel, while the x-axes (frequency) is constant and logarithmic. The thick line represents the average spectrum, the thin lines the standard deviations. Spectra were smoothed with a triangular window (5%).....	102
Figure 35 – Deconvolution results: Impulse Response Function (IRF) spectra in the frequency domain, at the centre of the tunnel below the crest (panel a) and at the bottom (panel b), in the North-South direction (upstream-downstream). The crest of the dam was used as reference. The Green function is considered between 0.1 and 15 Hz, because of the filter effect on the signal. ....	104
Figure 36 – Deconvolution results: Impulse Response Function (IRF) spectra in the frequency domain, at the centre of the tunnel below the crest (panel a) and at the bottom (panel b), in the Est – West direction (tangent to the crest curvature). The crest of the dam was used as reference. The Green function is considered between 0.7 and 25 Hz, because of the filter effect on the signal. ....	105
Figure 37 – Impulse Response Function, deconvolved wavefield in the time domain; a) autocorrelation of the signal at the centre of the tunnel below the crest, with the bottom tunnel as reference; b) wavefield at the bottom of the dam. Bandpass filter 1-20 Hz. Please note that the scale is different per each panel. ....	108
Figure 38 – Deconvolution results: Impulse Response Function, deconvolved wavefield in the time domain for; a) autocorrelation of the signal at the centre of the tunnel below the crest, used as reference; b) wavefield at the bottom of the dam, divided in a causal and a-causal part ( $t < 0$ , left, and $t > 0$ , right, respectively). Bandpass filter 1-20 Hz. From this plot we can read the time delay between the acausal and causal peak and the difference in their amplitude, obtaining so shear wave velocity and damping of the structure. Please note that the scale is different per each panel.....	108
Figure 39 - deconvolved waveform, using the bottom as reference, at the centre of the tunnel below the crest, with bandpass filter between 4.5 and 6 Hz, first mode .....	110
Figure 40 - deconvolved waveform, using the bottom as reference, at the centre of the tunnel below the crest, with bandpass filter between 6.5 and 7.5 Hz, second mode. Please note that the scale is different per each panel.....	110
Figure 41 - deconvolved waveform, using the bottom as reference, at the centre of the tunnel below the crest, with bandpass filter between 8.5 and 9.5 Hz, third mode. Please note that the scale is different per each panel. ....	110
Figure 42 – deconvolved waveform, using the crest as reference, at the centre of the tunnel below the crest, with bandpass filter between 4.5 and 6 Hz, first mode. Please note that the scale is different per each panel. ....	111
Figure 43 – deconvolved waveform, using the crest as reference, at the centre of the tunnel below the crest, with bandpass filter between 6.5 and 7.5 Hz, second mode. Please note that the scale is different per each panel.....	111
Figure 44 – deconvolved waveform, using the crest as reference, at the centre of the tunnel below the crest, with bandpass filter between 8.5 and 9.5 Hz, third mode. Please note that the scale is different per each panel. ....	111
Figure 45 – Deconvolution results: Impulse Response Function (IRF) spectra in the frequency domain, at downriver right side of the tunnel below the crest (panel a) and at the bottom (panel b), in the North-South direction (upstream-downstream direction). The crest of the dam was used as reference. The Green function is considered between 0.5 and 20 Hz, because of the filter effect on the signal. ....	113

Figure 46 – Deconvolution results: Impulse Response Function (IRF) spectra in the frequency domain, at downriver right side of the tunnel below the crest (panel a) and at the bottom (panel b), in the Est – West direction (tangent to the crest curvature). The crest of the dam was used as reference. The Green function is considered between 0.1 and 12 Hz, because of the filter effect on the signal. .... 114

Figure 47 – Deconvolution results: Impulse Response Function, deconvolved wavefield in the time domain; a) autocorrelation of the signal at the downriver right side of the tunnel below the crest, with the bottom tunnel as reference; b) wavefield at the bottom of the dam. Bandpass filter between 1 and 20 Hz. Please note that the scale is different per each panel. .... 115

Figure 48 – Deconvolution results: Impulse Response Function, deconvolved wavefield in the time domain; a) autocorrelation of the signal at the downriver right side of the tunnel below the crest, used as reference; b) wavefield at the bottom of the dam, divided in a causal and a-causal part ( $t < 0$ , left, and  $t > 0$ , right, respectively). Bandpass filter between 1 and 20 Hz. Please note that the scale is different per each panel. .... 115

Figure 49 - deconvolved waveform, using the bottom as reference, at the downstream right of the crest tunnel, with bandpass filter between 4.5 and 6 Hz, first mode. Please note that the scale is different per each panel. .... 116

Figure 50 - deconvolved waveform, using the bottom as reference, at the downstream right of the crest tunnel, with bandpass filter between 6.5 and 7.5 Hz, second mode. Please note that the scale is different per each panel. .... 116

Figure 51 - deconvolved waveform, using the bottom as reference, at the downstream right of the crest tunnel, with bandpass filter between 8.5 and 9.5 Hz, third mode. Please note that the scale is different per each panel. .... 116

Figure 52 – deconvolved waveform, using the crest as reference, at the downstream right of the crest tunnel, with bandpass filter between 4.5 and 6 Hz, first mode. Please note that the scale is different per each panel. .... 117

Figure 53 – deconvolved waveform, using the crest as reference, at the downstream right of the crest tunnel, with bandpass filter between 6.5 and 7.5 Hz, second mode. Please note that the scale is different per each panel. .... 117

Figure 54 – deconvolved waveform, using the crest as reference, at the downstream right of the crest tunnel, with bandpass filter between 8.5 and 9.5 Hz third mode. Please note that the scale is different per each panel. .... 117

Figure 55 - sensors configuration for the ambient vibration tests performed in 2016, after the earthquake hit the structure. The sensors were deployed with the north axis in the radial direction; before starting the analysis they were rotated with the north axis in the upstream-downstream direction, as the one at the centre of the crest. .... 119

Figure 56 – deconvolved wavefield, using the sensor deployed at the downriver left side as reference, of all the 15 ambient vibration recordings, in the North South (panel a) and East-West directions (panel b) .... 120

Figure 57 – diagram of the recorded delay time per each sensor and its distance from the first sensor deployed at the downriver left of the dam, in the North-South direction (upstream-downstream direction, panel a) and in the East-West direction (orthogonal to the former, panel b). The dotted line indicates the trend line; the slope of this line is the medium velocity (N-S - 848 m/s ; E-W - 1030 m/s). .... 122

Figure 58 – deconvolved wavefield of ambient vibration recordings between two close receivers on the crest of the dam; after the earthquake, in the upstream-downstream, tangential and vertical directions. It can be seen as it is impossible to separate the two peaks related to the arrival of the causal and a-causal waves. Please note that the scale is different per each panel. .... 123

Figure 59 – deconvolved wavefield of ambient vibration recordings before the earthquake, in the upstream-downstream, tangential and vertical directions. Please note that the scale is different per each panel. .... 125

Figure 60 – comparison between the modal shapes obtained through the ambient vibration test after the earthquake (2016) and the forced vibration tests (1989 and 1993), with the un-deformed shape (black line) as reference. ....	128
Figure 61 – geo-mechanical characterization provided by the dam’s dealer. Geological section of the rock mass. ....	129
Figure 62 – Comparison between modal shapes identified through ambient vibration test (upper panel) and those calculated by the FEM model matched with the forced vibration test results(lower panel) – 1st vibrational mode .....	130
Figure 63 – Comparison between modal shapes identified through ambient vibration test (upper panel) and those calculated by the FEM model matched with the forced vibration test results(lower panel) – 2nd vibrational mode .....	131
Figure 64 – Comparison between modal shapes identified through ambient vibration test (upper panel) and those calculated by the FEM model matched with the forced vibration test results(lower panel) – 3rd vibrational mode .....	132
Figure 65 – Central transversal section of the case study dam (left); clamped shear beam model (right) ....	134

## LIST OF TABLES

Table 1 – List of possible application of the methods discussed in the present subchapter and their sample references as reported in Table 1 of Çelebi (2000). .....	57
Table 2 – list of surveys perform and the date in which they were performed; reservoir water level at the time of the surveys performed on the dam [meters above sea level] .....	72
Table 3 – list of earthquakes recorded by the monitoring system installed on the dam in February 2017.....	72
Table 4 – modal frequencies [Hz] identified through ambient vibration tests. ....	73
Table 5 – frequencies [Hz] identified through ambient vibration tests on the dam and comparison with the one obtained by Equation 14 for the first mode frequency estimation .....	83
Table 6 – sensors position and model definition .....	86
Table 7 – modal frequencies identified by the ambient vibration tests after the earthquake. We recall that in this case the level of water reservoir was 17 meters lower than the previous ambient vibration tests. ....	88
Table 8 – MAC values for the three modes identified by ambient vibration test after the earthquake. The values on the matrix diagonal should be 1 (autocorrelation) while those outside the diagonal should be close to zero; that indicates that the modes are linearly independent, as they should be. ....	90
Table 9 – magnitude, depth and distance between the dam and the epicenter of the five seismic events recorded by the monitoring system in 2017. On the right side, a scheme of the distribution of the events around the investigated dam.....	93
Table 10 – sensors used for the ambient vibration tests, their coordinates and the distance of each sensor form the first at the downriver left side of the dam, taken as reference. The orange columns are relative to the North-South (upstream-downstream) direction, while the blue one are relative to the East-West direction (orthogonal to the former). In the first column of each direction, the measured time delay is reported (when the deconvolved wavefield was clear enough for picking), in the second column the calculated velocity is reported. Those data are also reported in the graphic of Figure 57. ....	121
Table 11 – comparison between identified modal frequencies through forced vibration tests, FEM model matched and ambient vibration tests (AVT) before and after the Central Italy earthquake .....	127
Table 12– reservoir water level at the time of the surveys performed on the dam [meters above sea level]	127
Table 13 - geo-mechanical characterization provided by the dam’s dealer – estimation of the parameters .	129

# Acronyms list

AVT	Ambient Vibration Tests
EMA	Experimental Modal Analysis
FEM	Finite Element Method
FFT	Fast Fourier Transform
HVSR	Horizontal to Vertical Spectral Ratio
IRF	Impulse Response Function
MAC	Modal Assurance Criterion
MSC	Microseismic Intensity
NIMA	Noise Input Modal Analysis
OMA	Operational Modal Analysis
PDF	Probability Density Function
PSD	Power Spectral Density
SDOF	Single Degree Of Freedom
SSI	Soil-Structure Interaction
SSR	Standard Spectral Ration

# Thesis structure

In the **first chapter**, the motivation and objectives of the thesis are declared.

In **chapter 2** I will present a review about the state of the art of monitoring methods and regulations concerning dams, in order to set the framework in which the study has to be developed.

The **third chapter** is dedicated to the framework of buildings characterization techniques. A critical review of the state of the art about building monitoring and dynamical characterization of buildings using non invasive and low cost geophysics techniques as ambient vibration tests and seismic events monitoring is proposed. In particular, I will focus on the seismic deconvolution interferometric approach and its outcomes, in order to fulfil the thesis main target that is to test the possibility of using a set of parameters as a first level indication on dam structural integrity.

In **chapter 4**, the case study of a hydroelectric dam is shown with the aim of understand how geophysical methods, already successfully applied on buildings, can be used also on energy production facilities. These industrial plants are of many different kinds and differ from regular civil builds for many factors. In fact, they are characterized by structural complexity, long service life, and severe consequences to people, property and environment in case of failure. Their monitoring is therefore crucial, both in their normal exercise than in case of extraordinary events that may have consequences on the structure (for example earthquakes). On the other hand, monitoring methods may be complex to be carried on, since operativeness must be preserved during the entire time of the testing, since to stop the operations would mean a consistent monetary loss and in some cases can even be impossible. Finally, these kind of structures is strongly dependent from boundary conditions: not only external factors (such as wind, rain, ...), but also intrinsic factors, such as the level of the reservoir or its temperature, must be considered.

The dam analysed is located in Central Italy and suffered the Amatrice 2016 destructive earthquake. Fortunately, only non-structural damage has been reported. The results of three different testing campaigns will be compared: forced vibration tests and ambient vibration tests before the 2016 earthquake and ambient vibration tests after the 2016 earthquake. Moreover, a permanent monitoring system was installed on the dam, based on the results of the previous testing campaigns, and was able to record four earthquakes of magnitudes between 3.5 and 4. Data are analysed through spectral and interferometric methods in order to determine the set of structural parameters (i.e. shear waves velocity, structural damping and modal frequencies) which can be used to address further levels of investigation

In **chapter 5** I discuss the results obtained through seismic interferometry based on deconvolution, on the basis of the results exposed in chapter 4. The use of these techniques could become an important tool to provide support in decide when and how to organise an in depth experimental test on the dam. In fact, they can provide preliminary structural parameters that can be useful as an earliest step of a multi-level approach to the complex issue of dam structural integrity monitoring, useful to address further survey campaigns, optimizing their cost and efficiency.

In the conclusion (**chapter 6**), I debate the outcomes of this work, in the framework for which it was developed, and the possible future perspectives in the field.



# 1. Introduction

## 1.1 Motivation

Dams are considered strategic structures since their failure can have severe consequences on human life and on the environment. Although statics confirms a good structural behaviour, even under severe earthquakes, seismic testing and monitoring of dam structural behaviour is one of the problem of major interest, considering the socio-economic importance of their impact. In fact, in addition to the quality of design and construction, the safety of a dam, and of the inhabitants of the downstream towns, strongly depends on appropriate maintenance and proper surveillance to monitor its condition (ICOLD, 2000).

The issue gains even more relevance when it comes to existing dams, for which it can be necessary to perform new testing, because of changes in the structure itself due to aging or accidents, or because of changing in the regulations. In Italy, dealers of hydric or hydroelectric plants faces intricate issues in the safety management of infrastructures that reached (and often overcame) the service life expected when the structure was built. In fact the average age of Italian dams is over 66 years. We are thus fronting an infrastructural framework that need unceasing maintenance, ordinary and extraordinary, and non-stop high level of surveillance. Which is more, dams underwent a three-generations evolution of design and realization method and regulations, implicating an uneven safety level (ITCOLD, 2012). The majority of them was built when seismological knowledge and understanding of structural behaviour under dynamic load were much poorer than now.

Therefore, ordinary and extraordinary monitoring of dam structural integrity is an unavoidable duty, which can entail considerable extra technical and economic efforts for dam dealers or owners.

In the last decades, legislative measures imposed more technical fulfilments, none of which useless or worthless, but that worsen the organizational and economic commitment of the

dam dealer. Among the tests to perform, deformation, inclination and drifts, and their evolution over time, are of particular importance.

In addition to all the requirements, integrative investigations are due to the concessionaire: hydrological, hydraulic, material characterization and seismic. These fulfilments imply tests, studies and elaboration, leading to significant costs and technical efforts for the dealer, especially if the dealer is not having a considerable profit from the dam management. This eventuality, not unusual, becomes quite common for small reservoirs, also considering that the requirements are almost the same for big and small reservoirs. Therefore, reservoirs are increasingly being abandoned, leading to the lack of spread of low cost hydraulic resources exploitation on the territory. The only solution to this situation is to foster the opportunity and sustainability of a virtuous maintenance of dams.

In this framework, it would be a consistent advantage to find a cost-effective method for the preliminary evaluation of dam structural integrity conditions. In order to do so, it would be interesting to find an index of dams structural integrity condition, able to address further levels of investigation, optimizing their cost and efficiency. The index must be able to be used as a first check on possible variations in the structural characteristic of a dam, in case of shocks (artificially or naturally induced on the dam, i.e. seismic events or invasive operations), or due to normal aging. The researched index has to be provided through tests that should have at least three characteristics: being of immediate interpretation, being non-invasive – since the operativeness of dams must be preserved during testing procedures – and being able to detect also damage not visible at a sight inspection. Nevertheless, to be widely adopted by dams' managers, it should be a system with low installation and maintenance costs, not to overload companies with other obligations.

Therefore, this thesis proposes to use the shear wave velocity inside the structure and the damping factor of the dam as indexes. In fact, the shear wave velocity and the damping are immediately related to the shear stiffness of the dam itself, which is a good indicator of possible structural degradation. Thus, it would be feasible to detect potential structural damage whereas variations in the shear wave velocity are observed.

In order to obtain these indexes, the most suitable tests fulfilling all the requirements exposed above would be passive geophysical tests based on seismic deconvolution interferometry.

Geophysical passive tests, already widely adopted on regular buildings and infrastructures (as bridges), are based on ambient vibration or seismic events recording. Passive methods are by now extensively and successfully used in dynamic characterization of buildings, in microzonation studies and in soil-structure interaction preliminary assessment. An index provided by these techniques could become an important tool to provide real-time support in the decision-making process concerning dam ordinary and extraordinary structural integrity monitoring. This index, far from be exhaustive in describing the dynamic behaviour of a dam, would represent a preliminary step of a multi-level approach to the complex issue of dam structural monitoring and maintenance, useful to address further levels of investigation.

The aim of this thesis is therefore to propose to use the shear wave velocity and the structural damping obtained by interferometric analysis based on deconvolution of recorded seismic events or ambient vibrations. In this work, I discuss whether this method, postulated for buildings, could be profitably used as a first explorative approach to dam dynamical characterization, and to propose a guideline for the application of the method on dams.

In the case of promising results, the method would be important to enhance the monitoring methods already available for dams. Being the technique proposed a level zero method of investigation, useful to optimize cost and efficiency of further ones, this could lead to a significant advantage when approaching the complex issues of designing, prepare and perform structural tests on dams.

## 1.2 Objectives

The objective of this thesis is to test whether a set of parameters obtained through passive geophysical methods can be useful to support decision-making process concerning planning and organization of dam structural monitoring. These indexes, shear waves velocity, structural damping and modal frequencies, are successfully being determined for buildings. The aim of this thesis is to propose to use them also for addressing the issue of design and organization of structural monitoring campaigns on dams.

The structural characterization of dams is a very complex topic. The aim of finding cost effective and quickly available parameters that completely describes a dam structural behaviour would be fairly too ambitious if not even inconceivable. The storey drift, a significant parameter for the characterization of dynamic behaviour of buildings, is difficult to translate in the dam environment, where several different factors can be involved in the crest displacement. Moreover, in the case of dams experimental tests should be performed in a number of environmental scenarios to take into account all the factors that can affect modal parameters variations.

Anyhow, in the framework of a multi-level approach to dam dynamical characterization, a method able to provide useful preliminary information – although raw and incomplete – in order to address further levels of investigation about structural integrity of dams would be a significant advantage, especially if performed with low cost non-invasive techniques. Far from being exhaustive, the method could be complementary to conventional monitoring methods, providing evidences beneficial to address ordinary and extraordinary monitoring of dams structural integrity.

The monitoring system is usually requested by Authorities to improve dam safety both in ordinary condition and during emergencies (for example floods or seismic conditions). The ordinary monitoring include a numerical analysis of the structure to verify its behaviour under operating loads and loads associated to hypothetical scenarios of interest (i.e. earthquake). Extraordinary monitoring is, instead, necessary for the emergency management, whereas any of the scenario of interests (earthquake or floods) occurs.

The monitoring process involves the use of experimental tests. Nowadays there are several kind of tests that are used on dams. The most common one is the forced vibration test, useful to update or calibrate the numerical model. These tests, for their being quite expensive and logistically complicated, are usually performed few times in the operational life of a structure, and are not suitable to be used for continuous monitoring. On the contrary, geophysical tests are more suitable to be applied, for their being cost-effective and non-invasive. Furthermore, active tests may fail in the representativeness of the global behaviour of the structure. In fact, the outcomes may depend on the way in which the source is applied (in the case of the forced vibrations) or on the section selected for being analysed (in the case of tomography), and can result in a loss of important information.

Hence, it would be desirable to find a set of parameters – linked to dam structural characteristics – in order to address when and how to perform more detailed tests on the construction. The use of parameters obtained through passive geophysical tests is promising, both for their being cost-effective and non-invasive, that for not needing an artificial source. Moreover, they can capture the global response of the structure in its regular operativity condition. The results of these tests can be used in order to detect possible variations in the structural behaviour and to design further more detailed surveys, optimizing their cost and effectiveness.

Structural and seismic monitoring systems are already installed on several large dams. Obviously, in addition to installation and maintenance, these systems (weather based on permanent or periodic acquisitions) require the interpretation of the obtained data, based on physical or numerical models of the structure. The most advanced system can also offer real-time decision support.

Hence, the objective of this thesis is not to propose the installation of an additional monitoring system, but to check the possibility to analysis data that are usually already collected through seismic deconvolution interferometry, and to use the obtained results to design more in-depth tests. The aim of the work is to verify if the outcomes of the spectral interferometric approach, i.e. shear waves velocity structural damping and modal frequencies, could be a valuable index of structural integrity. This approach should be applied on data that are already available for the majority of large dams in Italy, not involving

any installation or maintenance of additional instruments. Which is more, it doesn't even require any artificial source, which are expensive and logistically complicated to apply. Besides, these parameters can be obtained from data acquired before and after any possible event of interest (for example an earthquake), providing a first indication of possible changes in the structural integrity that need to be focused.

As a first explorative attempt of application, a case study of a dam in Central Italy, that suffered the Amatrice 2016 earthquake, is analysed using seismic deconvolution interferometry. The obtained results have to be considered as a first response to an explorative attempt of optimizing dam monitoring. In case of positive results, further researches should be focused on integrating the use of these parameters as a first indication in the operative protocol of dam structural monitoring.

## 1.3 Confidentiality agreement

This thesis was born in the framework of a collaboration with private partners. They kindly allowed the publication of this thesis under a confidentiality agreement about the specific exposed case study. Hence, in this work, the dam analysed as a case study is not mentioned. Also the pictures, maps, planimetries and all other information that could lead to the identification of the structure are omitted.

## 2 Dam monitoring – framework and state of the art

With the term energy production facilities we refer to all existing kinds of industrial plants for production of Electric Power. These facilities are usually divided into two big categories: thermal power stations and renewable energy power stations. In the former class we find mainly fossil-fuel, natural gas, nuclear and geothermal. In the latter, hydroelectric, solar, wind (onshore and offshore), marine, osmosis and biomass are included. Among these, the hydropower plants with reservoir are the most efficient, being able to produce more than 200 times the energy required for their construction and operation (ITCOLD, 2012 *a*; Figure 1).

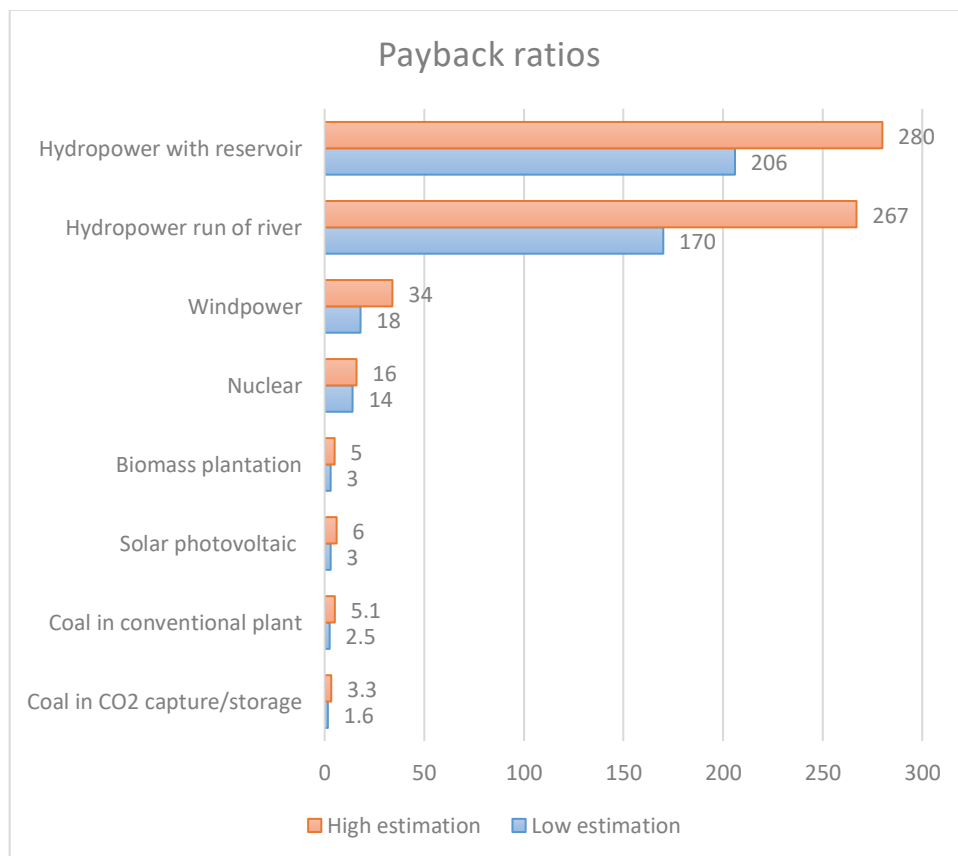


Figure 1 – comparison between the payback ratios of the different power plants. Among them, it is possible to see how the hydropower with reservoir is the most efficient (ITCOLD 2012, *a*)



A part from their structural complexity and long service life, energy production and distribution facilities differ from standard civil structures for many features:

1. Their failure can induce severe damage to people, property and the environment;
2. They are spread all over the territory;
3. Boundary conditions strongly influence the testing results and the tests as well: not only external factors (such as wind, rain, ...), but also internal factors, such as the level of the reservoir or wind strength have to be considered;
4. The operativeness of the facility has to be preserved: operations usually can not be stopped during the testing itself;
5. They are crucial also for the emergency management after a natural disaster;
6. They are usually covered by trade secret: it may be difficult testing to be accepted willingly by the company;
7. They are often contrivers and subject to NIMBY (Not In My Back Yard) syndrome.

Therefore, each power plant need to be regularly assessed and receive continuous structural health monitoring, in order to guarantee their reliability, safety and serviceability. It is very important to perform dynamic tests on every different facility, at many different operational situations, in different time period and every time something changes (earthquakes, aging, floods, ...).

Reported cases of failure or damage of dams are quite rare events. They involve mainly rock-fill dams, not mechanically compacted, and susceptible to dynamic load. Although a good structural behaviour is confirmed even under severe earthquakes, testing of dams is one of the problem of major interest, considering their socio-economic importance and the severe consequence that their failure may have. The issue gains even more relevance when it comes to existing dams, for which it is sometimes necessary to perform new testing, because of changes in the structure itself or in the regulations.

Safety condition, both of the dam itself than for the inhabitants of the downstream towns, strongly depends on appropriate maintenance and proper surveillance to monitor its condition, beside (of course) on the quality of its design and construction. Dam surveillance is defined as “the process of assessing the performance, safety and operability of the dam and reservoir”. The process embraces three activities: monitoring of dam and foundations; visual physical inspection; testing operational facilities. The monitoring term refers, therefore, to the “part of surveillance based on instrumentation and measurement” (ICOLD, 2000).

For arch dams the possibility of adopting simplified analysis is limited due to the fact that the response of these structures is depending on the superposition of contribution from a high number of modes, differently for what happens for gravity dams whose response is dominated by the first mode. Therefore, usually arch dams are verified through three-dimensional analysis, often in a linear elastic field. In this way it is possible to properly take into account interactions with the fluid and with the ground and even non-linear phenomena. Finite elements models allows a good representation of the real structural configuration and of its interaction with the fluid and the ground, as well as providing a precise picture of its tension-deformation status.

In the specific case of existing dams, it is advisable to rely on experimental testing on the dam, in order to increase numerical models’ accuracy. In particular:

- laboratorial and in-situ testing should be performed, to characterize in detail physical and mechanical materials’ parameters;
- using measures on the real behaviour of the dam over time, obtained through the static monitoring system, to obtain all information needed for the numerical model calibration;
- dynamic behaviour testing, and eventually numerical model calibration, through an experimental determination of the fundamental dynamic characteristics of the dam.

The level of detail of surveys performed for knowledge acquisition should be correlated to the economic and social importance of the dam and to the potential risk in the valley; it plays a key role in the definition of the degree of confidence of the results obtained by numerical analysis.

The modern approach to dam monitoring is that of developing an integrated system, which includes at the same time the monitoring of topographic, meteorological, hydrologic, hydrogeological, geotechnical and structural data. The monitoring activity can be performed through periodic in-situ surveys or through remote control, depending of the complexity of the situation and on the purposes of the analysis. Manual testing, generally used in case of emergency, has the advantages of being usually low cost, but on the other hand requires to take the risk of reaching the site immediately after the event. Vice versa, remote testing provides a huge quantity of data in real time, but is considered to be expensive, both for the cost of the instruments, than for the cost of installation and maintenance. (Loddo and Komin, 2015).

The monitoring system is usually requested by Authorities to improve dam safety both in ordinary condition and during emergency situation (for example floods or seismic conditions). The ordinary monitoring include a numerical analysis of the structure to verify its behaviour under operating loads and loads associated to hypothetical scenarios of interest (i.e. earthquake). Extraordinary monitoring is, instead, necessary for the emergency management, whereas any of the scenario of interests (earthquake or floods) occurs. Structural and seismic monitoring systems are already installed on several large dams. Obviously, in addition to installation and maintenance, these systems (weather based on permanent or periodic acquisitions) require the interpretation of the obtained data, based on physical or numerical models of the structure. The most advanced system can also offer real-time decision support.

In this chapter, I will briefly discuss the situation in Italy (Italian dams and Italian regulation) and then focus on the testing methods used for dam characterization and diagnosis. As stated in the introduction, the aim of this thesis is not that of proposing the installation of an additional monitoring system, but to propose ad integrative method for the analysis of data that are usually already collected.

## 2.1 Italian dams

A dam is defined as a work that, by blocking a section of a watercourse, intercepts its outflows and causes temporary accumulation (reservoir) in the valley preceding the section bounded.

With the term large dams are designed dams with an height superior to 15 meters or with a reservoir bigger than a million cubic meters. In Italy there are 534 large dams (data updated to February 2017, Ministero Infrastrutture e Trasporti; 2017), on which the competence is of the national Italian authority. Almost the 60% of those are hydroelectric dams (ITCOLD, 2014). In 2013, among 538 large dams, 13 were reported to be under construction, 92 in experimental operation, 402 in regular operation and 31 not in operation (Pascucci and Tamponi, 2013). A part from the large dams, in Italy there are more than 8.000 minor plants, managed at a regional level. The territorial distribution of large dams in Italy is represented in Figure 2. It can be noticed how dams are well distributed on the entire Italian territory, also in seismic prone areas.

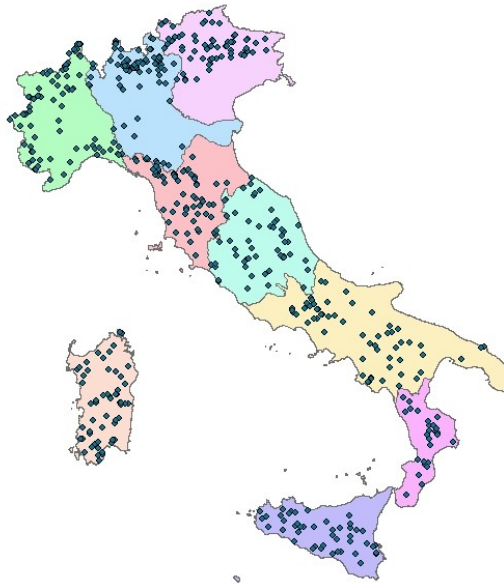


*Figure 2 – territorial distribution of Italian large dams (Pascucci and Tamponi, 2013). It can be noticed how dams are well distributed on the entire Italian territory, also in seismic prone areas.*

After having represented the backbone of the industrialization phase of the Italian history, contributing to the post-war economic recovery, from the 60s the realization of new dams – and especially hydroelectric ones – underwent an unfavourable phase. Several factors caused this process: financial restrictions, anthropization of Italian territory, competitiveness among other ways of water exploitation, regulations and administrative restrictions, hostility by stakeholders. Therefore, the dealers of hydric or hydroelectric implants faces intricate issues in the safety management of infrastructures that reached (sometimes overcome) the service life expected when the structure was built. In fact the average age of Italian dams is over 66 years old. The graph of Figure 3, represents the number of dams per year that were build and that underwent extraordinary maintenance intervention, in the history of Italian infrastructure. It is quite evident that we are thus fronting an infrastructural framework that need unceasing maintenance, ordinary and extraordinary, and non-stop high level of surveillance. Which is more, dams underwent a three-generations evolution of design and realization method and regulations, implicating an uneven safety level. In fact, more than the 65% of dams were built in the period between 1920 and 1970 and are therefore obsolete construction typology, with a high-incidence of rehabilitation interventions (Fornari, 2013).

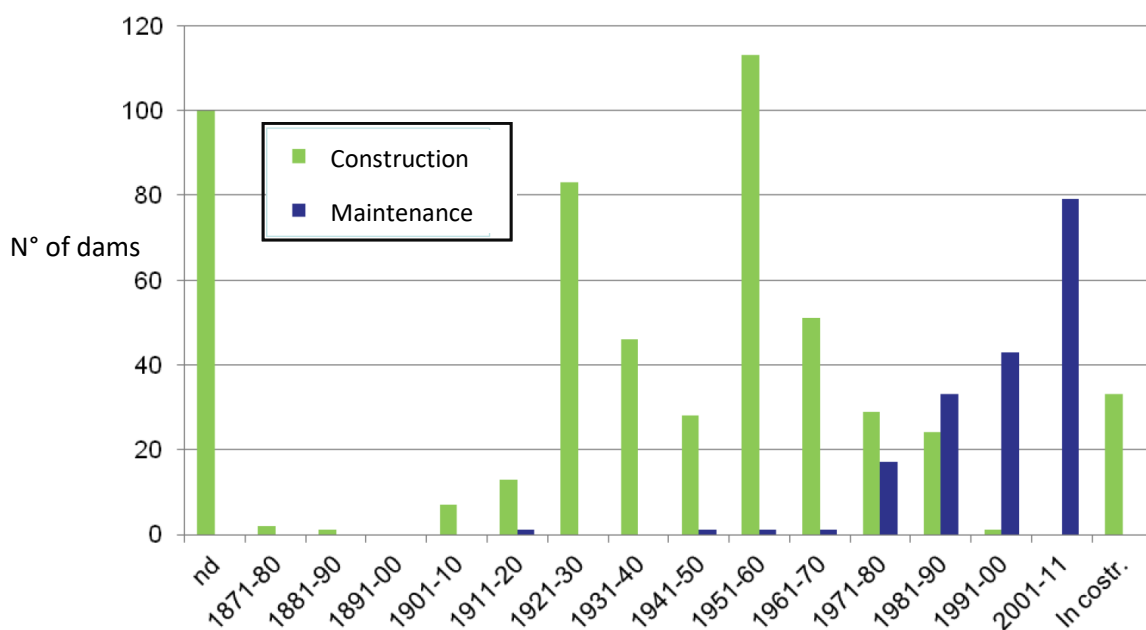


Figure 3 – history of construction and extraordinary maintenance intervention on Italian dams (ITCOLD, 2012)

The structural typologies of the Italian dams are represented in the histogram of Figure 4. In this graph, can be seen how there's a significant variability in the construction typologies, although the most common is the concrete gravity one. Other common typologies are the buttress, masonry gravity, earth filled dams and arc-gravity, all of which are suitable to be analysed through the seismic interferometric approach based on deconvolution that is exposed in the following chapters of this work.

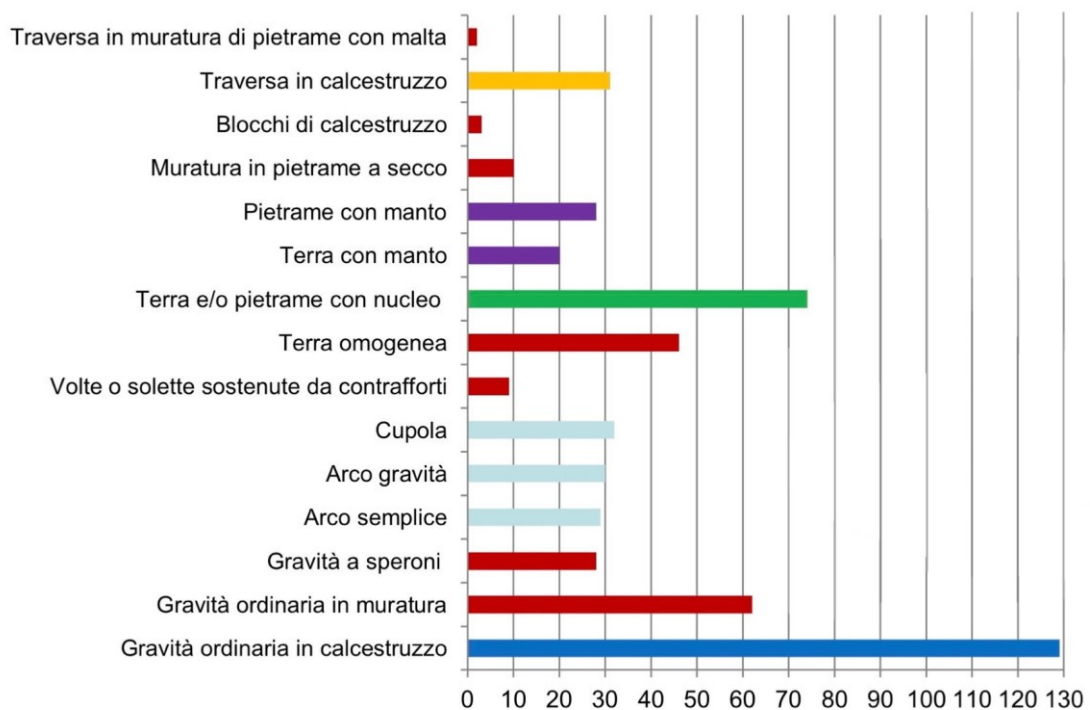


Figure 4 – structural typologies of Italian dams (Fornari, 2013). The concrete gravity dam (last one, blue bar of the histogram) is the typology most present for Italian dams, reaching nearly 130 dams. Other common typologies are the arch and arch-gravity ones, the buttress, masonry gravity, earth filled dams. On all these typologies, it is possible to apply the seismic interferometry approach based on deconvolution described in the following chapters.

## 2.2 Italian regulations about dams

The Italian code about dams is considered to be complex, since it is connected with several general provisions about civil defence and environment protection, therefore very difficult to accomplish from the side of the dam management.

The main existing regulation codes can be divided into two big classes:

- General regulator and administrative codes, regarding classification, geometric quantities definitions, process of approval for building or adjustment projects, obligations of the manager, supervision duties;
- Technical codes: detailed prescriptions about calculation and building;

The Central Authority for dams and hydric and hydraulic infrastructures collaborates with the Civil Defence Department in the framework of the national and regional warning system for the hydro-geologic and hydraulic risk, as a centre of competence (DPCM 2004). The Central Authority is called, in addition to the support to the functional centres on the analysis of hydrogeological phenomena, to give a special attention to real-time monitoring of large dams.

The recent 2014 technical code for dam design and construction (Ministero delle Infrastrutture e dei Trasporti, 2014) is applied to all the dams of the national territory. For dams with a height minor than 10 meters and with a volume of reservoir that does not exceed 100.000 m<sup>3</sup>, the competent administration can decide, case by case, which parts of the regulations have to be applied. The aim of these codes is to ensure, even in case of extreme events, that no release of water occurs and the safe controlled emptying of the reservoir (ultimate limit states). For strategic dams, also the serviceability condition (belonging to the Damage limitation states) is required. Eurocode 8 (2004) defines the Damage Limitation States as “those associated with damage beyond which specified service requirements are no longer met”. Section 2.2.3 of EC8 states that: “In structures important for civil protection the structural system shall be verified to ensure that it has sufficient

resistance and stiffness to maintain the function of the vital services in the facilities for a seismic event associated with an appropriate return period”.

The code gives the design criteria, the definitions of the dam characteristics (height, reservoir volume, etc...) and describes the structural typologies of dams, giving also criteria of choice among them. There are also the limit states for design descriptions (Ultimate and Serviceability) and the verification required, together with the actions to take into account.

The 2014 code takes into account also the monitoring requirements for the dam. It is prescribed that the projects of a dam must entail a general plan of maintenance, including the apparatus for the behaviour monitoring, both on the structure itself than on the foundation soils. In the plan also the type of instruments to be used and the frequency of the acquisition of each typology of data must be included, especially during the construction, experimental filling of the reservoir and during regular serviceability. Data acquisition and elaboration has to verify continuously that the behaviour of the dam corresponds to the one expected. The following parameters have to be observed and measured: water level of the reservoir, water volumes release, leakages, interstitial pressured, deformations and displacements of the structure and of the foundation soil, seismic events recording. The instruments used must be suitable for real-time remote transmission.

The methods allowed for seismic verification of concrete dams are the pseudo-static or the dynamic ones, using linear or non-linear numerical models.

As far as existing dams are concerned, unless otherwise specified, the general regulations of the 2014 codes have to be considered. In case of non-structural intervention, only the possible influence on the Ultimate and Serviceability State has to be addressed. The safety and design of interventions on existing dams must be in conformity with this code and with the technical codes for general constructions (NTC – Norme Tecniche per le Costruzioni), and must be based on the survey performed during dam construction and service and on the specific tests performed to assess the current conditions of the structure.

Safety verification must be carried out whenever a structural intervention occurs and must assess the safety condition before and after the intervention. Safety verification can entail the stability of the dam body, considering geological and hydrogeological conditions,



considering structural, geotechnical hydraulic and seismic factors. Interventions can entail adaptation, improvement, restoration, declassing, dismissing.

The 2014 code specifies that the preparation of the plan of investigations and surveys to identify the current condition of the dam must consider the data acquired in the phases of design and construction, as well as the data progressively acquired through the control system. The framing of the problems and of the causes that led to the need of intervention will include the description, documentation and critical analysis of the detected phenomena. It is suggested also the design of a model appropriate to reproduce the observed phenomena based on the framework of the available quantitative surveys, also with the purpose of assessing the assess the suitability of the proposed solutions.

Integrative surveys must be programmed, addressed to the mechanical characterization of the materials of the dam body, in addition to those on the foundation soils, with a specific focus on the seismic vulnerability assessment methodologies. For concrete and masonry dams, in situ and laboratory tests on samples are required to ascertain the characteristic of the materials and their variability within the dam body. The parameters obtained through non-destructive tests will be correlated to the direct measures obtained on samples.

For the existing dams, designed and built under previous technical codes, also possible dissimilarities between the current condition and the prescription of the 2014 codes for new dams must be verified.

## 2.3 Structural diagnosis

A measuring system for static or dynamic dam monitoring is a coordinated ensemble of several instruments able to acquire physical values and to elaborate the acquired information (ITCOLD, 1988).

Dam structural diagnosis is flawlessly addressed by an ITCOLD (2012, in Italian) publication, to which I am mainly referring in this chapter.

Structural diagnosis can be defined as the set of methods and techniques used in civil engineering to identify possible causes of abnormal behaviour in civil works. The diagnostic process is activated once anomalies in the structural response to loads are detected through observational methods, eventually followed by degradation signals. Structural diagnosis differs from regular structural assessment or check-up because the latter is generally performed as a precautionary measure. Although, those processes are often addressed with the same name since they usually require the same survey techniques.

In every diagnostic process, the activity is divided into four steps (ICOLD; 2000):

- Taking measurements with the instruments;
- Data checking;
- Data processing and analysis;
- Data interpretation and reporting of the results.

The principal methodologies used in dams diagnosis are:

- Visual inspections regarding not only the dam structure but also foundation, side, channels, pipes,...
- Experimental surveys for the characterization of materials of the system dam-foundation-reservoir. Usually a sample (of rock, concrete, water, etc...) is analysed in a laboratory, or without samples acquisition in case of geophysical tests (cross-hole, tomography, ...)
- Static monitoring, usually permanent or temporary in case of the investigation of structural behaviour under a specific load

- Dynamic monitoring, usually temporary if linked to the execution of vibrational tests, or seismic monitoring, permanent or temporary, when a system for seismic actions and structural response is installed on the dam or nearby it.

Laboratory tests are usually performed on cores belonging to the body of the dam. Of course, the dimension of the cores taken must be chosen in relation to the dimension of the dam elements. Through these test it is possible to determine several characteristics of the materials that make up the dam, such as their density, mechanical resistance, elastic modulus, permeability and thermic features. For chemical evaluation of materials' degradation (i.e. X ray, microscope, chemical analysis) only small samples can be used. It must be considered that in-situ testing are more significant than laboratory testing, since they avoid the interference in the sampling collection and the problems related to the representativeness of the sample. In fact, the size and the direction of extraction of the core samples have an influence on the resulting compressive strength, and the withdrawal of the core induces a tensional state in the sample itself, changing its properties.

In the last decades, thanks to the exponential improvements in the hardware and software developments, the used of automated performance monitoring of dams' structures and foundations underwent a considerable increase worldwide. Initially, automation included only transmission, acquisition and display of data, while at present time it include also analysis and archiving (ICOLD, 2000).

The information collected through these methods undergoes then a critical analysis and, currently, refers on mathematical models, on which the engineers rely in the interpretation phase. In this case, we usually benefit of models for structural identification, i.e. models which starting from the behaviour observed or registered allow retrieving the most plausible set of physical/mechanical parameters that control the behaviour. This is a back analysis problem, for the solution of which a series of methods, deterministic or stochastic, have been developed in the years.

## 2.4 Aims

The diagnostic activity on a generic system which interact with the environment evolving during time is necessary in relation to specific objectives, which should be analytically defined in a preliminary phase. Before starting the monitoring of a dam it is fundamental to ask the following questions: what, where, when, how and (especially) why to measure? The answer to this last question affects the conception, the realization, the management of instruments and teams that will practically apply the activities on the selected dams.

After the diagnostic process, a prognostic process must follow, in which possible structural behaviour of the dam are forecasted with their specific probability of occurrence. In case any intervention on the dam is considered necessary on the basis of the results of the diagnostic and prognostic phases, the identification of the specific measure that have to be adopted is then defined, in the perspective of maintenance, prevention or improvement of the dam's performance.

The diagnostic activity is therefore an essential link in the chain, considering the necessity of a feedback in the entire process, improving the efficiency, reliability and safety of the expected intervention. On the other hand, a diagnostic system must have some basic requirements such as: identification of all the significant parameters for the dam's structural behaviour; efficiency; sensitivity to variations; timely availability; promptness of elaborations. Last but not least, also the economic component must be considered, including not only direct costs but also potential costs avoidable thanks to the monitoring system method.

Structural diagnostic activities on dams can be divided into two very different categories: based on temporary survey campaigns or continue and systematic over time. While the latter kind of testing requires permanent equipment, the former kind entails high level competences and the use of special apparatus (which after the end of the testing have to be removed).

Moreover, in the peculiar case of dams, considering the interaction with the environment, the monitoring system should not include only the structure itself, but should be extended to the physical and even economic environment in which it exists.

From a mathematical and numerical point of view, many of the diagnostic purposes aims to the identification of values or properties of the structure that cannot be directly measured. Therefore, it often happens the occurrence of an inverse problem, i.e. the assessment of the causes starting by the knowledge of the consequences. Therefore, a model is unavoidable. Which is more, often in this kind of monitoring it does not matter the value measured, but its variation over time.

Consequently, it is desirable to consider the optimization of the structural monitoring system design and of the model taken as reference, in a perspective of the maximum efficiency at the minimum cost, with a sufficient measures detail. Actually, sensor installation for dynamic testing is a problem of major interest that is still waiting for a solution.

## 2.5 Geophysical and geomechanical testing

Geophysical and geomechanical tests can provide information on the stress-strain behaviour and the deformation condition of the system and are therefore widely used in structural monitoring. In fact, while visual inspection can only detect major degradation problems, methods based on waves and on low-energy sources to penetrate the concrete dam body are precious since they deliver direct answers and supplementary data, supporting other studies and more invasive methodologies as drillings.

The areas of application and the possible methodologies can be divided into two main categories: the tests for design of new dams (which are not considered in this thesis) and those for the existing dams. As far as the latter is concerned, the main aim is that of assessing the material, and especially their resistance, in order to verify if they match the design prescription. For this purpose, ultrasonic or superficial waves are mainly used directly on the dam body. Earth fill dams are instead tested with reflections and refractions techniques or with tomography, to verify the presence of drifts that may be index of earthquake damage or potentially fragile areas. GPR (Ground Penetrating Radar) and resistivity tests are instead used to detect possible cavities, while filtrations areas can be detected to resistivity measures. The concrete degradation is instead tested mainly through sonic and ultrasonic measures, besides the GPR.

Due to dams aging, it becomes assessing the condition of the structural part of a dam and keeping trace of their variations in time becomes increasingly important. An initial degradation leads to an acceleration of future major problems. Therefore, continuous monitoring of structural integrity is essential in order to enable a prompt intervention, ensuring dams' safety.

The most of these testing techniques can be performed in a non-destructive and non-invasive manner, without emptying the water reservoir, which is a consistent economic and technical advantage. Though, at the present time, the most common geophysics techniques used are refraction/reflection or sonic ones, for which the main ambition is to assess the integrity of materials: usually they don't include an interferometric or modal approach.

McCan and Forde (2001) proposed an interesting review on existing Non Destructive Tests. Sonic inspective methods, based on the wave-velocity detection through tomographic cross-section, give useful information on major elements; on the other hand data are of difficult interpretation and the cost of the test is moderately high. Conductivity tests, instead, are low cost but have a maximum penetration depth of only 1.5 meters, which is not enough in the investigation of a dam section. Therefore, sonics are usually used as complementary to radar testing techniques, that measure electromagnetic wave velocity; the disadvantage is that this tests are expensive and they require high level skill for data interpretation. Also vibration testing allow to obtain information on the dynamic behaviour of the structure (i.e. modal shapes, damping,..) but have a very high cost and there's a difficulty in data quantification.

Seismic methods can significantly contribute also to ordinary monitoring, since they can detect less consolidated materials and the degradation of mechanical parameters. In seismic interferometry, velocity values variation can suggest a different degree of water saturation, by which it is possible to assess the quality of the porous concrete (Karastathis et al., 2002).

One of the main advantage of the passive techniques is that they don't need any artificial source. This aspect, beside the cost savings, implies that there are much less interferences into the physical system, therefore these tests are replicable. Possible variations in the measured parameters are certainly ascribable to a variation in the structural conditions and not to a variation in the boundaries condition caused by the source itself.

## 2.6 Dynamic monitoring

Dam dynamic monitoring consists in equipping the dam-foundations-reservoir system with a permanent network of sensors which perform a continue or periodic testing of the system's behaviour. Physical quantities usually measures include causes – such as water level and temperature – and consequences – such as displacements, deformation, stress.

On the other hand, dam dynamic monitoring is linked to complex phenomena which embrace: geometry of the structure, dam-foundation interaction, dam-reservoir interaction, non linear phenomena, environmental effects (especially thermic). Dynamic testing is able to provide an overall picture of the system dam-foundations-reservoir, taking simultaneously into account all the effects. The goal of dynamic testing is that of obtaining the “modal experimental model” that consists in the definition of: transfer functions, eigenfrequencies, modal shapes, damping factors. It is important to keep in mind that the modal experimental model relates to a particular status of the structure (i.e. reservoir water level and temperature distribution) since the values of these parameters may change in case of condition variations.

Data collected through dynamic testing are useful, but it must be considered that stress levels induced on the dam during the tests are always much lower than those induced by a seismic event. Therefore, the behaviour of the structure is defined in a linear-elastic field, while the non-linear behaviour is assigned to the seismic surveillance system.

Obviously, for the dynamic monitoring it is necessary to obtain data relative to its behaviour under loads that disrupt its static condition. The source can be artificial – forced vibration test – or natural – ambient vibration test. In the latter case, the source could be micro-seismicity, waves, wind, and etcetera. Dynamic analysis is based on the structural response to these external loads and entails three phases: dam excitation, structural response recording and data interpretation.

Forced vibration tests usually entails sinusoidal forces, varying from few hundreds Newton to 200kN, applied to the structure through one (or more) mechanical exciter, made of two eccentric masses counter-rotating. The resulting source is a force with a constant direction



and variable amplitude. It is also possible to use a mechanical exciter made of a single rotating mass. A more complex system is instead the hydraulic one, using inertial masses. The difference, in this case, is that the source time variation can be discretional, but, on the counterpart, the intensity is lower. Anyhow, the amplitude of the force used in the ambient vibration tests is always very small, therefore the dam shows a linear behaviour. The intensity is chosen only in relation to the amplitude of the response signals, in order to optimize the signal to noise ratio. Although, it is important to verify the assumption of a linear behaviour of the dam, varying the level of intensity to check the variations in the outcome parameters.

The structural response is then recorded through high-sensitivity transducers, as velocity, acceleration, relative displacement and hydrodynamic pressure values. With the forced vibration test it is possible to detect the first 3 to 6 vibrational modes, those that contributes significantly to the structural response. Consequently the frequency range usually investigates is between 2 and 25 Hz, depending on the dimensions of the dam.

The installation position and the number both of the source and the sensors should be carefully addressed, depending on the complexity of the vibrational modes of the dam. The ITCOLD in 2012 recommended the use of a number of sensors between 25 and 40.

## 2.7 FEM updating and modal matching

Numerical models are used for design purposes in order to simulate the response of different possible configurations of a structure, or, for existing dams, to obtain the characteristic of the structure, in order to update the model, to make it able to reproduce the structural behaviour.

Mathematical models based on the Finite Elements Method (FEM) are commonly used for structural behaviour interpretation with a diagnostic purpose. In the case of dams, strongly influenced by boundary conditions, it is essential to fit the model on data acquired in situ. In particular, the combination of numeric modelling and non-invasive investigation methods based on dynamic testing (forced vibrations or ambient vibrations) is increasingly gaining importance. The process, named “structural identification”, aims to the updating of FEM models in order to reduce the difference among the experimental response and the numeric model results. Chiefly, several non-destructive diagnostic methods highlighted how the arise of damage conditions implicates a reduction in the structural stiffness, resulting in a variation in the modal response of the structure. Hence, modal frequencies, modal shapes and deformation energy can be used to obtain information on damage extent and localization.

Experimental tests are fundamental to check the reliability of the estimation of the mechanical and thermal parameters used in the F.E.M. model. To do so, the results of the in situ and laboratory test should be used throughout the life cycle of the dam: in the design phase, during the construction and during regular operation. In this way, using both punctual surveys (laboratory) and global maps of shear and compression waves velocity, obtained through geophysical tests, it is possible to assess the consistency of the material of the structural body of the dam, assigning different physical and mechanical characteristics also to the same type material.

## 2.8 Examples

The static monitoring of the structural part of a dam involves both the external actions (i.e. water level variations, temperature variations, acceleration at the soil in case of seismic events) and the structural or hydraulic response to them such as drift, velocities and/or accelerations in case of seismic events, internal temperatures, interstitial pressures, leakages (ITCOLD, 2012 c). In the following subchapters, few examples of dam structural monitoring in Italy and abroad are reported, with the aim of clarifying how structural monitoring is currently performed on dams. Although dams monitoring has a long history (in Italy ambient vibration tests on dams are used from the late 90s; Castro et al, 1998), in this part of the thesis only few and recent case studies are reported, to have a clue of the current state of the art about dam monitoring practices.

### 2.8.1 Seismic monitoring

Antonovskaya et al. (2017) highlights the importance of a fusion between different monitoring systems. In fact, they affirm, every monitoring system utilizes its own specific sensors, communication protocols, and timing, but we can often see an excessive amount of sensors, duplicating the functionality of others with varying precision. The combination of data recorded by the different systems has the disadvantage of having different time intervals for measurements, that does not permit simultaneous data acquisition and processing. Moreover, there may be the artificial limitation of continuous data acquisition (i.e., recording of seismic events only).

Jian et al. (2017) underlines that the merit of strong motion records lies in the abundant information on structural dynamic nonlinearity, but that strong motion records of arch dams that have experienced earthquakes are very limited. In fact, existing observational databases

are insufficient, and therefore the studies based on the databases of actual dams are few. In the paper, the authors present a work based on data collected thanks to a permanent monitoring system installed on the dam since 2001, which was able to record about 20 earthquakes with a magnitude up to 8. They were able to demonstrate how the identified resonant frequency of the dam decreased with the increase in the water level in the reservoir.

Wang et al. (2017) present an investigation of the seismic cracking behaviour of Guandi concrete gravity dam, located in the highly seismic zone of China. The authors carry out three dimensional nonlinear finite element analyses, considering the Concrete Damaged Plasticity (CDP) model to consider concrete cracking under seismic loading. The authors' conclusions include the consideration that in the spirit of performance based earthquake engineering, seismic fragility analysis using abundant strong motion records should be performed.

Also Dunben and Qingwen (2016) worked on the damage assessment focusing on the remaining seismic carrying capacity after an earthquake occurs. In their work, they analyse the response and damage distribution, in the case study of the Koyna concrete gravity dam. The results are obtained considering the concrete damage plastic constitutive model and, especially, by using time-frequency localization performance of wavelet transform, for different amplitude seismic events.

Although there are several studies simulating the damage or failure of a dam using numerical models, it is not easy to find studies that assessed a real damage due to a seismic event that hit a dam. In the next subchapter, a case study of an Italian dam that suffered L'Aquila 2009 earthquake is reported, even if in this case no damage was detected on the structure.

## 2.8.2 Seismic verification

The dam of Sella Pedicate belongs to the ensemble of dams that compose the Campotosto reservoir (Central Italy). Part of the dam is a gravity concrete structure, while a part of it is earth filled. The crest is 638.38 m long. The height of the dam is of 26.50 m according to the D.M. 24.03.82. After the 2009 L'Aquila earthquake, the Civil Defence required the structural verification of the dams belonging to the Campotosto reservoir, considering the Maximum Credible Earthquake action (MCE) triggered by the Campotosto fault. The verification is reported as a case study in the ITCOLD *Potenzialità, limiti e possibili sviluppi delle tecniche di identificazione strutturale per la diagnostica delle dighe*, subchapter 5.4, 2012.

The seismic behaviour of the dam was assessed through structural non-linear dynamic analysis, which simulated the potential non-linear behaviour of the dam. A F.E.M. model, with a high definition, in order to be representative of the dam, was developed. For this purpose, the first approach to the problem was the set of the model and its calibration, using the measures of the displacement monitoring system installed on the dam.

Laboratory tests were performed on samples extracted from two vertical cores. The cores were performed from the crest and reached 5 meters of foundation rock. The results highlighted a concrete of a good quality, homogeneous and well preserved.

On the dam geophysical tests were performed as well, mainly on the central section of the dam and on a lateral one. The results were the tomograms, maps of the velocity of the P waves inside the structure. Also sonic and cross-hole tests were applied, obtaining the shear waves velocity in addition to the P-waves velocity. The results of the geophysical tests (reported in Figure 5) confirm the homogeneity of the concrete.

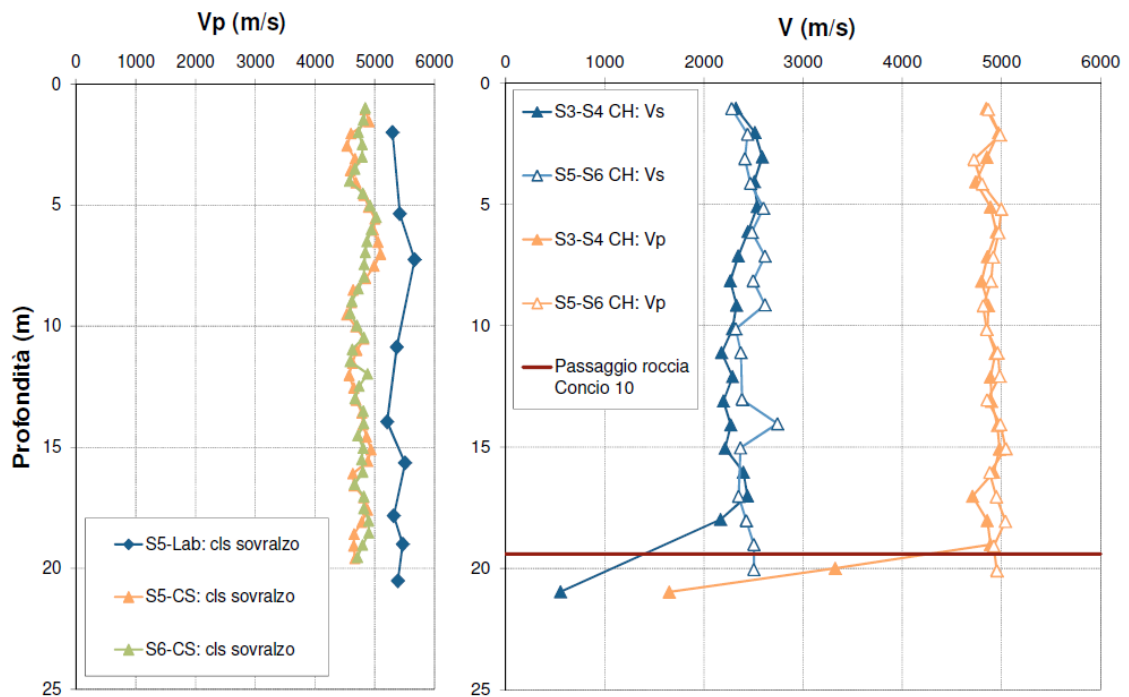


Figure 5 – velocity profile of the P-waves (left) and shear waves (right) for two sections of the dam, calculated through sonic cores (CS), cross-hole tests (CH) and laboratory analysis, on the Sella Pedicate dam, as reported in ITCOLD 2012 c.

The monitoring system installed on the dam entails the measure of the environmental parameters (water reservoir level and air temperature) and of the upriver-downriver displacement (through pendulum). Moreover, 20 thermometers measure the temperature inside the body of the dam and two thermometers (immersed in water) the temperature of the up-river wall.

The detailed analysis of results can be found in the document ITCOLD, 2012 c.

### 2.8.3 Ambient Vibration Tests

Abdulamit et al. (2017) presented the application of ambient vibration tests on three buttress dams built between 1960 and 1980 in Romania: Stramtori - Firiza dam, Gura Raului dam and Poiana Uzului dam.

The measurements campaigns are part of the long-term monitoring of dams. Vibration data were acquired in two dam operation conditions: with and without running of hydro-mechanical equipment (right side and left side of Figure 6 respectively). In each case two samples of 3 minutes length with a sampling frequency of 100 Hz were recorded. The measurement direction was transversal to dam axis (towards downstream). Several layout configurations with group of 5 sensors per each were used, in different period of the year (summer, autumn, winter). Fourier spectral analysis was used to estimate (from ambient vibration records) modal frequencies of investigated dams.

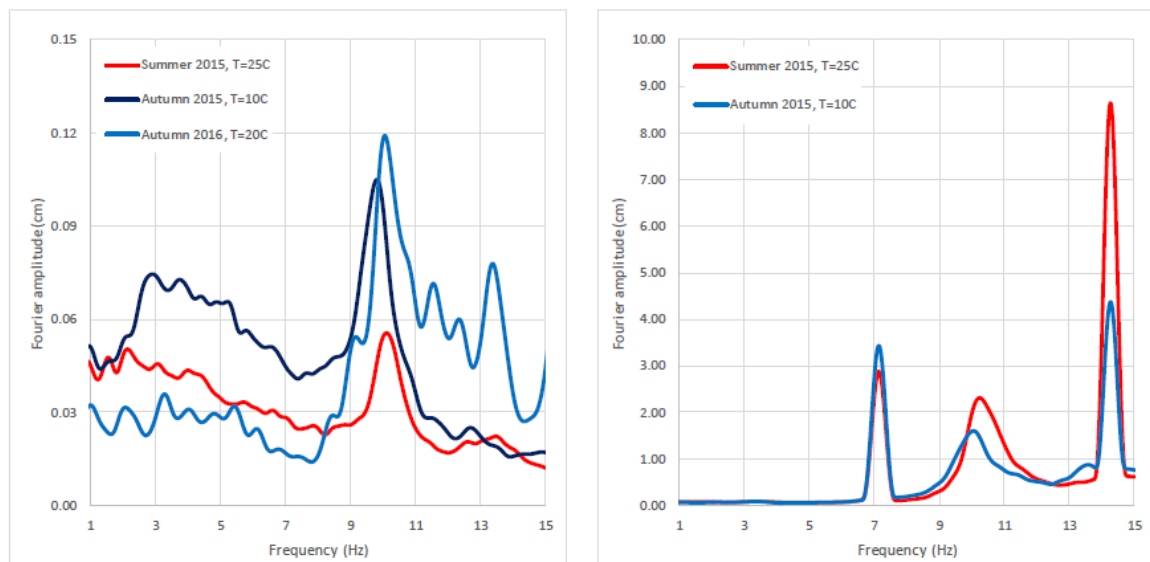


Figure 6 – example of average amplitude Fourier spectra for a central buttress without (left) and with (right) running of hydro-mechanical equipment as reported in Abdulamit et al. (2017).

## 2.8.4 Seismic Investigation for Characterization

Capizzi et al. (2016) exposed the application of seismic tests for the characterization of the concrete conservation on a gravity concrete dam. They performed three seismic tomographies (TS4, TS10 and TS14) and a vertical seismic profile (DH) on the dam body. In addition a continuous core drilling (BH) was also performed and used to calibrate seismic surveys. All seismic surveys were performed using the digital seismograph X610-S (M.A.E.).

Three 2D seismic tomographies were carried out in the body of the dam, energizing on the upstream and receiving signals on the downstream face. The receiving points were spaced of 2.5 meters, while the source points were positioned with spacing of 1 meter. A total of 704, 888 and 744 raypaths were used for TS4, TS10 and TS14 respectively. Figure 7 shows the results of the tomographies as reported in Capizzi et al. (2016).

The results of the vertical seismic profile (DH), acquired with a vertical sampling interval of 1 m showed P-wave velocity ranging between 3800 m/s and 4750 m/s and S-wave velocity ranging between 1100 m/s and 2520 m/s.



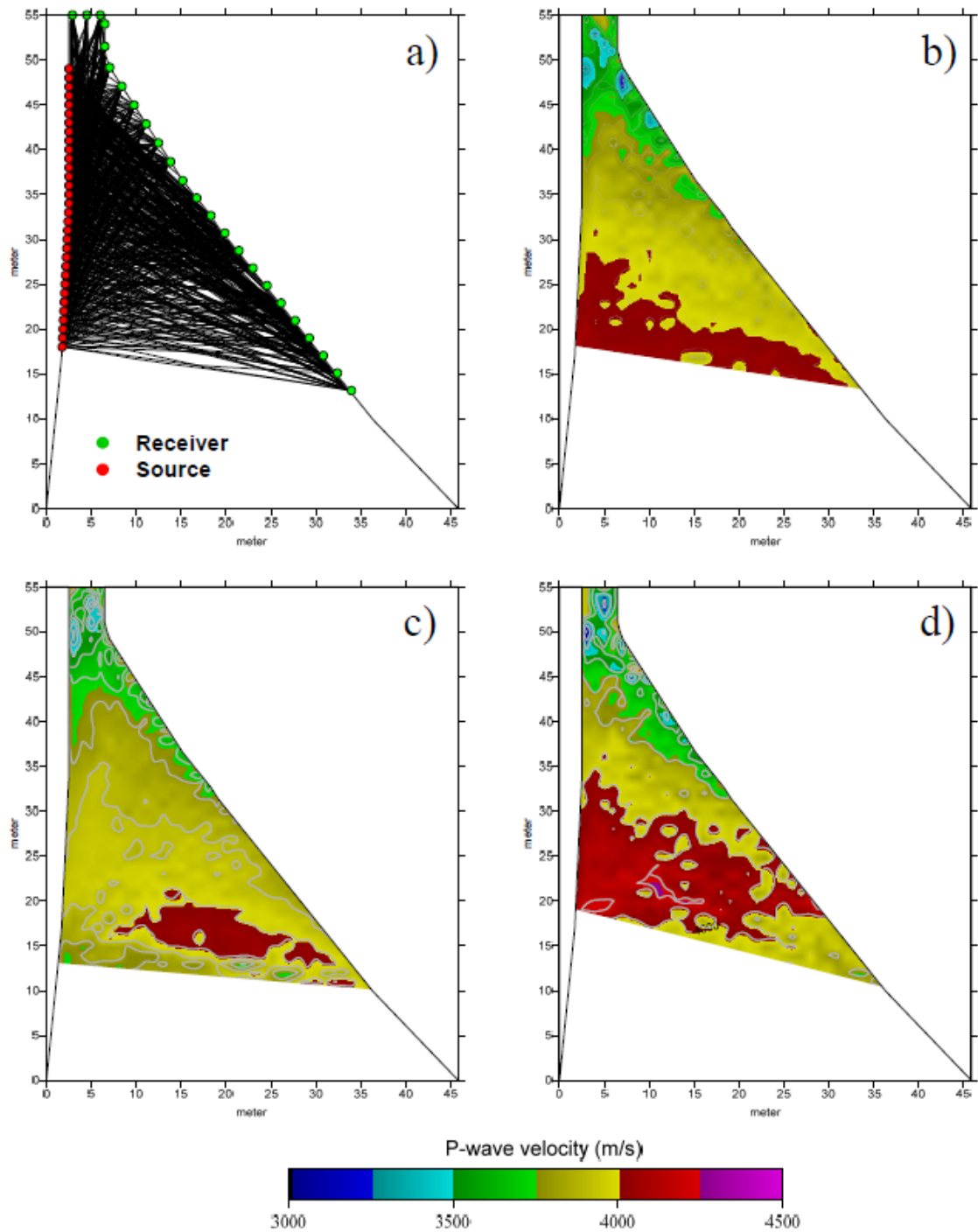


Figure 7 - An example of curved raytracing obtained for TS4 section (a) and P-wave tomographic model obtained for TS4 (b), TS10 (c) and TS14 (d) sections, as reported by Capizzi et al. (2016)

# 3 Experimental structural analysis methods

## – framework and state of the art

### 3.1 Soil-structure interaction

The dynamic interaction between the near-surface soil and the structural response of the building is named soil-structure interaction (SSI).

SSI affects the dynamic behaviour of the structure, increasing time period and damping, and modifying the input ground motion with respect to a free soil surface. Therefore, SSI is important for performed-based design of structures, design technique that is increasingly used in the last decades. The assessment of soil-structure interaction includes the site response analysis, which consist in the calculation of the response of a soil profile. On the other hand, studies on soil-structure interaction are not sufficiently developed, mainly because of a lack of experimental or field-based case-studies that demonstrate its effects on structural response (Bolisetti and Whittaker, 2015).

Soil-structure interaction effects have undergone a large number of studies since long time, but usually focusing only on the seismic input evaluation or on damage modelling. Recently, the attention was moved to estimating the influence of buildings in the amplification, and in particular how the fundamental vibrational mode of a building can influence microtremor analysis (Gallipoli et al., 2004). Two important effects can happen in that case: resonance between the building and its foundation soil if the seismic response of both is in the same frequency range; constructive interference within some frequency ranges between the wave fields generated by the vibration of the buildings, leading to a variation in the frequency and amplitude of ground motion (Gallipoli, 2004). The possibility that, during an earthquake, buildings are capable to significantly influence ground motion was theoretically postulated by Wong and Trifunac (1975) and Bard et al (1996) and then experimentally

evaluated (Jennings, 1970, Kanamori et al. 1991, Guéguen et al. 2000, Mucciarelli et al. 2002). The simplest model for evaluating the energy flow is a damped oscillator, with one degree of freedom which represents the building and a stiff foundation with two degrees of freedom: horizontal translation and ground rotation (Trifunac et al. 2001).

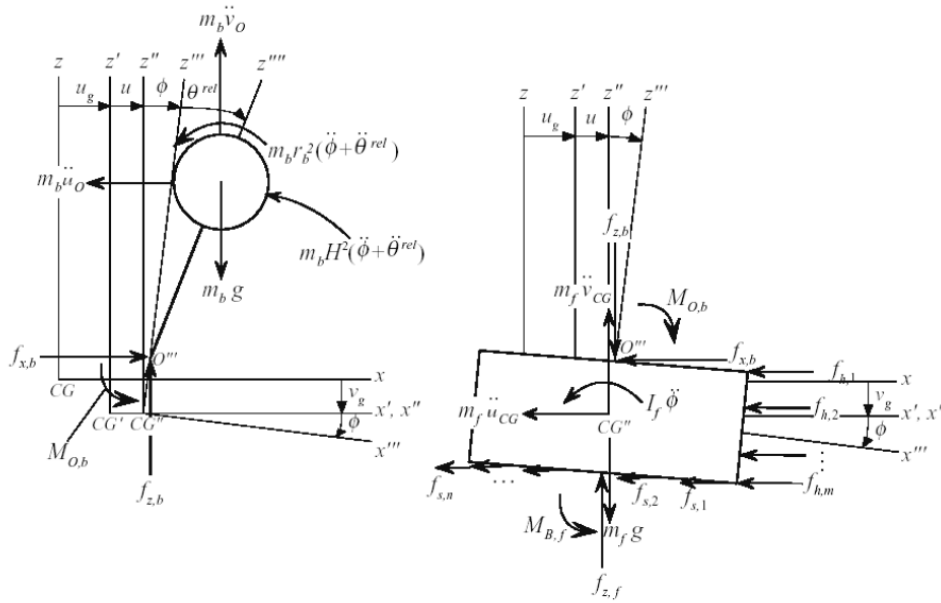


Figure 8 – Trifunac et al., 2001; forces involved in the soil-structure simplified model of a building: a damped oscillator, with one degree of freedom which represents the building and a stiff foundation with two degrees of freedom: horizontal translation and ground rotation.

Considering this model, it will be possible to estimate an equivalent frequency given by:

Equation 1

$$\frac{1}{\tilde{\omega}^2} = \frac{1}{\omega_1^2} + \frac{1}{\omega_R^2} + \frac{1}{\omega_H^2}$$

Where:  $\omega_1 = 2\pi/T_1$  is the frequency of the structure with a rigid foundation, while  $\omega_R = 2\pi/T_R$  and  $\omega_H = 2\pi/T_H$  represents rotational and translational frequency respectively, depending on the foundations and on the foundation ground.

As shown in Trifunac et al. (2001) for the San Francisco earthquake (Figure 9), the energetic contribution from the building to the soil can be a significant fraction of the initial energy. Petrovic and Parolai (2016) demonstrated that the energy radiated back by the structure is of the order of 10% of the energy of the input wavefield at a borehole depth of 145 m in the 1–10 Hz frequency band. Moreover, if the energy from the structure is focused on the same frequency range of the soil, the resulting motion will be the sum of the contributions, leading

to an increased amplitude and length of the motion. This factor is more important the heavier buildings are and the more soft and stratified is the soil (Wolf and Song, 2002). Therefore, it is especially important to consider it in the case of big power plants with a complex ground foundation situation, as dams and windmills are.

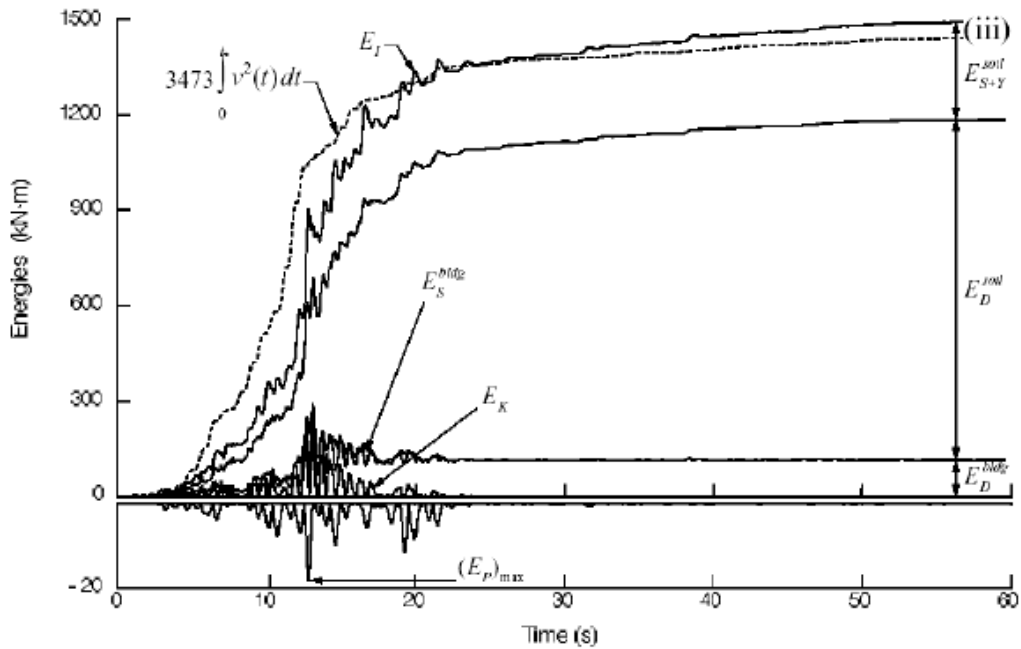


Figure 9 – energy contribution of all the forces considered in the San Francisco earthquake; the energetic contribution of from the building to the soil can be a significant fraction of the initial energy (Trifunac et al., 2001)

## 3.2 Dynamic characterization of existing structures

Dynamic characterization (i.e. identification of natural frequencies, mode shapes, damping ratios) is crucial for existing buildings, in order to assess the condition of a structure. Results can be used to calibrate the numerical model through the elastic properties of the structure; to detect variations in the structural behaviour after damage or after a retrofiting intervention; to predict the structural behaviour in case of seismic event (Michel et al., 2008; Michel et al., 2010). In fact, there are significant uncertainties related to the real and actual conditions of the structure, in terms of construction properties (geometry, materials, ...) as well as non-physical parameters such age and maintenance (Masi, 2009).

The dynamic behaviour of structures is determined by several external factors on very different timescales (Navarro and Oliveira, 2006; Clinton, 2006 and references therein). Variations in the modal parameters can result from a change in the boundary conditions (e.g., fixed- or flexible-base structure), mechanical properties (e.g., reinforcement or retrofiting), or the elastic properties of the material (e.g., Young's modulus) (Mikael et al., 2013). A wide literature has proven transient and/or permanent variations to occur during seismic excitation, due to the non-linear response of the structure and/or of the soil, the opening/closing process of cracks, and (if permanent) structural damage (Mucciarelli et al. 2004; Mikael et al., 2013 and references therein). In fact, structural damage usually results in loss of structural stiffness, which is characterized by a drop in the natural frequency. However, measurable change in recorded natural frequency has been recognised in concrete buildings, concrete dams and woodframe buildings, even during small shaking events; hence, not all the changes in natural frequency can be attributed to structural damage. In fact, the frequency can be shorten by more than 20% during seismic events without reporting structural damage, while up to a 7% drop of frequency can happen even during forced vibration tests (Clinton, 2006 and references therein). The recoverable frequency decrease can reach the 50% during excitation, while a 60% of permanent drop in frequency has been identified as a limit for collapse (Gallipoli et al., 2016 and references therein). Anyway, the frequency recovery may require a long time, with the consequent possibility of false alarm situation (Gallipoli et al. 2016).

Nevertheless, under strong motion, the observed drop of the structural frequency is mainly dominated by variations of the structural stiffness due to opening and closing of cracks, while the soil-structure interaction properties variation and the atmospheric conditions show a low amplitude frequency drop that can be neglected (Michel and Guéguen, 2010 and references therein).

The identification of the variation of dynamic parameters of a structure is important since they depend on mass and stiffness of the structure itself. While the mass can be considered unchanged whatever the state of the structure, the stiffness is influenced by the structural modifications such as reinforcing and damage (Michel et al., 2008). Being related directly to the stiffness of the building, natural frequencies in particular are a sensitive indicator of structural integrity and can be easily tracked for structural health monitoring or long-term building analysis (Mikael et al., 2013). In fact, the damaging process in structures during seismic events produces a permanent increase of the fundamental period due to the permanent loss of structural stiffness (Guéguen et al., 2014 and references therein). Correlating damage level and changes in dynamic characteristics of a structure forms the basis for non-destructive damage evaluation (NDE) techniques (Ponzo et al., 2010 b and reference therein) and they are widely used in structural health monitoring. The NDE methods are classified according to Stubbs et al. (2010, and references therein) into four levels, according to the information provided: 1) methods that only identify if damage has occurred; 2) methods that identify if damage has occurred and its location; 3) methods that identify if damage has occurred, determine its location and severity; 4) methods that identify if damage has occurred, determine its location, severity and impact. Each one of those levels of damage identification requires a gradual increasing amount of data and more complex algorithms, and consequently increasing costs with higher error probability (Ponzo et al. 2010 b).

Damping ratio, on the contrary, is not commonly used as a damage indicator, since it is not an intrinsic parameter of the building. In fact, being dependent on several structure and soil characteristics, and also on soil-structure interaction, its determination is complex problem as much from a theoretical point of view as empirically (Vidal et al., 2013; Navarro and Oliveira, 2006). Damping factor variations are influenced not only by the amplitude of motion but also by the time variations of the factors mentioned above (Guéguen et al. 2014).

Therefore, damping values should be considered only as a general information, since the variations of these factors due to friction in the connection, dissipation of heat and/or plastic deformation of the soil can modify the damping of the structure (Navarro and Oliveira 2006). Also Vidal et al. (2013) proved damping ratio to be a bad indicator of damage in structure since the variation showed with earthquake damage degree are quite small and sometimes the same order as the measurement errors. Anyhow, information about damping can enrich the quality and quantity of the knowledge on the global damage.

The methods belonging to the first level are generally based on the variation of the fundamental vibration frequencies and/or damping and are convenient because they are simple, robust and require a reduced number of sensors installed within the structure. (Ponzo et al., 2012).

There are many different techniques to perform a dynamic characterization of a structure or to assess soil-structure interaction, which are divided into two big categories: numerical models and experimental surveys. Finite-elements methods (linear and non-linear) for soil-structure interaction analysis have gone through a significant development, also thanks to increasingly available computational resources (Bolisetti and Whittaker, 2015). However, analytical prediction methods can be less accurate than artificial and natural vibration tests because of structural idealizations and uncertainties involved in the simulations, failing in representing the true behaviour of the structure. Therefore, computational models should not exclude experimental data, useful for model calibration and validation, since they can reflect the true dynamic behaviour of a structure (Perez-Ramirez et al., 2016). Moreover FE models are not accurate enough in the identification of modal parameters, particularly as far as operational testing of large structures is concerned (Reyndersa et al., 2010). Therefore, experimental surveys are crucial to validate the hypothesis and to detect eventually possible mistakes in the model conceptualization.

To identify the vibrational modes of a structure there are several techniques, which can be divided into parametric and non-parametric methods. When using a parametric method, the parameters of the model are updated to fit the recorded data in frequency or in time domain, whereas non parametric methods use only signal processing tools (Michel et al., 2008).

We should underline once more that neither models nor experimental surveys are enough by their own to completely characterize a structure or its interaction with the soil beneath it, especially for big, complex and strategic structures (as power production plants). Experimental tests are a preliminary or an integrative instrument to collect information about the structure and cannot replace numerical models. Stubbs et al. (2010) proposed the algorithm reported in Figure 10.

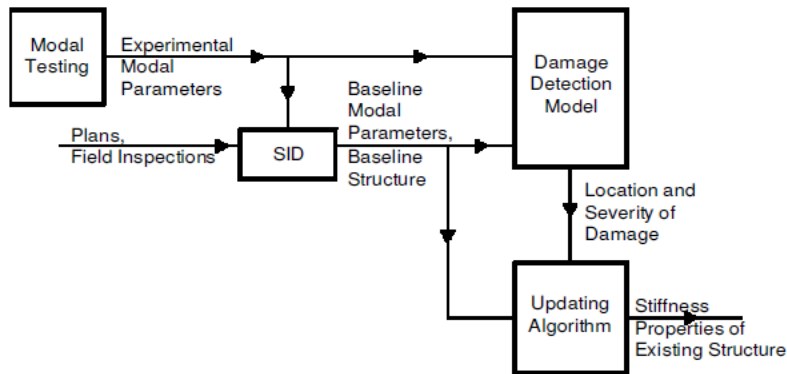


**Figure 1. Schematic of approach used to identify stiffness properties of as-built and existing structures.**

*Figure 10 – Scheme of the approach for the properties evaluation of existing buildings proposed by Stubbs et al. (2010) [SID stands for System Identification].*



### 3.3 Experimental methods for dynamic characterization of structures

In recent years experimental methods gained popularity, after the prevailing of numerical methods in the 80s and 90s. The main reason is that the instruments used to perform the tests underwent significant improvements as far as their quality, price and sensitivity are concerned. Moreover, new methods were developed for the processing of the acquired data (see the Guéguen et al., 2014 European Review; Stubbs and al., 2010).

To reliably diagnose civil engineering structures is a necessity not only for public and strategic building, but also for ordinary and industrial structures. The main goal is to assess their vulnerability and support decision making on structural improvements. The lack of information (quality of materials, ageing, structural integrity, degradation due to long-term, intense operational demands ...) on the structure that commonly raise the level of diagnostic uncertainty can be overcome by dynamic tests, as a first efficient diagnostic level, not substituting an accurate modelling (Hans et al., 2005; Michel et al. 2010; Gallipoli et al., 2016). Monitoring is vital considering the increasing number of aging structures and infrastructures exposed to seismic risk (Gallipoli et al., 2016). Moreover, a systematic overestimation of structural periods as defined by codes and a consistent difference from theoretical models has been demonstrated (Ditommaso et al., 2013; Gallipoli et al., 2010, Chiauzzi et al 2012 ).

Experimental methods include in-situ surveys on the real structure and laboratory test on a part of a structure or on a reduced model of the structure. Experimental tests are an essential tool for the dynamic characterization of civil engineering structures, through the identification of their main dynamic parameters: vibrational frequencies, natural mode shapes and viscous damping ratio (Di Marcantonio and Ditommaso, 2012). As stated in the subchapter above, dynamic characterization is essential within a wide range of research and application fields. Its results can be used for dynamic response prediction, finite element model updating, structural health monitoring and vibration control engineering (Bindi et al., 2015; Fujino and Abe, 2002).

In situ testing method consists in recording with synchronized accelerometers the responses of a structure on the bandwidth between 0 and 50 Hz (Hans et al., 2005). Through in situ experimental testing on real structures (EMA, Experimental Modal Analysis) it is possible to detect phenomena which would be otherwise difficult to reproduce or identify in the case of idealized laboratory experiments. Which is more, in-situ experiments avoid the delicate issues related to the interpretation of the results in terms of scale similarities interference at reduced scale or enlarged time. On the other side, the range of load that we can apply to the structure is limited and the structure itself might be only partially known (Boutin and Hans, 2009).

Field monitoring of existing structures for structural diagnosis is attractive for civil engineering, since it allows to reduce the uncertainties of the risk assessment procedures, developing assessment tools and evaluating the actual state of the structure through real-time methods. In fact, it is possible to use these methods for the identification of elastic properties of structures and infrastructures, detection and localization of structural changes, design of monitoring systems and operational warning (Guéguen et al., 2014). Moreover, this makes it possible to monitor the evolution over time of a structure's safety conditions, becoming a fundamental tool for rapid damage assessment (Guéguen et al., 2014; Mikael et al. 2013; Clinton et al. 2006; Karapetrou et al., 2016).

Experimental testing provide valuable information about construction quality, service behaviour and performance of structures. It is important to perform full scale dynamic testing in order to validate or update numerical models of the building. The knowledge of elastic parameters that mainly dominates the response of the building to a seismic shake, i.e. frequency and damping, can reduce the range of errors and uncertainties for the representation of the vulnerability curves (Michel et al., 2011; Navarro and Oliveira, 2006). Consequently, the models can better reflect the in-situ, as built, boundary conditions, structural stiffness and connectivity, energy dissipation and inertia properties (Chen et al., 2014). In fact, the response of a structure under seismic loading reflects the actual response of a structure incorporating the complexity of its design and the boundary conditions, including soil-structure interaction (Guéguen et al., 2014). As exposed in Trifunac (1999), when we measure the natural frequency of a structure through the use of accelerometers deployed on it, we obtain a combination of the fundamental fixed-base period of the

structure, as well as the rocking and horizontal translation frequencies of the same structure if it moved as a rigid body on the flexible soil.

There are many different kinds of experimental tests on buildings and on structures, depending on the aspect it is necessary to address (see Table 1), which use different exciting sources: induced vibration, records of earthquakes or explosions; ambient vibration tests or microtremors (Navarro and Oliveira 2006; Huang and Lin, 2001; and references therein). Fast monitoring procedures, able to provide useful information on the damage extension on a large number of strategic structures during and after seismic events, using a limited number of sensors per each structure, are gaining ground (Gallipoli et al., 2016).

The amplitude of the excitation of the structure is different for each method, therefore introducing some variability (Clinton, 2006). As reported in Hans et al. (2005 and references therein), for ambient vibrations the level of horizontal acceleration is of the order of  $10^{-5}$  –  $10^{-4}$  g (at the top and at the bottom of the structure respectively) and the density of probability of the random signals follows a Gaussian distribution, which means that the structure responds to a white noise imposed motion. In the case of harmonic forced vibrations, the induced horizontal acceleration can be about 10 times larger ( $10^{-4}$  –  $10^{-3}$  g at the bottom and top respectively). Shock tests, realized by impacting the upper part of the structure by means of a heavy mechanical shovel, can be thousands times greater than ambient vibration, with a recorded peak acceleration of the short impulse of about 10-2 g even on the ground floor. Anyhow, all those methods have acceleration amplitudes that remain in the elastic domain.

Forced vibration tests are very expensive, since they require big and sophisticated instruments, and their application to a great number of buildings assumes prohibitive costs (Navarro and Oliveira, 2006; Gallipoli, 2009). Yet, the answer of the tests is quick and precise, since the input is known, allowing the determination of force response relationships (Bukanya et al., 2012). Clinton (2006) highlights that forced vibration tests differ from ambient and earthquake motions in how energy is imparted to the system, in addition to their differences in amplitude. In fact, forced vibration tests are performed through one or more shakers located at the top of the building, which emits a continuous, single frequency, steady state vibration that flows down the structure (see also Trifunac, 1972). On the other

hand, in ambient and earthquake vibrations, the energy reaches the structure from the bottom and travels to the roof, reflects and dissipates (Navarro and Oliveira 2006; see subchapter 3.5) and contains a wide range of frequencies. Moreover, ambient vibration tests are favoured in comparison to forced vibration tests because in the first case parameters are obtained from data acquired in an operational condition and not in a laboratory one (Reynders, 2012). Which is more, Trifunac (1972) highlighted that the high modes at the top level of analysed buildings show a difference between the mode amplitude determined by ambient vibration and forced vibration, due to the participation of all the modal shapes as a consequence of the application of the force to the structure.

The use of earthquake recordings is cheaper, especially if low cost sensors as MEMS (proven to be reliable, see Gallipoli et al., 2016) are used. On the other hand, it is necessary to maintain a permanent instrumentation in the building (which supposes high costs) and in areas of low to moderate seismicity the amount of time required to gather a significant number of recordings with satisfactory signal to noise ratio is too long (Bonney-Claudet et al., 2006). In fact, well instrumented buildings are few, and the number of moderate to strong earthquakes which occur per year close to them are limited. Therefore, weak to moderate earthquake are usually recorded, limiting the analysis to the range of linear deformation as in the case of forced vibrations (Bindi et al. 2015).

Practical issues for vibration recordings are the layout of measurement arrays and the frequency and time length of recordings. The number of recorded points depends on the height, complexity and accessibility of the building, The frequency of sampling depends on the greatest frequency we want to estimate (Michel et al. 2008, and references therein). Çelebi (2000) proposed a guideline for the seismic instrumentation of buildings. In the guideline, the author underlines several important steps: selection of structures to be instrumented (structural parameter, site-related parameter, probability of seismic events, expected shaking,...); requisite information to optimize the instrumentation schemes (both from cost and data points of view), including site visit. After those steps, the author highlights that it is important to perform tests on the selected structures to determine dynamic characteristics through ambient or forced vibration tests, and to perform the consequent dynamic analysis.

Both for ambient and forced vibration tests, the detected displacement are very small, although in the case of forced vibration the motion may be several orders of magnitude greater than the ambient vibrations (Trifunac, 1975). Michel and Guéguen (2010) underline that ambient vibrations cause differential motion along the structure, produced by multiple sources, while the earthquake can be considered as a single input loading. Therefore, ambient vibration highlights a torsional modes that is usually not activated during seismic events. Also, the complexity of the ground ambient wave field produced by ambient vibrations can explain the small variations in amplitude and frequency.

Table 1 – List of possible application of the methods discussed in the present subchapter and their sample references as reported in Table 1 of Çelebi (2000).

<b>GENERIC UTILIZATION</b>
Verification of mathematical models (usually routinely performed) (e.g. Boroschek et al, 1990)
Comparison of design criteria vs. actual response (usually routinely performed)
Verification of new guidelines and code provisions (e.g. Hamburger, 1997)
Identification of structural characteristics (Period, Damping, Mode Shapes)
Verification of maximum drift ratio (e.g. Astaneh, 1991, Çelebi, 1993)
Torsional response/Accidental torsional response (e.g. Chopra, 1991, DeLalera, 1995)
Identification of repair & retrofit needs & techniques (Crosby, 1994)
<b>SPECIFIC UTILIZATION</b>
Identification of damage and/or inelastic behavior (e.g. Rojahn & Mork, 1981)
Soil-Structure Interaction Including Rocking and Radiation Damping (Çelebi, 1996, 1997)
Response of Unsymmetric Structures to Directivity of Ground Motions (e.g. Porter, 1996)
Responses of Structures with Emerging Technologies (base-isolation, visco-elastic dampers, and combination) (Kelly and Aiken, 1991, Kelly, 1993, Çelebi, 1995)
Structure specific behavior (e.g. diaphragm effects, Boroschek and Mahin, 1991, Çelebi, 1994)
Development of new methods of instrumentation/hardware (Çelebi, 1997, Straser, 1997)
Improvement of site-specific design response spectra
Associated free-field records (if available) to assess site amplification, SSI and attenuation curves
Verification of Repair/Retrofit Methods (Crosby et al, 1994, Çelebi and Liu, 1997)
Identification of Site Frequency from Building Records (more work needed)
<b>RECENT TRENDS TO ADVANCE UTILIZATION</b>
Studies of response of structures to long period motions (e.g. Hall et al, 1996)
Need for new techniques to acquire/disseminate data (Straser, 1997, Çelebi, 1997, 1998)
Verification of Performance Based Design Criteria (future essential instrumentation work)
Near Fault Factor (more free-field stations associated with structures needed)
Comparison of strong vs. weak response (Marshall, Long and Çelebi, 1992)
Functionality (Needs additional specific instrumentation planning)
Health Monitoring and other Special Purpose Verification (Heo et al, 1997)

### 3.4 Ambient vibration tests

If until the 90s traditional modal analysis (forced vibration tests) were preferred because of the accuracy of the corresponding system identification techniques, in the last decades ambient vibration recordings are favoured for the determination of dynamic behaviour, damage detection, retrofitting evaluation or model updating, mainly due to their low cost (Nakamura, 1989; Nakamura 2000; Ventura et al., 2005; Michel et al. 2008 and references therein).

With ambient vibrations we denote an ensemble of small amplitude seismic waves which can be recorded everywhere on the earth's surface. Bonnefoy-Claudet et al. (2006), in the literary review on seismic noise, define noise as "the generic term used to denote ambient vibrations of the ground caused by sources such as tide, water waves striking the coast, turbulent wind, effects of wind on trees or buildings, industrial machinery, cars and trains, or human footsteps, etc." The noise wave field consists primarily of fundamental mode Rayleigh waves. Its origin depends on frequency: it is mainly due to human activities at frequencies higher than 1 Hz, when it systematically exhibits daily and weekly variations, while at lower frequencies (between 0.005 and 0.3 Hz) the variation of seismic noise is correlated to natural activities, such as oceanic waves and meteorological phenomena (Bonnefoy-Claudet et al., 2006). The waveform so generated is therefore used as a white random seismic source for what takes the name of Ambient Vibrations Tests (AVTs) (Farrar and James III, 1997). The expected range of acceleration values for ambient vibration tests is  $10^{-7}$  to  $10^{-4}$  g (Michel et al., 2008).

Ambient vibration tests have been increasingly used for earthquake engineering activities and research activities, leading to an abundant scientific literature (see the European review by Guéguen et al, 2014, and the references therein). In fact, in many cases the classical methods for the estimation of seismic behaviour and vulnerability of existing buildings (earthquake recordings and forced vibration) are inadequate both technically than financially, therefore can be used only on few case studies (Michel et al., 2010; Gallipoli et al., 2008). Ambient vibration tests represent a valuable alternative, since they were

demonstrated to be as accurate as active methods for the determination of vibrational modes parameters (Trifunac, 1975; Hans et al., 2005; Vidal et al., 2013 and references therein). The success of ambient noise analysis is due to their being a quick, efficient and inexpensive technique (Navarro and Oliveira, 2006), mostly because only a short duration of time series data may be needed to obtain stable results (Guéguen et al., 2014; Vidal et al., 2013). The time necessary to complete forced vibration tests is about five times longer than ambient vibrations experiments, and requires a lighter measuring equipment, a small team and therefore a reduced field effort (Trifunac, 1975). Which is more, ambient vibration tests can be performed at any time without interrupting the activities (factor that is extremely important when it comes to power plants) and are immediately ready for analysis and interpretation. On the other hand, due to the difficult testing conditions they are undertaken, AVTs requires special attention, controlling the test setup and accuracy in the analysis and interpretation of acquired data (Chen et al, 2014).

Ambient vibrations are recorded using three-components seismic stations. If the aim is to identify only the structural vibration modes, one instrument is enough; otherwise, if the goal is to evaluate modal shapes, estimate the damping factor or determine the values of drifts, several synchronized instruments should be used. The instruments should be installed in a vertical array at the centre of the building to detect the translational modes, with the sensors axes parallel to the longitudinal and transversal direction of the structure. To address the issue of torsional modes, instead, the vertical array of instruments should be placed far from the rotational axis (in a corner of the building, far from the centre). Torsional modes, produced by geometrical or mass/stiffness irregularities in plan or elevation, are especially important since they can origin an asymmetrical distribution of lateral loads, which is the main cause of heavy structural damage (Kotkar and Patankar, 2017).

For ambient vibration tests it is impossible to determine the input load, since, in contrast to forced vibrations and earthquakes recordings, the excitation is transmitted to the structure by external forces spread along the structure (wind), by the ground (seismic ambient noise) and by internal forces (human occupancy). That's the reason why those techniques are called output-only or operational modal analysis (OMA) or Noise Input Modal Analysis (NIMA) (Sevim B. et al., 2013; Brincker et al.,2003 ;Michel et al., 2008 and references

therein). Output only modal analysis works better in cases where boundary conditions plays a central role and where the loading level plays a central role (Brincker et al., 2003).

Ambient vibration tests only provide information about the linear elastic response of structures, because of the low level of excitation and consequently small deformations (Ivanović et al., 2000; Vidal et al., 2013). Anyhow, one of the major uncertainty in the assessment of seismic vulnerability of structures is to define their (even elastic) model. Which is more, ambient vibrations modal analysis methods provide an effective tool for short- and/or long-term monitoring of building health indicators, such as aging effects or after extreme events (Mikael, 2013). In fact, useful information for detecting and quantifying post-earthquake damage is the variation of elastic properties of the structure, therefore ambient vibration tests can contribute to the damage evaluation in the immediate after-event (Guéguen et al. 2014). Also when planning a monitoring system ambient vibration recordings can be useful to establish an upper bound for the frequency domain where the fundamental frequency is contained (Figure 11), making it is possible to use a limited domain for the interferometric analyses and for the S-Transform of the IRFs (Ponzo et al. 2012).

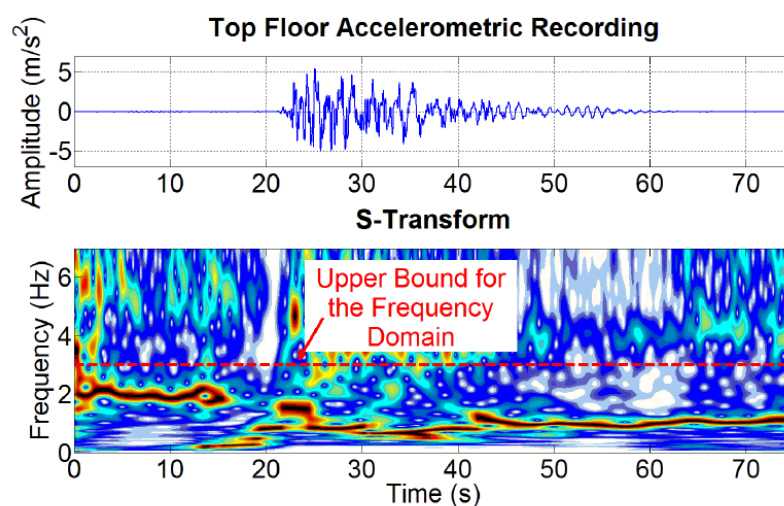


Figure 11 – Example of S-Transform of an accelerometric recording with the upper bound of the frequency domain highlighted, as reported in the work of Ponzo et al. (2012).



The ambient vibration data acquired can be analysed through several methods. Among the most common, there is the Peak Picking (PP) method, which consists in calculating the Fourier transforms of short time windows (several seconds) and picking the value of the frequency peaks of the average spectrum. Each peak provides a point of the modal shape, than normalised by dividing it by the value at the reference sensor; the fundamental one is defined by the lower frequency peak while higher frequencies are correlated to higher modes. This method gives accurate estimation of modal shapes only if the modes are well separated (Michel et al., 2008). An improvement of this method is the Frequency Domain Decomposition (FDD, Bricker et al. 2001) that consists of decomposing the power spectral density (PSD) matrices into single-degrees-of-freedom systems. The PSD matrices are the Fourier transforms of the correlation matrices between all the simultaneously recorded signals so that no a priori model is supposed (Michel et al., 2008 and references therein).

Techniques based on Fourier transform (Trifunac 2001) provide good results when the response of the system is stationary, but fail when the system exhibits a non-stationary, time-varying behaviour, as in the case of strong earthquake motion (Ponzo et al, 2012). In the field of non-stationary response, the S-Transform analysis (Stockwell et al.,1996) in the time-frequency domain shows a good resolution and offers a range of fundamental properties such as linearity and invertibility; Ponzo et al. (2012, and references herein) successfully use the S-Transform in combination with the interferometric analysis (see next subchapter 3.5).

The random decrement technique (RDT) has been shown to be useful in the determination of the damping of dynamic systems subject to unknown random excitation, such as microtremor vibration (Navarro and Oliveira, 2006). In the RDT, stacking a large number of windows with identical initial conditions, the impulse response of the structure is revealed, given that ambient vibrations remain stationary and contain a random and impulse element (Mikael et al., 2016 and references therein).

Gallipoli et al. (2009, and references therein) proposes a comparison on the results obtained through SSR (Standard Spectral Ratio; Parolai et al., 2005), HVSR (Horizontal to vertical Spectral Ratio; Nakamura 1989), NonPaDAn (Non Parametric Dynamic Analysis; Mucciarelli and Gallipoli 2007) and HBW (Half Bandwidth method), finding a substantial agreement

between them. Which is more, they found that the results obtained from those technique applied on ambient vibrations are comparable to the ones obtained from their application on small seismic events recordings. A slight decrease of the fundamental frequency in the latter case (small seismic events) is due to the fact that even during small amplitude earthquakes the soil and/or the buildings undergoes non-linear phenomena. Their conclusions are that SSR is found to be the most reliable method for assessing frequency, while NonPaDAn is preferable for the damping estimation. A simple method of modelling structural response to ground motions is to convolve the fundamental mode building response with a nearby reference recording of ground motion (Clinton, 2006).

### 3.5 Seismic Interferometry and Deconvolution

As seen in the previous chapters, the response of a building to a dynamic load depends on the properties of the structure and the coupling to the soil below it. Thus, in the structural monitoring one of the major issues is to separate the building response to a seismic action from that of the soil. In fact, the frequencies detected through experimental testing are dependant not only on the structure itself but also on soil-structure interactions. In particular, Şafak (1995) demonstrated that the dominant frequency recorded in a building subjected to SSI is always smaller than the dominant frequencies of the fixed-base building, and smaller of the one of the foundation without structure. Hence, the standard mode frequency estimation can be not appropriate for the monitoring of a structure without considering its environment – which is particularly important for dam structural damage identification.

Thus, the main advantage of the interferometric approach is the capability of removing the dependency on the source excitation and the effect of the ground coupling (Snieder and Şafak, 2006). In addition, this technique is the possibility to study the waves propagating between receivers without requiring a source at one of the receivers' locations: the response is independent of the excitation and it is irrelevant if the sources are coherent or incoherent (Snieder and Şafak, 2006). Hence, deconvolution interferometry can be used both on earthquake recordings and on ambient vibrations, although in the latter case results depend on radiation losses at the base of the building, because of the simultaneously action of several internal sources (Nakata and Snieder, 2014). It must be highlighted that the following formulation is valid assuming the response of the structure and foundation soil to be linear and time invariant. This is true when analysing ambient vibration recordings, whereas seismic events can cause variations in the dynamic properties both of the structure and of the ground, even if of moderate intensity and increasingly with the amplitudes of motion (Trifunac et al., 2001). Anyhow, to obtain stable deconvolved waveforms, a stacking

procedure is applied to the deconvolution computed, both in the case of earthquake recordings that for ambient vibrations, in order to reduce the noise to signal ratio.

The core of this method is the determination of the impulse response function (IRF) of the structure, getting in this way a useful insight on the spatial distribution of the wave field inside it, while on the other hand the vibrational approach analyses the soil-building system as a whole (Bindi et al., 2015). In fact, the transfer function is based on the Fourier transform but involves the ratio between waves recorded at different heights of the structure.

Through deconvolution interferometry, we can estimate the velocity of the waves that propagate inside the structure, based on the distinction among wave fields at different levels of the building (Nakata et al., 2013). In fact, we can easily deduce the velocity of shear waves inside the structure, a parameter that is linked to the dynamic characteristics of the building only (Snieder and Şafak, 2006; Bindi et al., 2015 and references therein).

We will now analyse in detail the basic concepts underneath the technique.

The transfer function of a linear system involves an input function  $f(t)$  and output function  $y(t)$ , where  $t$  stands for time. Since the system is linear, the differential equation can be described as a linear combination with constant coefficients:

Equation 2

$$a_n y^{(n)} + a_{n-1} y^{(n-1)} + \dots + a_0 y = f(t)$$

And Equation 2 can be easily solved through Fourier transform:

Equation 3

$$[a_n (i\omega)^n + a_{n-1} (i\omega)^{n-1} + \dots + a_0] \cdot Y(\omega) = F(\omega)$$

Where  $F(\omega)$  represents the Fourier transform of the input and  $Y(\omega)$  the Fourier transform of the output. We can so define as transfer function the following:

Equation 4

$$H(\omega) = \frac{Y(\omega)}{F(\omega)} = \frac{\text{output spectrum}}{\text{input spectrum}} = \frac{1}{a_n (i\omega)^n + a_{n-1} (i\omega)^{n-1} + \dots + a_0}$$

If we assume the structure to behave as a linear time invariant system for the entire or for a part of the seismic shaking,  $H(\omega)$  represents the system transfer function in the frequency

domain. Hence, it is possible to represent the system function in the time domain (i.e., the defined IRF) by computing the inverse Fourier transform of  $H(\omega)$

Equation 5

$$h(t) = F^{-1}(H(\omega))$$

Where  $F^{-1}$  is the inverse Fourier transform (Ponzo et al., 2012).

Assuming the station deployed on the top as a reference we can obtain information about the wave field propagated into the structure. On the other hand, if we assume the station at the bottom as a reference station, we can extract the IRF of the building (Figure 12) (Ponzo et al., 2012). In this way, the frequencies corresponding to all the peaks of the transfer function are oscillation frequencies of the system. (Di Marcantonio and Ditommaso, 2012). In the assessment of buildings, we usually take as a reference the measure performed in the basement; for different structures, such as dams, the bedrock layer close to the dam can be used instead.

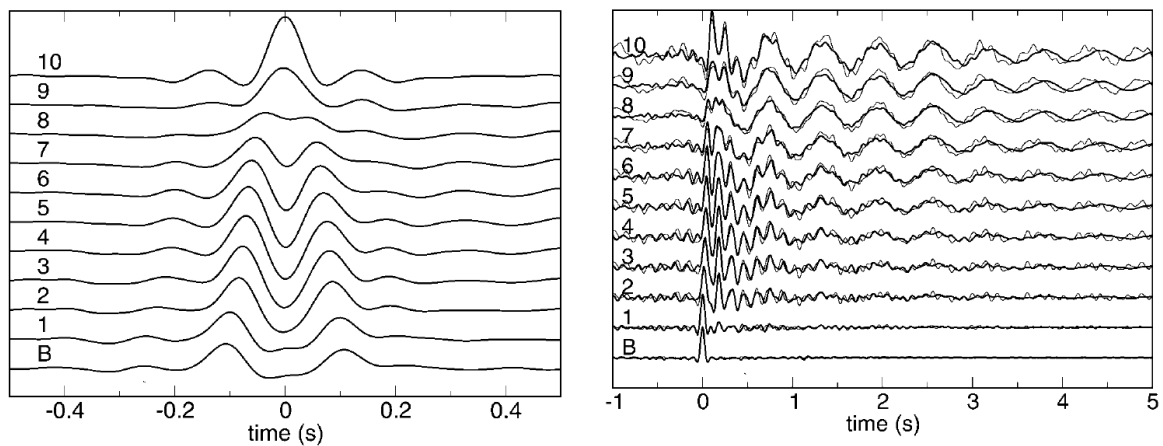


Figure 12 – Figure from the work of Snieder and Şafak (2006): wave field obtained using the station located at the top floor as reference (on the left) and Impulse Response Function obtained using the bottom as reference station.

With some hypothesis, through this technique it is possible to obtain the Green's function, which represents the wave propagation between two receivers installed at different levels of the structure (Lobkis and Weaver, 2001). It is important to recall that the IRFs are just a special case of Green functions, with zero initial conditions and a Dirac Delta (unit impulse function) as input.

It is known that a wave field generated by a generic source between two receivers A and B can be expressed in the frequency domain as the convolution between the Green's function  $G(t, \mathbf{x})$  and a source wavelet  $w(t)$  as (Wapenaar et al, 2010):

Equation 6

$$u(r_{AB}, t) = w(t)G(r_{AB}, t)$$

Deconvolution is therefore given by:

Equation 7

$$D(A, B) = \frac{u(r_A, s)}{u(r_B, s)} = \frac{w(t)G(r_A, s)}{w(t)G(r_B, s)} = \frac{G(r_A, s)}{G(r_B, s)} = \frac{G(r_A, s) G^*(r_B, s)}{|G(r_B, s)|^2}$$

and we can see how the source contribution is annulled in the expression above (Cao, 2016). Moreover, being the Green function a complex function, the operation in the last part of the equation above has the aim of having the modulus as denominator.

As stated before, in the time domain and considering the hypothesis of a time-invariant system, interferometry consists in the deconvolution of the signal  $u(z_B, t)$ , recorded at a reference location, from the signal  $u(z_A, t)$ , recorded at a generic location. Being interested in the wave field, it is preferable to express the deconvolution in the Fourier domain. According to Snieder and Şafak (2006), deconvolution as a function of the angular frequency ( $\omega = 2\pi f$ ) can be written as:

Equation 8

$$D(\omega) = \frac{U(z_A, \omega)}{U(z_B, \omega)}$$

where  $U(\omega)$  represents the Fourier transform of the signal  $u(t)$ .

In this approach, a regularization parameter  $\varepsilon$  is introduced to control the degree of filtering applied to the spectral ratio in order to stabilize the Impulse Response Function (Bindi et al., 2015). In fact, the function would become unstable close to the notches in the spectrum relative to  $(z, t)$ , since the denominator goes to zero (Snieder and Şafak, 2006). The  $\varepsilon$  parameter is a positive number whose value determines the degree of filtering applied to the solution: increased values of  $\varepsilon$  reduce the effect of numeric instabilities, increase the smoothness of the solution, but on the other hand decrease the spatial resolution of the solution (Ponzo et al., 2012). The above expression for deconvolution becomes therefore:

Equation 9

$$D(\omega) = \frac{U^*(z_B, \omega)}{|U^*(z_B, \omega)|^2 + \varepsilon} U(z_A, \omega)$$

Following the work of Snieder and Şafak (2006), the deconvolution of the motion recorded at a generic height ( $z$ ), with respect to the motion recorded at the highest floor ( $z = H$ ) can be expressed as:

Equation 10

$$T(z, \omega) = \frac{u(z, \omega)}{u(z = H, \omega)} = \frac{1}{2} [e^{ik(z-H)} e^{-\gamma|k|(z-H)} + e^{ik(H-z)} e^{-\gamma|k|(H-z)}]$$

Where  $k$  is the wave number =  $\omega/c$ ,  $c$  is the shear wave velocity of the building, and  $\gamma$  the viscous damping. In this equation,  $T(z, \omega)$  describes the response of the system when a virtual source is acting at the top of the building at  $t = 0$ . The first term describes an a-causal up-going wave ( $t < 0$ ), the second term the causal down-going wave ( $t > 0$ ). As derived above in this subchapter, we underline once more that  $T(z, \omega)$  is independent from the reflection coefficient at the base of the structure, and therefore independent from the coupling with soil.

As stated above, The IRFs in the time domain are used to estimate the average shear wave velocity by measuring the observed time delay  $\tau$  between the a-causal and causal pulses: the average velocity between the height  $z$  and the top is given by  $\beta = D/\tau = 2(H - z)/\tau$ . The delay time, in fact, represents the time shear waves require to propagate once up and once down the building (Snieder and Şafak 2006).

It is known, from the theory on wave propagations, that the shear wave velocity can be expressed as:

Equation 11

$$c = \sqrt{\frac{\mu}{\rho}}$$

Where  $\mu$  represents the shear modulus while  $\rho$  the mass density of the structure. Being  $c$  related to the structural stiffness, if damage occurs, it would imply a reduction of stiffness and therefore a lower wave velocity. In this way, seismic interferometry can be useful to detect possible structural damage. In fact, Clinton et al. (2006) demonstrated that there is a

logarithmic correlation between frequency reduction and maximum recorded acceleration. As seen above in this chapter, ambient vibration and forced vibration tests can be used for the estimation of modal frequencies of a building and modal frequencies temporarily or permanently decrease when an earthquake hit the structure, representing a reliable indicator of damage occurrence. Actually, it is widely known that natural frequencies are proportional to the square root of the stiffness, and inversely proportional to the square root of the mass. If the mass of the structural system does not change considerably (as usually does not in the comparison between before and after a seismic event), a variation in the natural frequency corresponds to a major stiffness decrease (Clinton et al. 2006).

Following the work of Snieder and Şafak (2006), there are two ways of interpreting the deconvolved response of a structure: as a superposition of waves, as seen above, or as a superposition of modes. It should be highlighted that the normal modes of a structure depend also on the coupling with the foundation soil; thus, the modes obtained through deconvolution are not the normal modes of the building, as they depends merely on the structure. Anyhow, always considering the model of a cantilevered shear-beam, the relation between the shear wave velocity and the period of the structure can be written as:

*Equation 12*

$$T_0 = \frac{4H}{c}$$

It should be noticed that a shear wave propagates inside the structure (up and down) twice in the period  $T_0$ , with a double change of polarity.

To extract information on the fundamental mode without the contamination of higher modes, a band-pass filter centred on the frequency of interest can be applied (Ponzo et al., 2012).

When propagating inside the structure, seismic waves attenuate due to radiation losses at the basement and intrinsic attenuation, but the deconvolved wave field is not subject to radiation losses. Therefore, the wave field decay in time only depending on intrinsic damping of the structure (Snieder and Şafak 2006). From the IRF we can easily retrieve information about the equivalent viscous damping factor applying the logarithm decrement method on the waveform at the top floor (Ponzo et al., 2012). The asymmetry between the causal and



a-causal IRF can be used for the estimation of intrinsic attenuation (Newton and Snieder, 2012).

Being the damping coefficient  $\gamma$  dependent on the quality factor  $Q_s$  through the expression:  $\gamma = 1/2Q_s$  (Snieder and Şafak 2006), the ratio between the amplitudes of causal and a-causal pulses,  $A^+$  and  $A^-$  respectively, is used, in the effective bandwidth  $\omega_{eff}$ , for the estimation of the quality factor as follows (Snieder and Şafak 2006, Bindi et al., 2015):

*Equation 13*

$$\frac{1}{2Q} = \frac{\ln(A^-/A^+)}{\omega_{eff} \tau}$$

In chapter 4, these methods will be applied to the case study: a dam located in Central Italy.

## 4 Case study: a Dam in Central Italy

The selected case study is a concrete arch-gravity dam located in central Italy. The structure is monolithic, without any expansion joint, and the crest is at 870.0 m on sea level height. The crest is 6 meters wide, while the bottom section is 40 meters large (see Figure 13). The dam's height is of 55.5 meters, with a reservoir maximum capacity of 12.5 Mm<sup>3</sup>. The inclination of the upstream side of the wall is of the 4%, while the downstream one has a 70% inclination up to 854.5 m level and then goes almost vertical to the top. There are three longitudinal inspection tunnels (at 824.3, 846.3 and 865.5 meters on the average sea level).

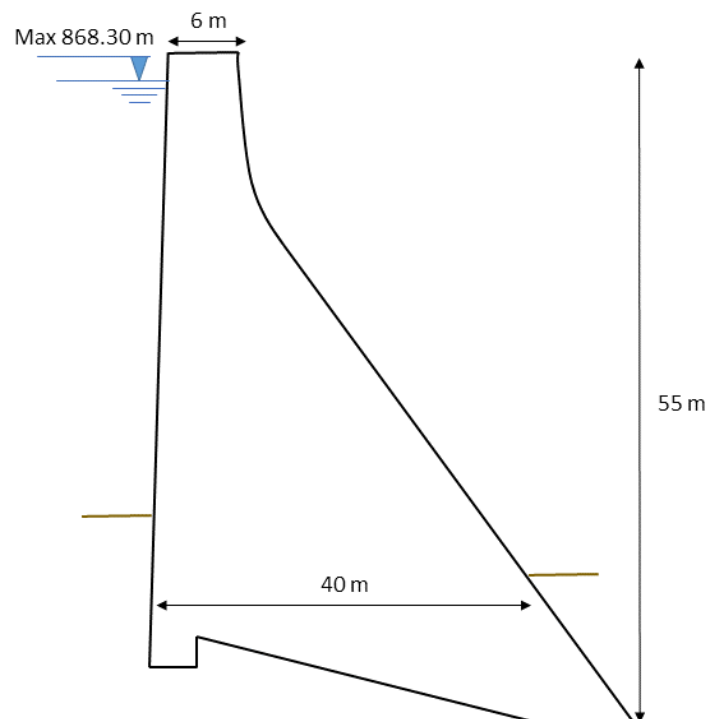


Figure 13 – geometry of the central transversal section of the dam

On the dam several survey campaigns were performed in different time periods (see Table 2). Unfortunately, the experimental tests on the dam were performed by several actors in various time periods, disparate instruments, different array configurations, for different purposes and – especially – with variations in reservoir water level. In this chapter, the results of those different kind of tests are reported, while in the next chapter they are discussed and compared.

Two dynamic forced vibrations tests were performed in the past (July 1988 and May 1993), on the basis of which a finite element model was developed. In 2015 I performed an ambient vibration survey, together with an OGS team, with tri-axial digital high resolution tromographs (Tromino, Moho®).

After this field campaign, one year later, the Central Italy earthquake of the 24th August 2016 happened and hit the structure, causing non-structural damage. Visible damage to the parapet of the crest and of the control cabin were reported. Moreover, visible cracks on the crest were described, but only involving the road pavement and not the structure behind it.

Soon after, in December 2016, the Civil Defence Department repeated the ambient vibration tests on the dam. These test preceded the installation of a permanent dynamic monitoring system (installed in February 2017), part of the Seismic Observatory for Structures (*Osservatorio Sismico delle Strutture*). The monitoring system recorded five seismic events (listed in Table 3), which are analysed in this thesis using deconvolution interferometry. The results obtained after the earthquake are compared with those of the surveys performed before.

As already stated in Chapter 2, the estimation of dynamic response of the dam to loads is quite complicated, as it depends on several factors, such as design input, reservoir water level, interaction with the foundation and through the foundation and the soil (Calcina et al., 2014). The survey campaigns were performed in different periods of the year and with different water levels of the reservoir, as summarized in Table 2. In the following subchapters the results of those different surveys are exposed and compared.

Table 2 – list of surveys perform and the date in which they were performed; reservoir water level at the time of the surveys performed on the dam [meters above sea level]

Tests	Date (DD/MM/YYYY)	Reservoir level [m.a.s.l.]
Forced vibration tests	07/1988	866
Forced vibration tests	05/1993	865.3
Vibration tests (before earthquake)	02/07/2015	867
Vibration tests (after earthquake)	15/12/2016	849.6
Permanent monitoring	19/02/2017	
Maximum reservoir lever	-	863.3

Table 3 – list of earthquakes recorded by the monitoring system installed on the dam in February 2017

Date and time [UTC]	Mw	Depth	Lat	Long
2017/02/20	3.9	11	42.5	13.26
2017/06/29 21:41	3.5	11	42.64	13.21
2017/06/30 00:25	3.8	12	42.63	13.21
2017/07/01 19:17	3.6	8	42.65	13.32
2017/07/22 02:13	4.0	13	42.57	13.33

## 4.1 Forced vibration tests

Two dynamic forced vibrations survey campaigns were performed on the dam in the past (July 1988 and May 1993). The survey were performed with a reservoir water level at 866,00 m.a.s.l. and 865,30 m.a.s.l. respectively (see Table 2).

The report signed by the engineers who performed the tests states that data processing highlighted difficulty in the interpretation, showing a non-linear dynamic behaviour and significant dissipative phenomena. The transfer functions they calculated showed maximum amplification not enough evident, and differences in the phases could be noticed, which were interpreted as possible material discontinuities in the longitudinal direction. Moreover, damping values associated with the first vibrational were quite high (8-10%), confirming important dissipative phenomena. Anyhow, surveys allowed identifying the range of the first three fundamental modes (listed in Table 4) and the corresponding deformed shapes, which are displayed in Figure 14. The first forced vibration campaign, in 1988, had identified also the fourth and fifth modal frequencies, but not the corresponding modal shapes. Therefore, in Table 4 only the results related to the first three modal frequencies identified by the second vibration test (1993) are reported.

Table 4 – modal frequencies [Hz] identified through ambient vibration tests.

	Frequency 1 <sup>st</sup> mode	Frequency 2 <sup>nd</sup> mode	Frequency 3 <sup>rd</sup> mode
Medium	5.1	6.8	9.1
Mininum	4.8	6.3	8.8
Maximum	5.5	7.3	9.4

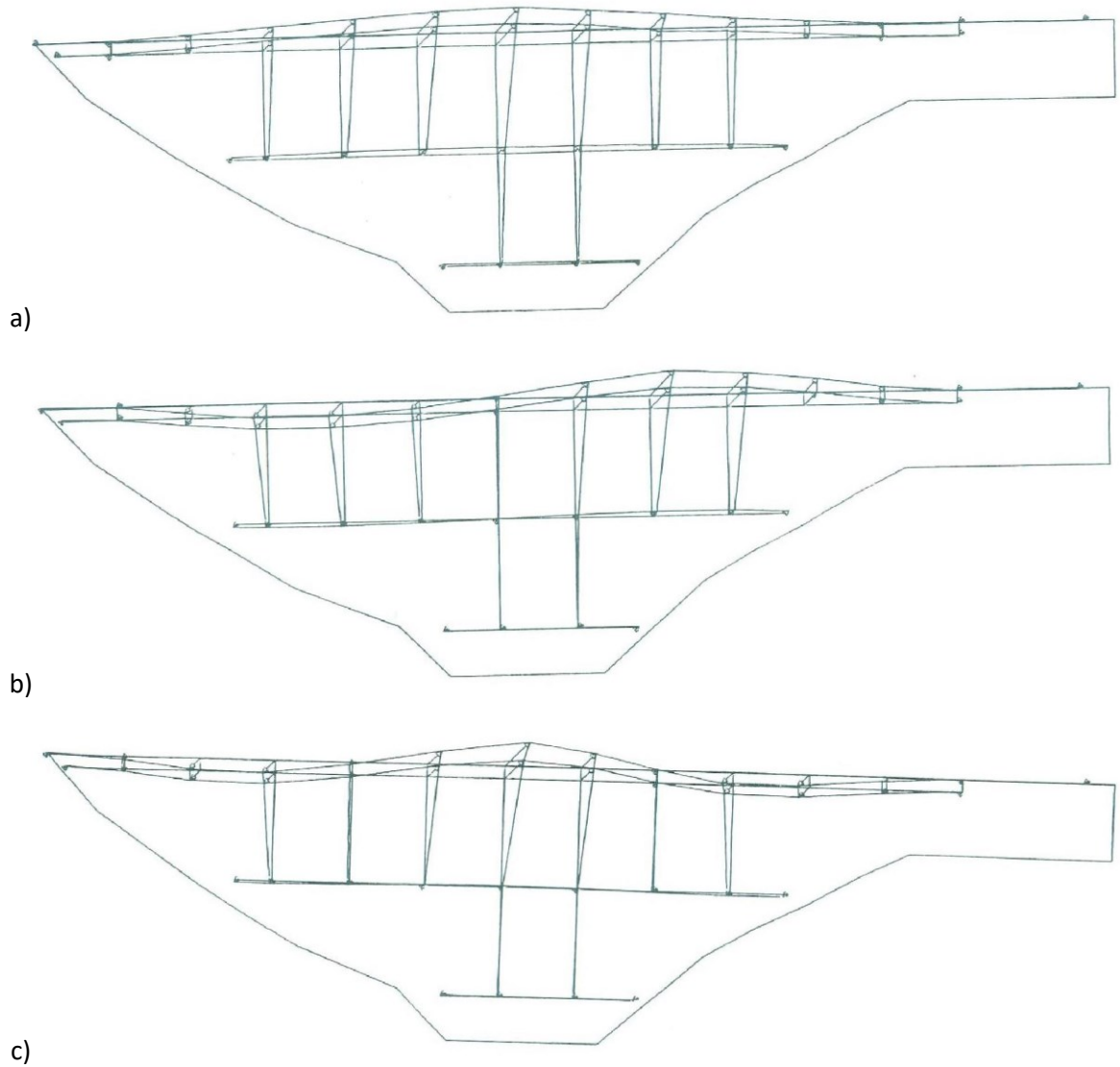


Figure 14 – modal shape identified through forced vibrations test: a) 1<sup>st</sup> mode (around 5.1 Hz); b) 2<sup>nd</sup> mode (around 6.8 Hz); c) 3<sup>rd</sup> mode (around 9.1 Hz). The deformed shape of the first and third mode are symmetric, while the one of the second mode is anti-symmetric.

## 4.2 Ambient vibration tests before the earthquake

In the 2015 (before the earthquake), I performed, together with an OGS team, an ambient vibration test on the dam.

We installed the sensors in 7 points on the crest and inside the three internal tunnels, as shown in **Figure 15**. All the measures were referred to the one made on a bedrock outcrop at the side of the dam. The measures were executed on a short time (4 hours) in order to avoid changing in the conditions throughout the testing period.

Unfortunately, we had only three Tromino stations available, two of which without the GPS antenna. Hence, measures were not synchronized. Though, all the measures have been referred to an ambient vibration measure on bedrock or free-field and the SSR analysis were performed on simultaneous time windows (although without the GPS time reference). Nevertheless, we can perform anyway the SSR analysis on the data, since the transfer function is calculated using the average among several time windows, and assuming the ambient vibration field to be stationary in a short time period.

Ambient vibrations were recorded for 12 minutes on the structures and 30 minutes on free-field soil, at a sampling rate of 128 Hz. In the analysis, the smoothing was fixed to 3% for the measures on structures, 10% for those on free-field soil.

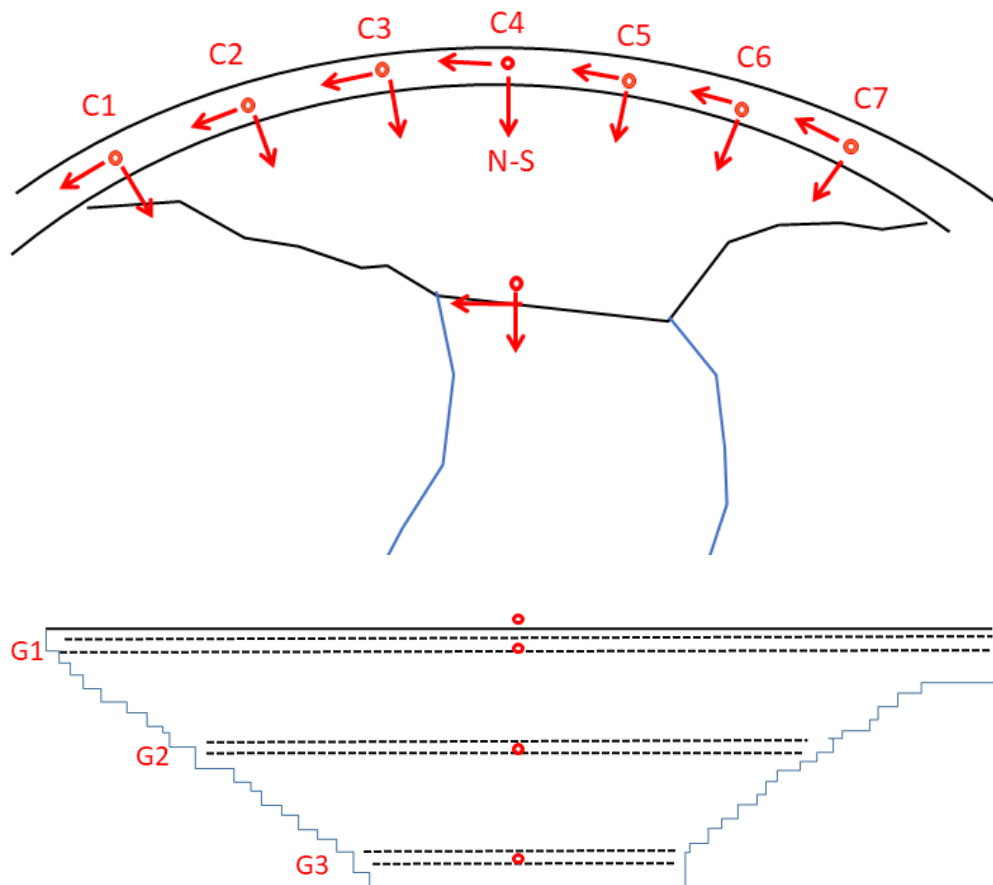


Figure 15 – Dam planimetry (a) and front view (b) with test sites locations.

The HVSR curve on the bedrock outcrop close to the dam (Figure 16, panel a) is flat, as expected. The three component spectra showed in Figure 16 panel b) highlighted instead some peaks at 6.5 Hz on all the three components, that is the reason why the peak can't be found on the HVSR curve. In fact, since the HVSR technique comprises the ratio among the horizontal and vertical components, a peak that is present on all the components will not be present on the HVSR curve. A peak on all the three components of the motion is usually attributable to an artificial interference. Moreover, it is clear that the curve is not reliable below the frequency of 1.5 Hz, where only instrumental noise can be found. Also after 20 Hz the curve is not significant. Therefore, the only part of the curve that can be interpreted is between 1.5 and 20 Hz. The H/V stability diagram (Figure 16, panel c) does not show any interference, therefore no windows selection had to be performed.

In view of these results, the noise source acting on the dam can not be considered as white excitation. Therefore, it comes to the necessity of separating the response of the dam from



that of the soil behind it. This was done with the SSR technique (Standard Spectral Ratio) and will be done with the deconvolution technique in the following subchapters.

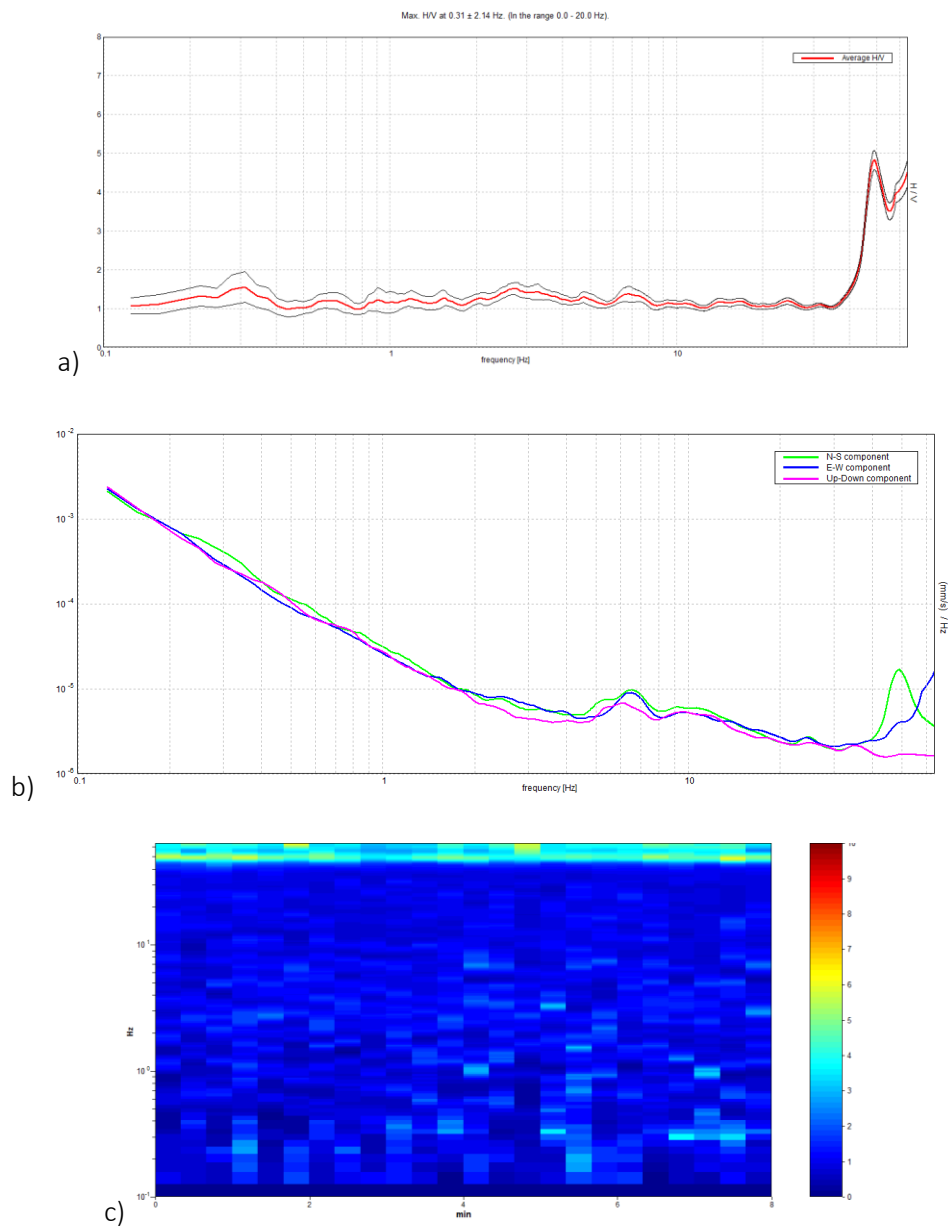


Figure 16 – a) H/VSR on the bedrock reference (AR site); b) three component spectra diagram on the bedrock testing site (AR); c) H/V stability bedrock testing site (AR).

In Figure 17 the SSR curves for all the testing site on the crest are displayed. The SSR analysis of the measures performed on the crest of the dam shows clear amplifications on the horizontal N-S component around 4.8, 6.9 and 8.7 Hz (Figure 17, panel a). At 7 Hz frequency we can find also amplifications on the vertical component (Figure 17, panel c), verifying the hypothesis of this being a structural rocking vibrational mode. It can be noticed that in the transversal direction (i.e. tangential to the crest curvature) the dam is very stiff and, as expected, there is no amplification on the SSR curves (Figure 17, panel b).

The amplifications displayed on Figure 17 are to be considered as qualitative and not quantitative. Moreover, since the measures were not synchronized because the instruments used didn't have the GPS, the information about the phases is lost. It is hence impossible to retrieve the deformation shapes from these results.

In the following figures (Figure 18 to Figure 22) the SSR curves are displayed separately in order to highlight their characteristics. It is possible to notice that only the testing sites AC2 and AC3 (Figure 18 and Figure 19) show an amplification of the vertical component for the second mode, which can be linked to a rocking phenomena of the structure.

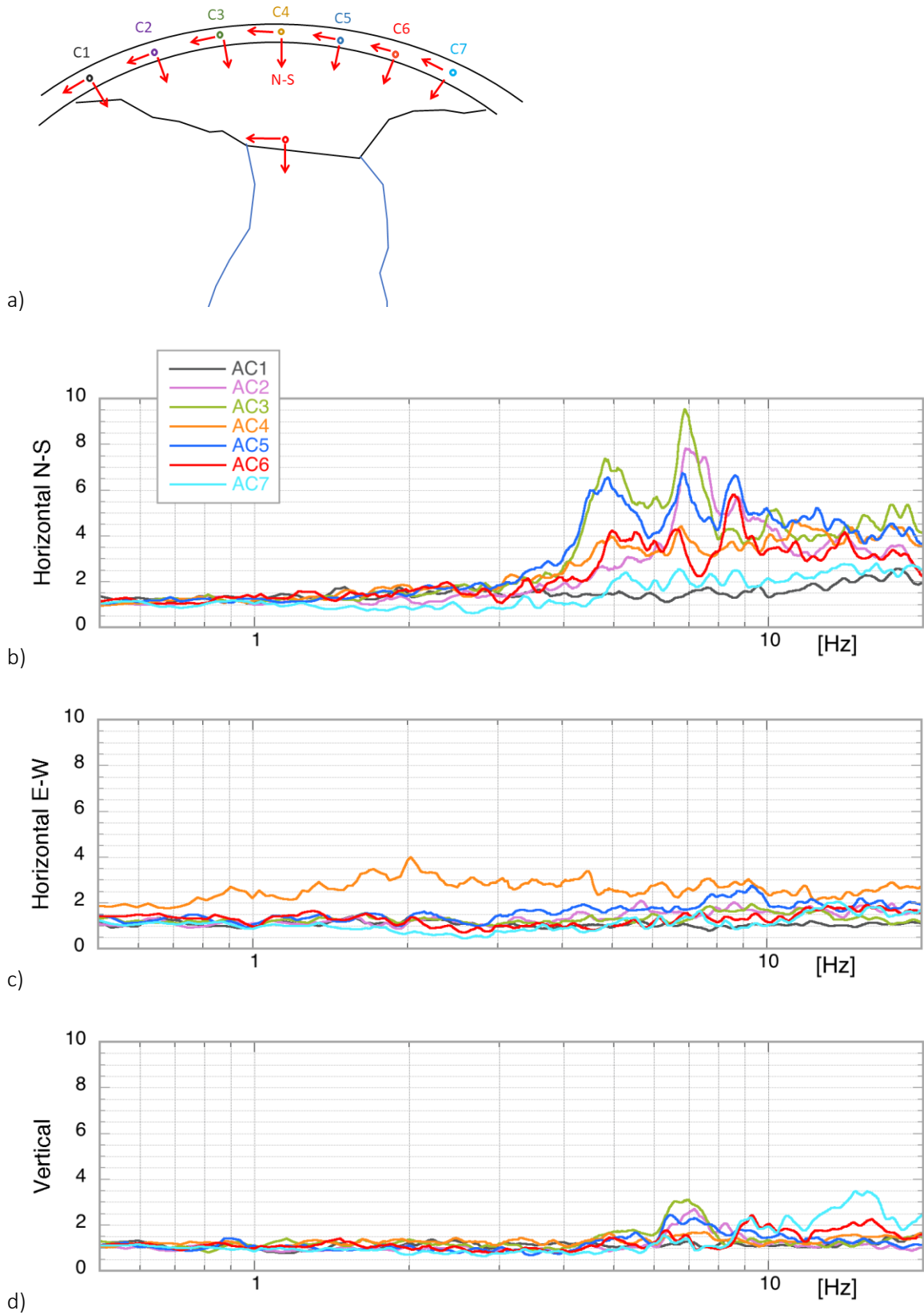


Figure 17 – Standard Spectral Ratios in the three components, for testing sites on the crest, related to the bedrock measure. Measuring points are reported in panel a); panel b), c) and d) relate to N-S, E-W and vertical directions respectively.

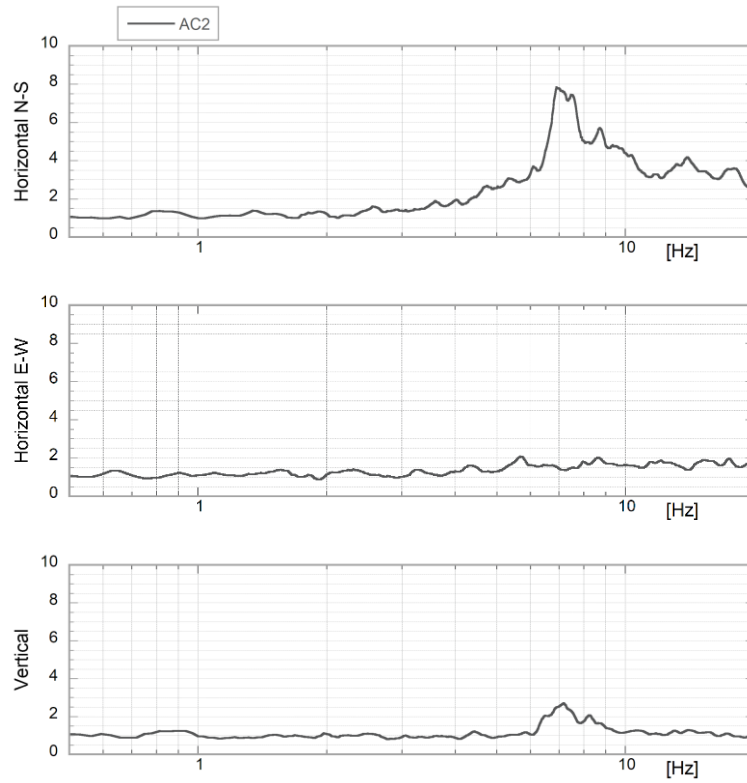


Figure 18 - Standard Spectral Ratios in the three components (N-S, E-W and vertical), for testing site AC2 on the crest, related to the bedrock measure.

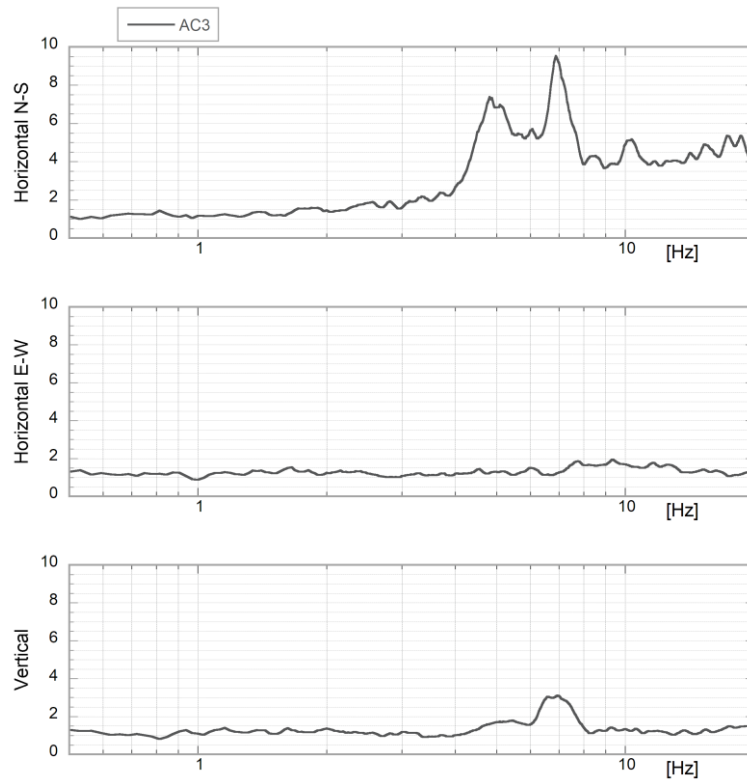


Figure 19 - Standard Spectral Ratios in the three components (N-S, E-W and vertical), for testing site AC3 on the crest, related to the bedrock measure.

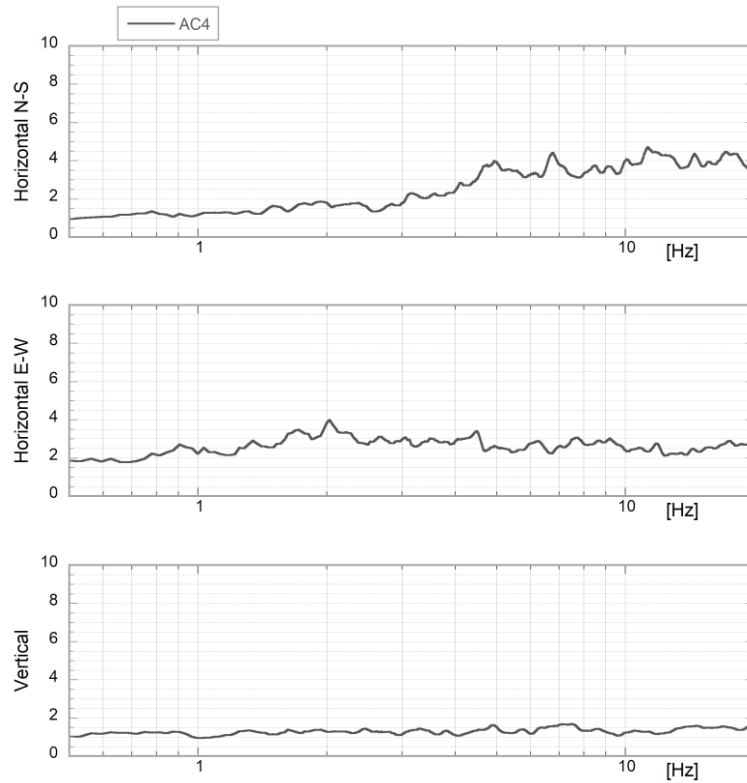


Figure 20 - Standard Spectral Ratios in the three components (N-S, E-W and vertical), for testing site AC4 on the crest, related to the bedrock measure.

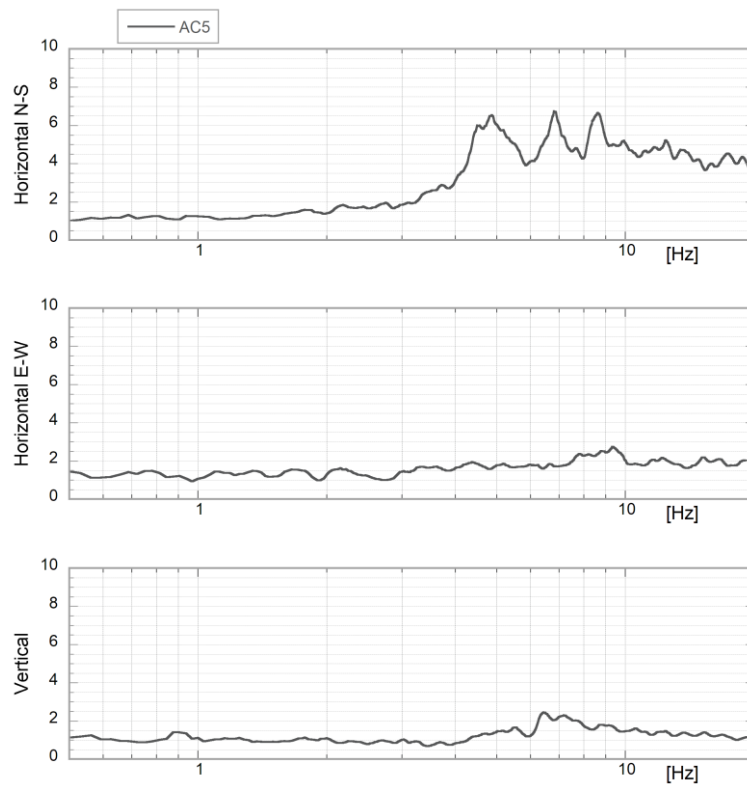


Figure 21- Standard Spectral Ratios in the three components (N-S, E-W and vertical), for testing site AC5 on the crest, related to the bedrock measure.

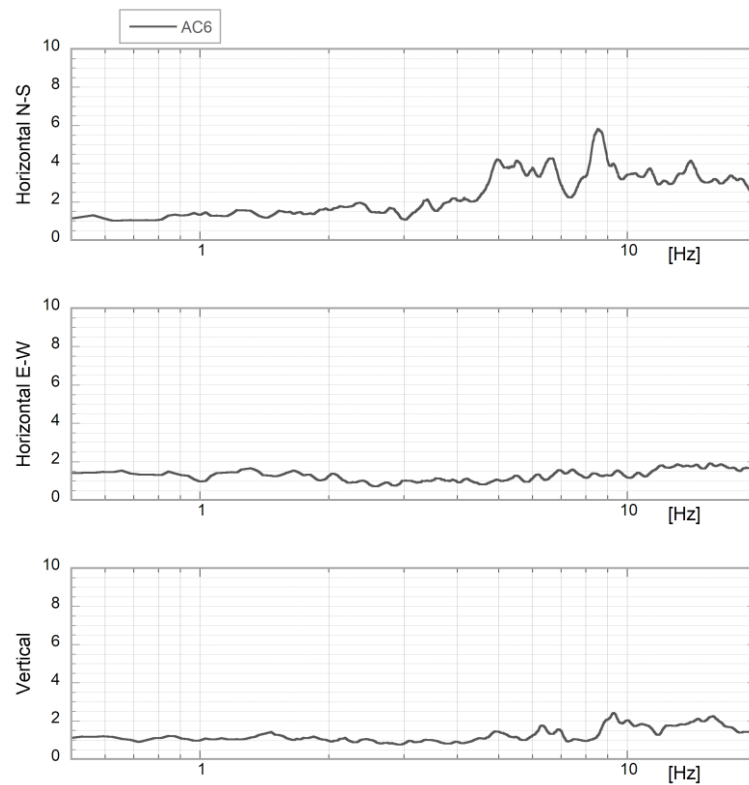


Figure 22- Standard Spectral Ratios in the three components (N-S, E-W and vertical), for testing site AC6 on the crest, related to the bedrock measure.

The main frequency identified has been compared to the one obtained from Equation 14 proposed by Priscu et al. (1985) for the estimation of the fundamental mode frequency of an arch dam assuming a full reservoir condition:

Equation 14

$$f_0 = \frac{1}{0.1 + 0.2 \left( \frac{H}{100} \right)}$$

where  $f$  is the natural fundamental frequency and  $H$  the dam height (meters). According to this formula, the theoretical fundamental frequency of the dam, if it was considered as an arch dam, is equal to 5.2 Hz. According to ambient vibration tests, instead, the main frequency results equal to 4.8 Hz. The (slight) difference between the theoretical and experimental frequency values can be explained considering the structure is a mixed arch-gravity structure and possible aging effects. Moreover, the equation neglects the crest length and thickness and the water level of the reservoir that, as we saw above, is a very

important in the frequency identification (Calcina et al., 2014). Anyhow, these values are in a good agreement with those obtained by the forced vibration tests, considering the errors that are always associated to the measures.

*Table 5 – frequencies [Hz] identified through ambient vibration tests on the dam and comparison with the one obtained by Equation 14 for the first mode frequency estimation*

	Frequency 1 <sup>st</sup> mode	Frequency 2 <sup>nd</sup> mode	Frequency 3 <sup>rd</sup> mode
Frequency	4.8	6.9	8.7
Theoretical	5.2	-	-

It is important to highlight that ambient vibration tests should be performed frequently, in order to highlight possible changes in the structural behaviour, necessarily under the same conditions. In fact, test results can be strongly affected by changes in the boundary conditions, such as: air and water temperature, water level, pore pressure and uplift, rock deformability (De Sortis and Paoliani, 2005). Hence, monitoring should be performed continuously, and this is the main advantage of using ambient vibration noise recordings. In fact, other type of analysis, such as those using forced vibration or earthquakes recordings, can not be performed continuously, since they depend on the presence of the source (artificial or natural, respectively).

During the several case studies exposed in this chapter, the level of the reservoir underwent little changes, as listed in Table 2. As already stated, the reservoir water level is the boundary condition that majorly influences the analysis results. This aspect will be addressed in the discussion and comparison of results, in chapter 5.

### 4.3 Ambient vibration tests after the earthquake

After the 2016 Central Italy earthquake, the Italian Civil Defence Department (Seismic Monitoring Territorial Service – *Servizio Monitoraggio Sismico del Territorio* - MOT) together with the Italian Ministry of Infrastructures and Transportation (M.I.T. - Central Dam Management – *Direzione Generale per le Dighe*) went on the same dam to perform ambient vibration tests again. This survey was done on the 15<sup>th</sup> December 2016, approximately one year later than the previous ambient vibration tests. The aim was to identify the vibrational modes of the structure and eventually their variations after the earthquake that hit it causing non-structural damage. Visible damage to the parapet of the crest and of the control cabin were reported. Moreover, visible cracks on the crest were described, but only involving the road pavement and not the structure behind it.

The dynamic characterization of the structure preceded the installation of a permanent dynamic monitoring system, installed in February 2017, which became part of the Seismic Observatory for Structures (OSS – *Osservatorio Sismico delle Strutture*). In this subchapter, I summarize the main results of the report provided by the Civil Defence Department. Those results will be used only as a comparison with the analysis performed in this work.

During the test, the level of the reservoir was at 849.06 m above sea level (see Table 2).

For these tests, 15 velocimeters LE-3Dlite (own frequency 1 Hz) connected to digital seismic recorder MARSlite MO, from Lennartz Electronic, were used. LE-3Dlite sensors are compact high performance instruments, in the three seismometric components.

Figure 23 shows the position and the direction of the installed sensors. The North axis was oriented in the radial direction of the dam's crest.



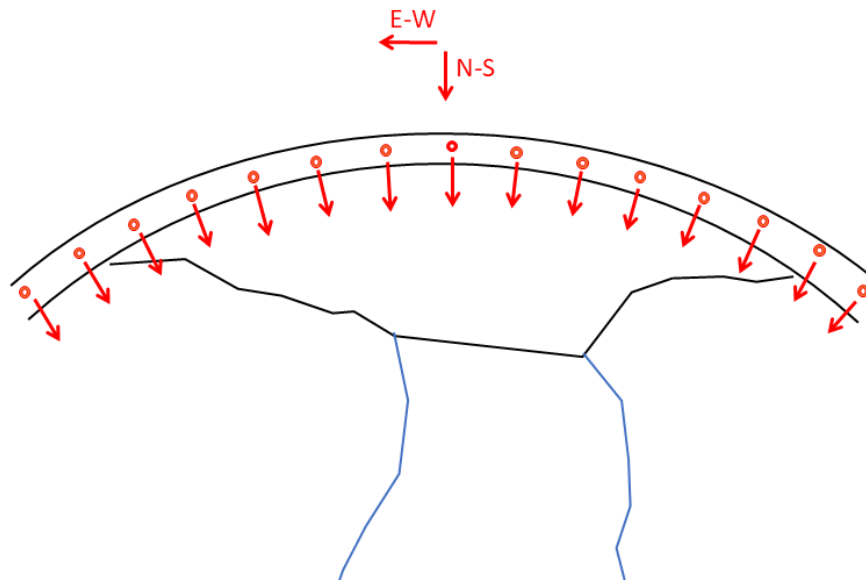
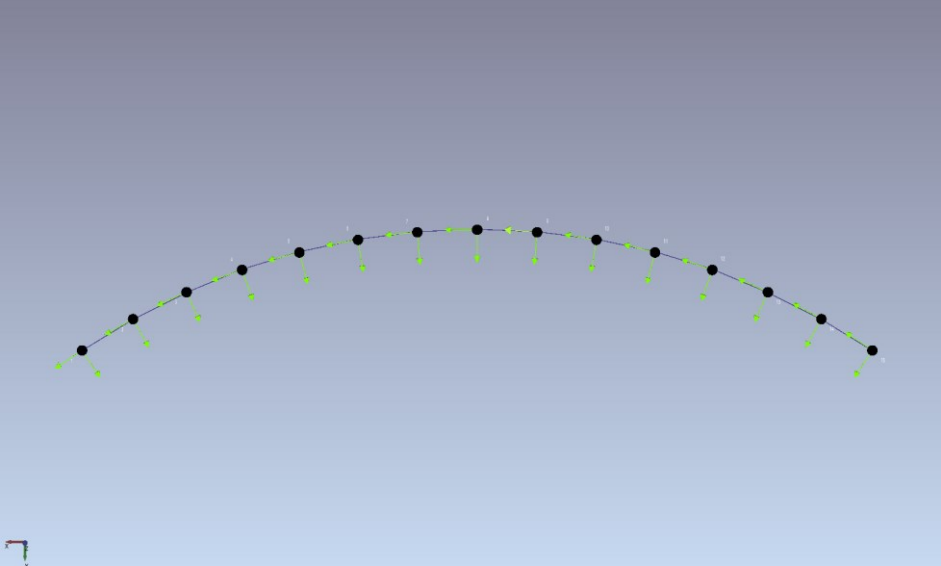


Figure 23 – sensors configuration for the ambient vibration tests performed in 2016, after the earthquake hit the structure. Each sensor was directed in the radial direction; before the analysis, data were rotated to be directed in the upstream-downstream direction, as the sensor at the centre of the crest.

A two-dimensional numerical model was created, in which at each joint were assigned the dynamical components measured. Table 6 shows the coordinates and the geometry of the model.

Table 6 – sensors position and model definition

Sensor	X	Y
A 112	83.87	25.64
A 106	73.04	18.98
A 101	61.69	13.27
A 108	49.89	8.54
A 107	37.73	4.82
A 104	25.31	2.15
A 114	12.70	0.54
A 111	0.00	0.00
A 109	-12.70	0.54
A 113	-25.31	2.15
A 103	-37.73	4.82
A 105	-49.89	8.54
A 110	-61.69	13.27
A 102	-73.04	18.98
A 100	-83.87	25.64



The tests performed are based on the ambient vibrations recordings. The recording started at 12:00:00 UTC for a two hours time period with a sampling frequency of 200 Hz.

The vibrational model of the structure identification, in terms of frequencies and modal shapes, was performed using the ARTEMIS software, applying the CFDD procedure, Curve-fitting Frequency Domain Decomposition (Jacobsen et al., 2008). As all the methods of the Operational Modal Analysis, the technique would be not dependant on the source applied on the structure if we assume this source as white noise. On the contrary, as seen through the spectra recorded on a reference station in the previous subchapter, the source signal is often not a white excitation. Therefore, it is important to apply techniques which are able to separate the contribution of the structure itself from that of the soil and of the source, as the deconvolution method exposed in the subchapter 3.5 and applied in the next subchapter to our case study.

In

Figure 24, the spectral density matrix in the frequency domain is shown. From these spectra we can identify the range of frequency of interest in this specific case study, and we can measure the frequencies of the first three peaks, corresponding to the first three modes, to be compared to those obtained through the first ambient vibrations survey in 2015 and to the results of the FEM model calibrated through the forced vibration test results. The power spectral density is displayed in the three directions, North-South (blue curve, upstream-downstream direction), East-West (red curve, in the tangential direction) and vertical spectral (green curve). The significant differences in the amplitudes showed by the three spectra confirms that the tangential direction is much stiffer than the upstream-downstream direction, and the two are anyway presenting much higher amplifications than the vertical one. Only for the second mode frequency (6.9 Hz) an amplification on the vertical component can be detected, suggesting a potential rocking component.

Those results support the choice of ignoring the tangential direction in the deconvolution interferometric analysis that will be exposed in the next subchapter. This assumption is essential for the application of the method, that is formulated only for a clamped shear beam model. I will discuss this issue in chapter 5.

Singular Values of Spectral Densities of All Test Setups

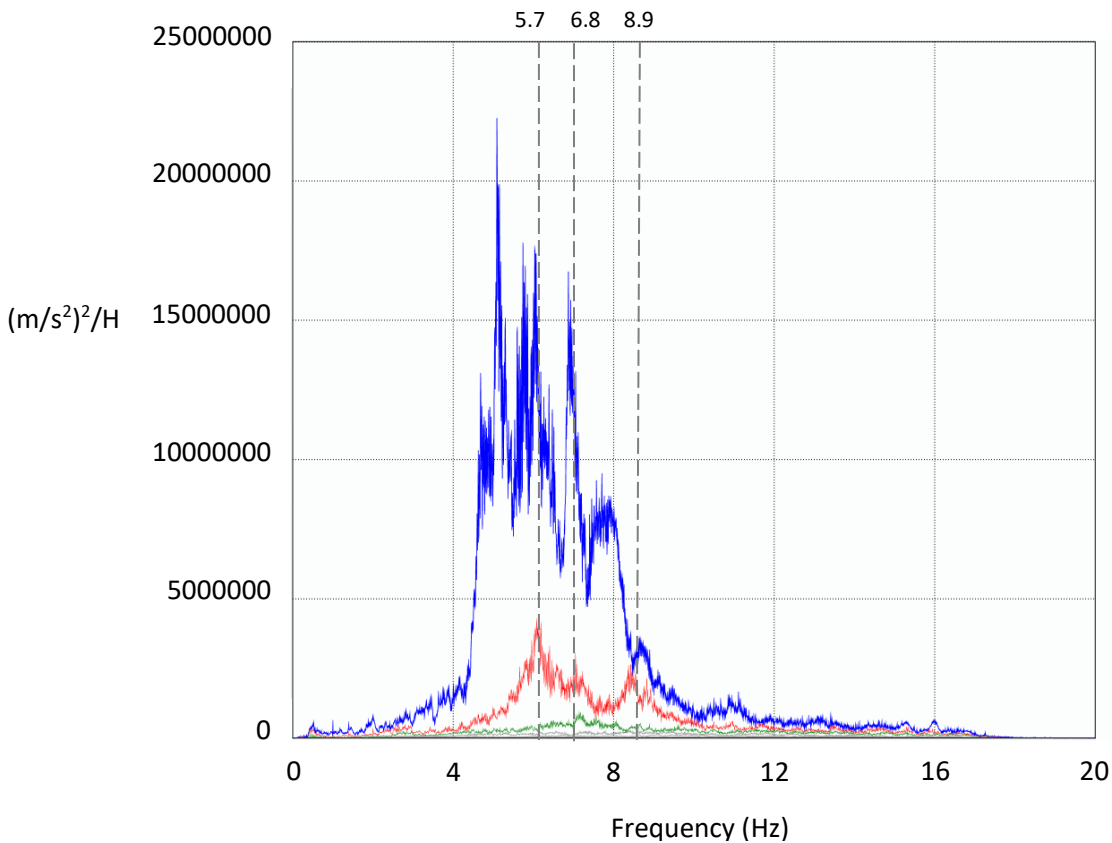


Figure 24 – Spectral density matrix in the frequency domain determined by ambient vibration tests after the earthquake; the blue line is the North-South direction, the red one the East-West and the green one the vertical direction. As can be noticed (and as could be expected), the main amplifications are on the North-South component, while the East-West component presents much lower amplifications and the vertical component almost no amplification. The only exception is the 6.9 frequency that shows amplification also on the vertical component, indicating a probable rocking motion. The power spectral density is also useful to see what is the range of frequencies of interest in the specific case.

Table 7 – modal frequencies identified by the ambient vibration tests after the earthquake. We recall that in this case the level of water reservoir was 17 meters lower than the previous ambient vibration tests.

	Frequency 1 <sup>st</sup> mode	Frequency 2 <sup>nd</sup> mode	Frequency 3 <sup>rd</sup> mode
Frequency	5.7	6.9	8.9

The identified modal shapes are represented in Figure 25. From this figure it is possible to see that the first and the third mode show a symmetric modal shape, while the second mode is anti-symmetric. All the modal shapes highlight higher deformation on the down-river right side of the dam, which was also the part that suffered non-structural damage after the 2016

earthquake. This behavioural asymmetry could not be detected by the ambient vibration tests, since (by chance) the vibrational source was applied on the other side of the dam.

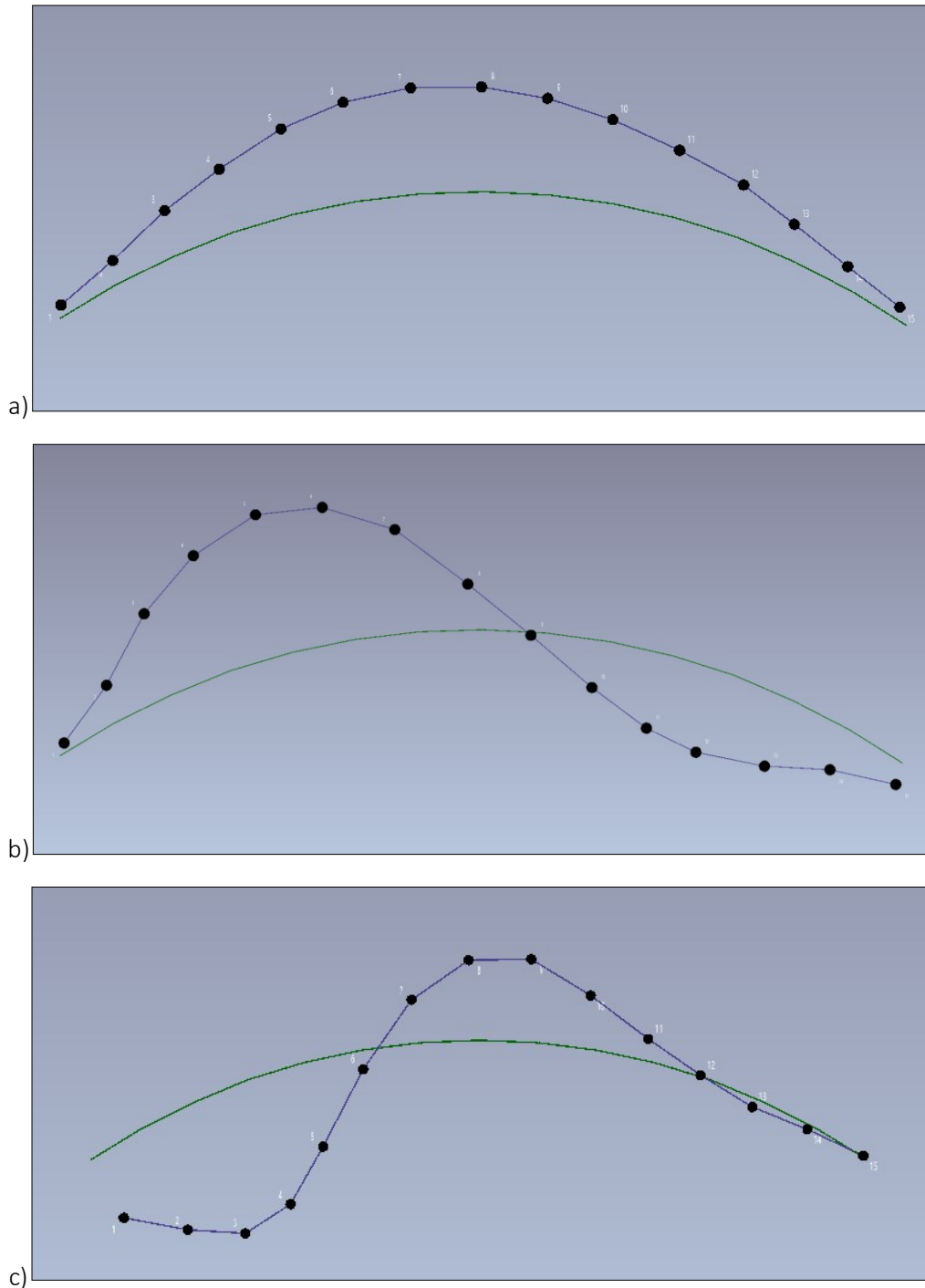


Figure 25 - Modal shape identified by the ambient vibration tests after the earthquake. Black dots line represents the displacement from the undeformed shape (green line) per each sensor. Panel a) 1st Mode - 5.737 Hz ; Panel b) 2nd Mode - 6.87 Hz; Panel c) 3rd Mode - 8.896 Hz. It is evident how the downriver-right side of the dam show major deformability. This is actually the side of the dam that showed non-structural damage after the 2016 earthquake.

To verify the reliability of obtained results, the MAC (Modal Assurance Criterion) numbers were calculated. Modal Assurance Criterion (MAC) (Allemang and Brown, 1982) is a statistical parameter for the investigation of the correlation between mode shapes, measuring the degree of consistency (linearity) of the modal vectors estimated, quantified in a scalar:

Equation 15

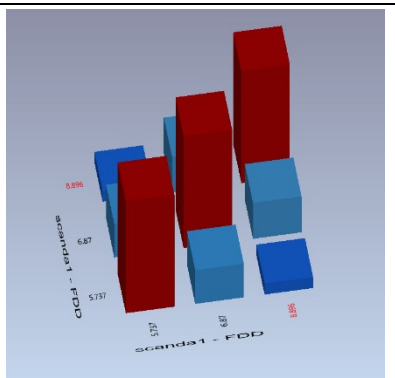
$$MAC(\Phi_1, \Phi_2) = \frac{|\Phi_1^H \Phi_2|^2}{|\Phi_1^H \Phi_1| |\Phi_2^H \Phi_2|}$$

Where  $\Phi_1$  and  $\Phi_2$  are two modal shapes and H denotes the Hermitian matrix (complex conjugate transpose) of the vector it applies to (Allemang, 2003).

MAC factors have a value included between 0 and 1, for orthogonal and parallel vectors respectively. If the MAC value is close to 1 the modes are well correlated, while if it tends to zero is an indicator of not correlated modes. In Table 8, the MAC numbers are presented. On the principal diagonal of the matrix, there are unitary values (coinciding vectors), while all other values are close to zero, therefore the three modes are almost orthogonal. If the modes are orthogonal, they can be considered linearly independent, as structural modes should be. Therefore, the MAC works as a consistency check of the modes estimated.

Table 8 – MAC values for the three modes identified by ambient vibration test after the earthquake. The values on the matrix diagonal should be 1 (autocorrelation) while those outside the diagonal should be close to zero; that indicates that the modes are linearly independent, as they should be.

MAC	5.737 Hz	6.87 Hz	8.896 Hz
5.7 Hz	1.00	0.301	0.098
6.9 Hz	0.301	1.00	0.32
8.9 Hz	0.098	0.32	1.00



## 4.4 Seismic Monitoring

The monitoring system was installed on the dam in February 2017. Three accelerometers were installed, two of which were deployed inside the tunnel immediately below the crest and one in the lowest of the three tunnels, at the bottom of the dam (Figure 26). As showed in Figure 26, the accelerometer deployed at the downstream right of the dam was installed with the main axis forming a  $19.43^\circ$  angle with the vertical direction. Therefore, the data were rotated before the analysis, so to be with the north axis in the upstream-downstream direction, as for the sensor at the centre of the crest. The two accelerometers on the crest had two orthogonal channels, one directed in a radial direction (North-South) and the other by the tangent (Est-West), without the vertical direction. Hence, hereafter in this chapter, the analysis is performed only on the horizontal components. Anyway, as highlighted in the study of Bindi et al. (2015), the wavelength of P waves in the vertical direction are often too long to measure the time delay between the pulses. In fact, wavelength is related to the velocity of propagation of the signal. For P waves, that are much faster than shear waves, the time needed to propagate from the bottom to the top is usually too short to be measured with the sampling frequency normally used for these test. Moreover, as we saw in the subchapter 3.5, the modal parameter of the structure are majorly related to the shear wave propagation and not to the P-waves propagation. Thus, even if we do not analyse the vertical component we are not missing any useful information.

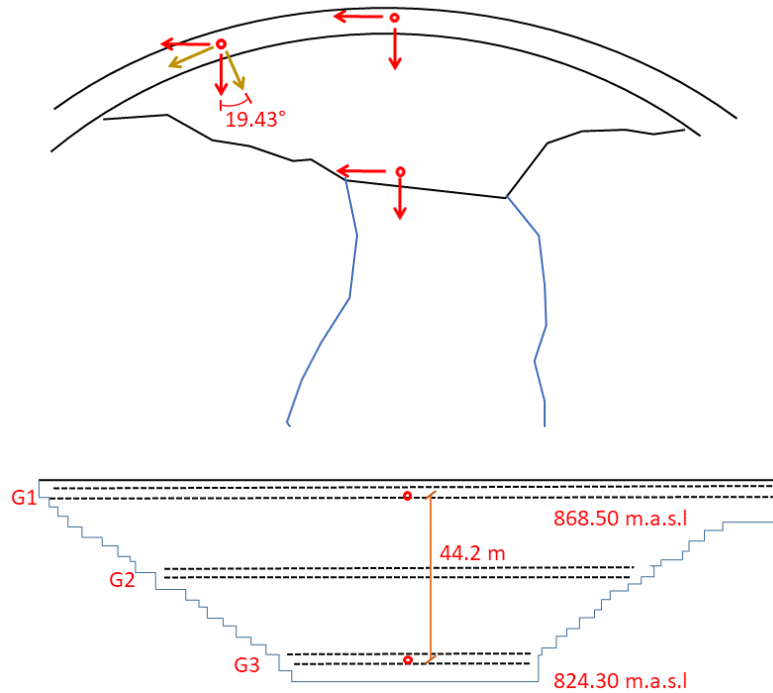


Figure 26 – position of the sensors of the permanent monitoring system: two in the tunnel immediately below the crest of the dam (G1) and one in the lower tunnel (G3). The sensor on the downriver-right side of the tunnel below the crest was installed with the North axis forming a 19.43° angle with the upstream-downstream direction. Hence, before the analysis data were rotated to be in the same direction as the central sensor.

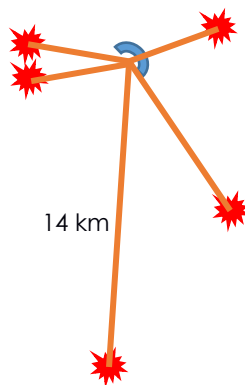
The accelerometers recorded five seismic events of magnitude between 3 and 4 (see Table 9). The recorded signals are analysed and the results are stacked in order to increase the signal to noise ratio. As an example, the waveforms of one recorded event (the magnitude 4 at 9 km distance) are displayed in Figure 27. From these waveforms it can be noticed that in the North-South direction (left panels) the accelerations recorded at the centre (panel a) and at the side (panel c) of the dam are comparable, slightly higher on the side of the dam. In the East-West direction (right panels), the acceleration recorded on the side (panel b) is noticeably higher than the one at the centre (panel d). The acceleration recorded at the bottom of the dam is, on the contrary, lower on the East-West direction (panel f) in comparison with the North-South one (panel e).

From Figure 28 to Figure 32 the time – frequency analysis using the Stockwell transform (Stockwell et al., 1996) is shown for each of the five events recorded.



Table 9 – magnitude, depth and distance between the dam and the epicenter of the five seismic events recorded by the monitoring system in 2017. On the right side, a scheme of the distribution of the events around the investigated dam

Magnitude [Mw]	Depth [km]	Distance [km]
3.9	11	14
3.5	11	4.9
3.8	12	5
3.6	8	4.2
4.0	13	9.3



In the following subchapter (4.5), I apply the deconvolution interferometry technique to these recordings.

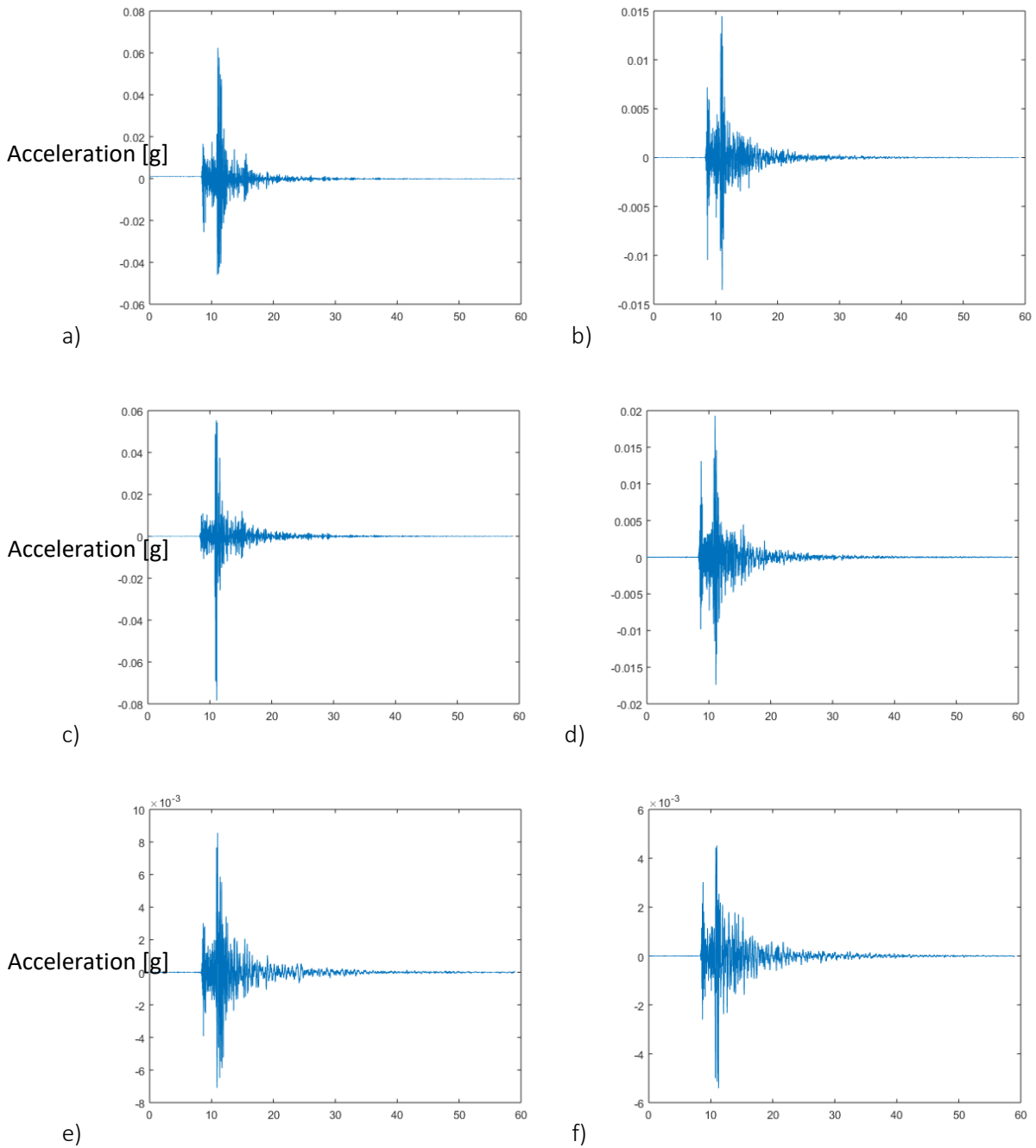


Figure 27 – seismic event of magnitude 4 and 9 km distance: waveforms recorded at centre of the crest of the dam (panel a and b), at the downriver right side (panel c and d) and at the bottom of the dam (panel e and f). On the left side (panels a, c and e) there are the waveforms recorded in the North-South direction (upstream-downstream direction), while on the right side (panels b, d and f) those on the East-West direction (orthogonal to the previous). Please note that the scale is different per each panel.

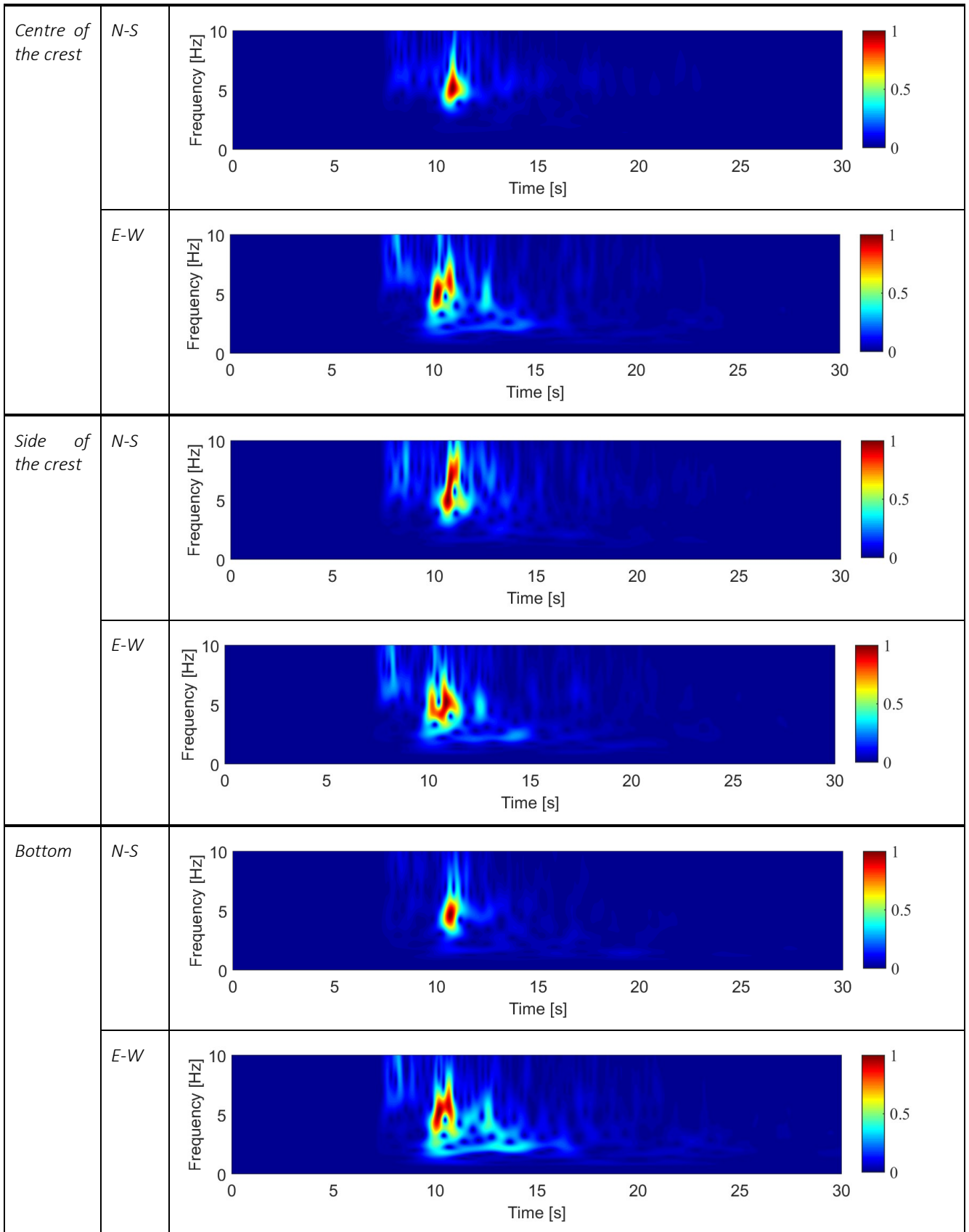


Figure 28 – time - frequency analysis using the S-Transform (using the code written by Stockwell published in Stockwell et al., 1996) of the M3.9 event at 14 km distance

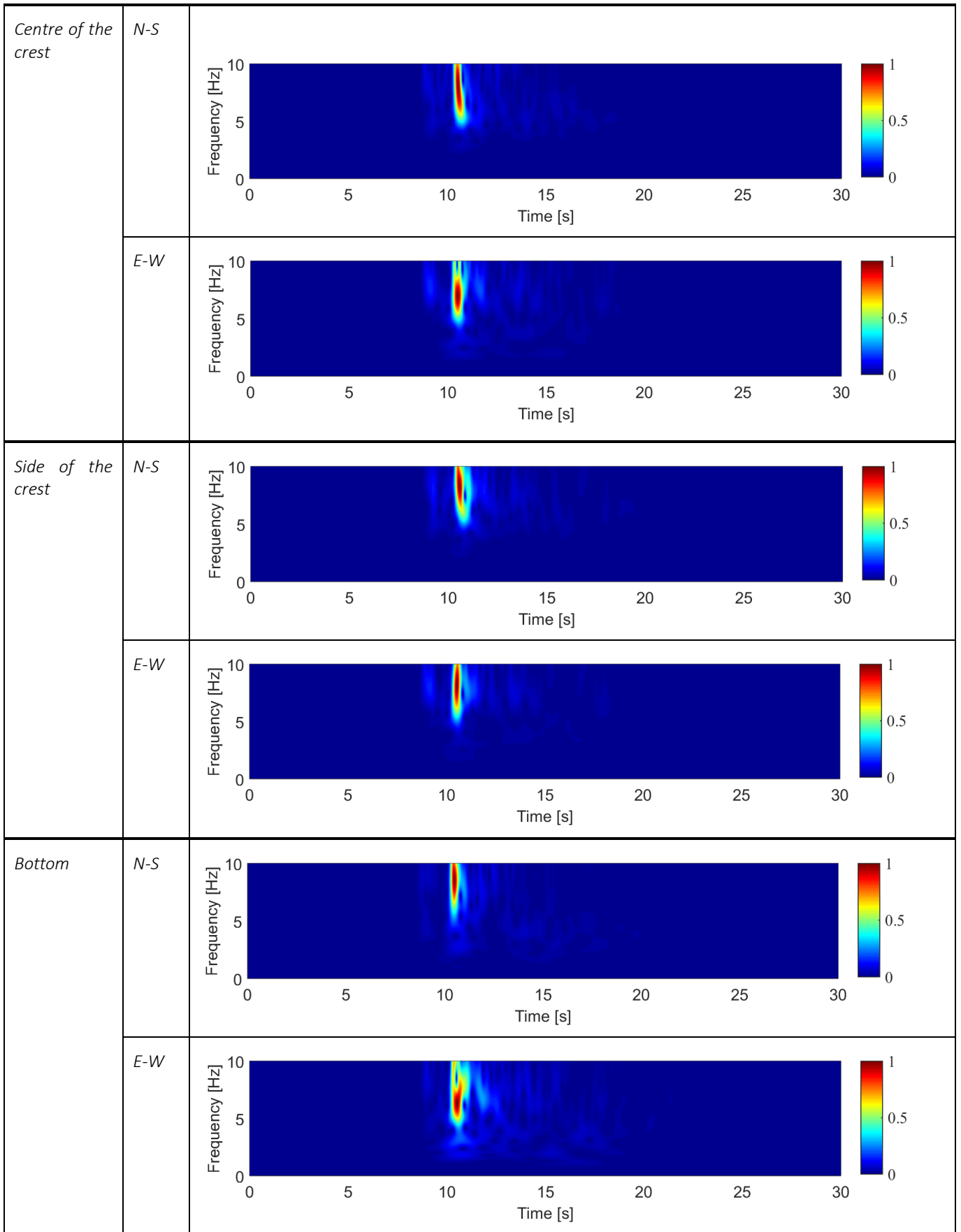


Figure 29 – time - frequency analysis using the S-Transform (using the code written by Stockwell published in Stockwell et al., 1996) of the M3.5 event at 4.9 km distance

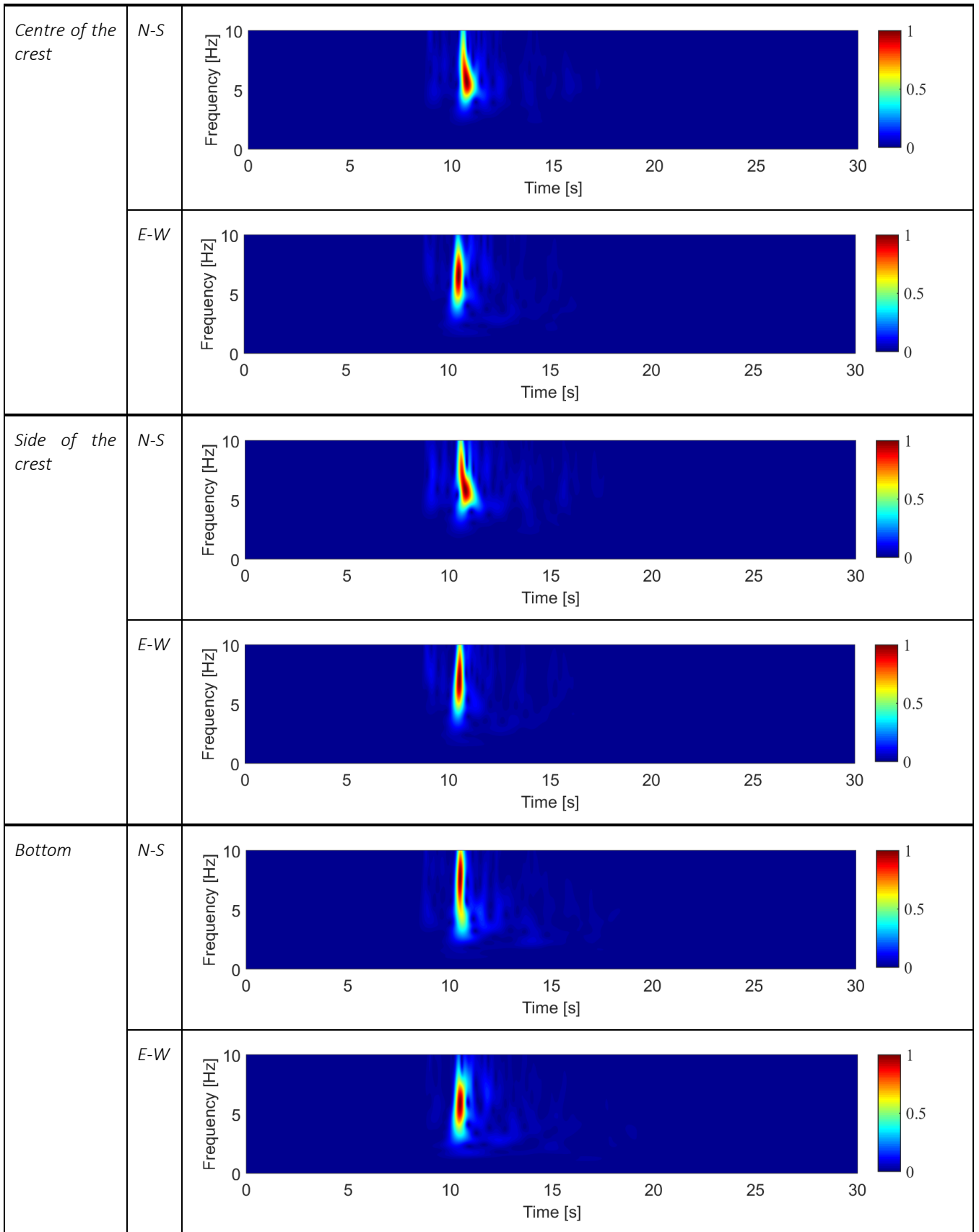


Figure 30 – time - frequency analysis using the S-Transform (using the code written by Stockwell published in Stockwell et al., 1996) of the M 3.8 event at 5 km distance

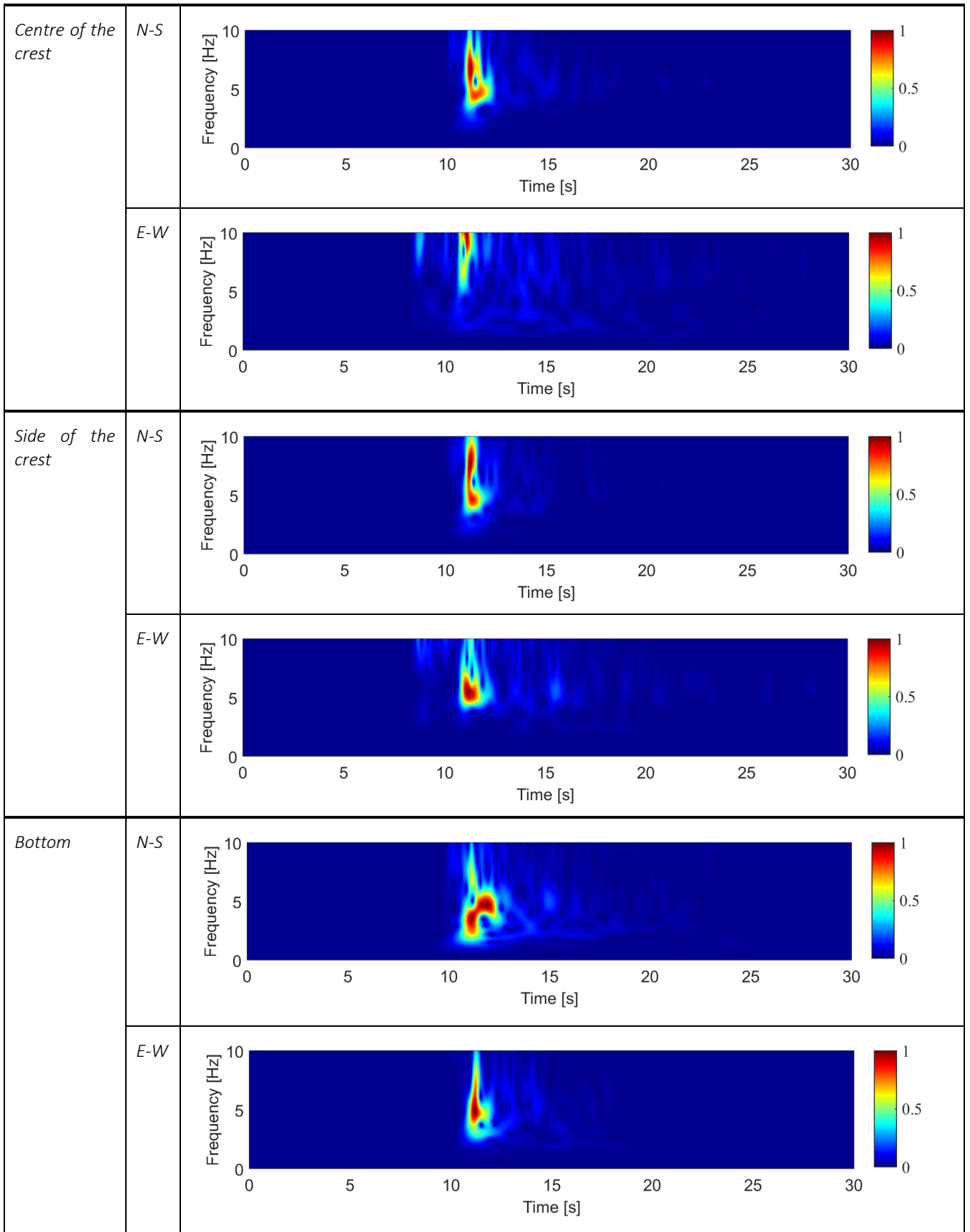


Figure 31 – time - frequency analysis using the S-Transform (using the code written by Stockwell published in Stockwell et al., 1996) of the M 3.6 event at 4.2 km distance

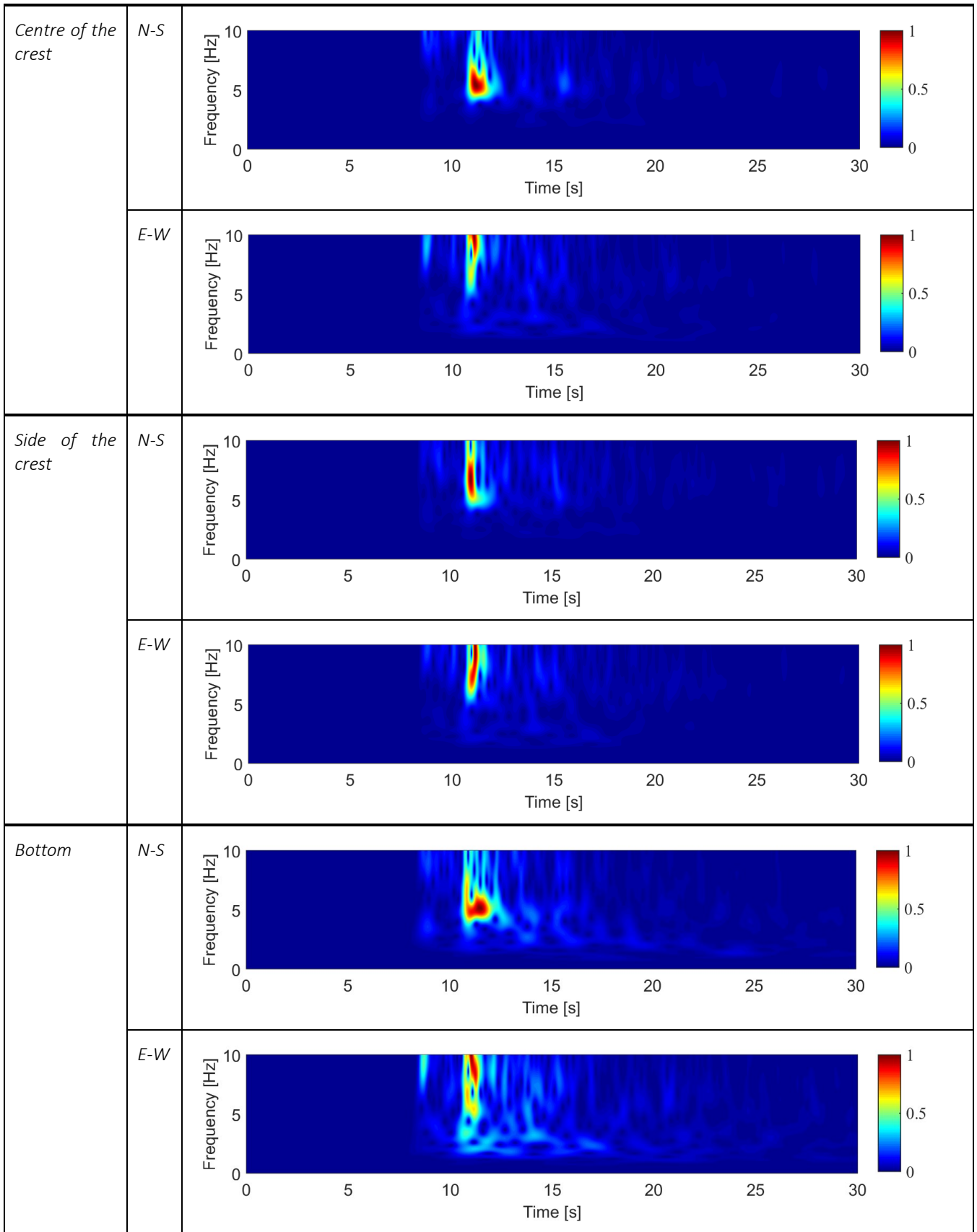


Figure 32 – time - frequency analysis using the S-Transform (using the code written by Stockwell published in Stockwell et al., 1996) of the M 4 event at 9.3 km distance

## 4.5 Deconvolution applied to earthquakes recordings

In the following subchapter, I apply the interferometry deconvolution technique exposed in the subchapter 3.5 to the earthquakes recorded (Table 9) by the permanent monitoring system, described in the previous subchapter 4.4, of the dam in Central Italy.

Parolai et al. (2009) demonstrated that deconvolution is not sensitive to windows selection. Hence, hereafter in this chapter, results are obtained without any window selection: the window contains the entire length of the event.

The first figures of this subchapter are only reported as an example of the spectra of the signals recorded on the dam. Figure 33 represents the Fourier Spectra in the two directions (N-S, corresponding to the upstream-downstream direction, and E-W, orthogonal to it) recorded in the tunnel below the crest and in the tunnel at the bottom of the dam, expressed in a double logarithmic scale. The dependence of the motion-variability on the frequency is highlighted by the differences in the spectra amplitudes (Petrovic and Parolai, 2016). This difference is emphasized in Figure 34, representing the average transfer function, i.e. the ratio between the spectra of the recording at the top of the dam and the one at the bottom of the dam. The average is performed on the values of this ratio per each recorded event. All the results showed from now on in this subchapter should be intended as the average between the responses to the seismic events recorded. A different method will instead be used for ambient vibration data recording, in the next subchapter. The transfer functions can be used for the estimation of the modal frequencies of the structure. In this case, the three modes are identified around the frequencies of 5.7 Hz, 6.8 Hz and 9 Hz, as expected from the results of the previous modal identification tests exposed above.

It is important to underline that the entire treatment in the work of Snieder and Şafak (2006) is appropriate only for tall buildings, for which the motion is basically one-dimensional. As far as the dam is concerned, being the structure very stiff in the transversal direction (in the direction tangent to the curvature of the crest, recorded by the East-West component of the sensors), it is possible to consider the problem as a one-dimensional problem in the



upstream-downstream direction, at least for the application of the interferometric approach. This issue will be better addressed in the chapter comparison and discussion (chapter 5).

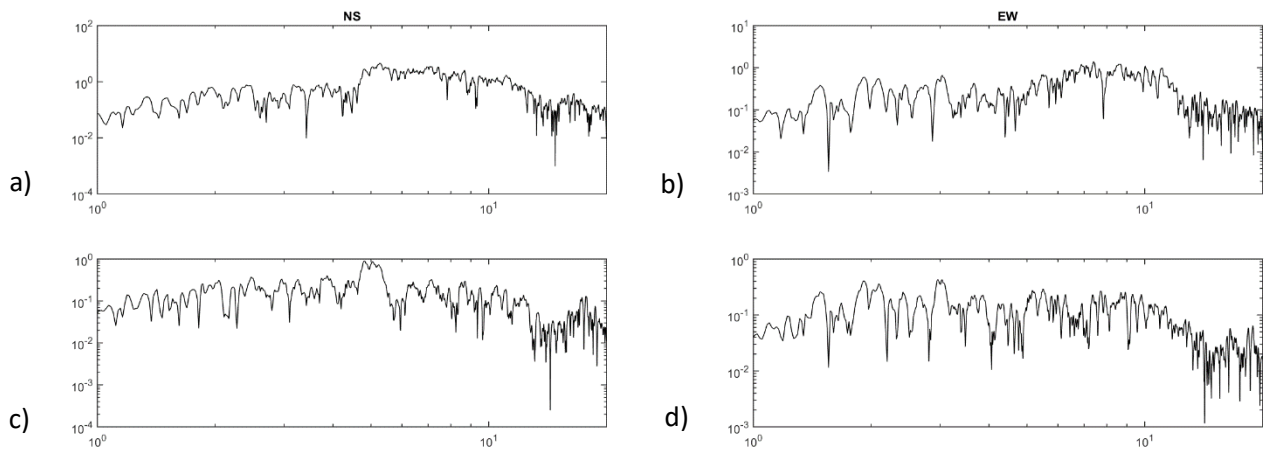


Figure 33 – FFT spectra recorded on the top tunnel (panels a and b) and on the bottom tunnel (panels c and d) for the North-South and North-West directions (left panels and right panels respectively), for the seismic event of magnitude 4 at 9 km distance (log log graph). Please note that the scale is different per each panel.

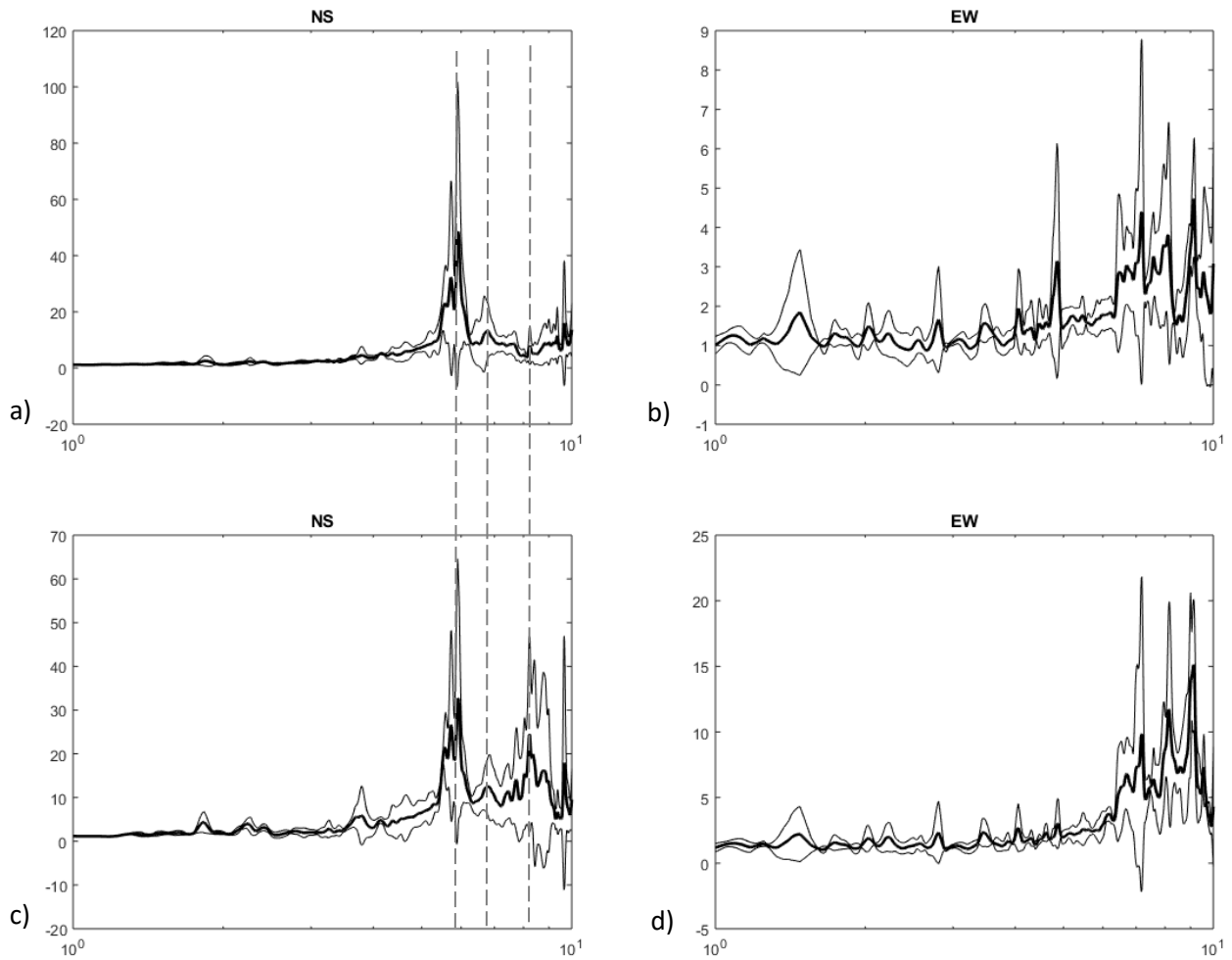


Figure 34 – transfer function calculated as the average of the ratio between the spectra at the tunnel below the crest and the one at the bottom tunnel of the dam per each event recorded, in the North –South and East – West directions (left side and right side respectively). Recordings at the centre (panels a and b) and at the downriver side (panels c and d) of the tunnel below the crest. The dashed lines indicates the frequency of the first three vibrational modes. Please note that the scale on the y axes is different per each panel, while the x-axes (frequency) is constant and logarithmic. The thick line represents the average spectrum, the thin lines the standard deviations. Spectra were smoothed with a triangular window (5%).

### 4.5.1 Recordings on the central transversal section

In Figure 35 and Figure 36, we can see how the filter operates on the signal. In fact, in the upper panels of these figures, the self correlated signal is shown. If the signal was not filtered, we would see a curve corresponding to the value of 1 for the entire spectrum of frequencies. The fact that the spectra amplitudes are decreasing before 1 Hz and after 20 Hz indicates the range of frequencies in which the Green Function is calculated. The lower frequency range limit is given mainly by the instrumental noise, that below 1 Hz is dominant, while the upper limit is given by the stabilizing coefficient  $\varepsilon$  in the deconvolution formula:

*Equation 9*

$$D(\omega) = \frac{U^*(z_B, \omega)}{|U^*(z_B, \omega)|^2 + \varepsilon} U(z_A, \omega)$$

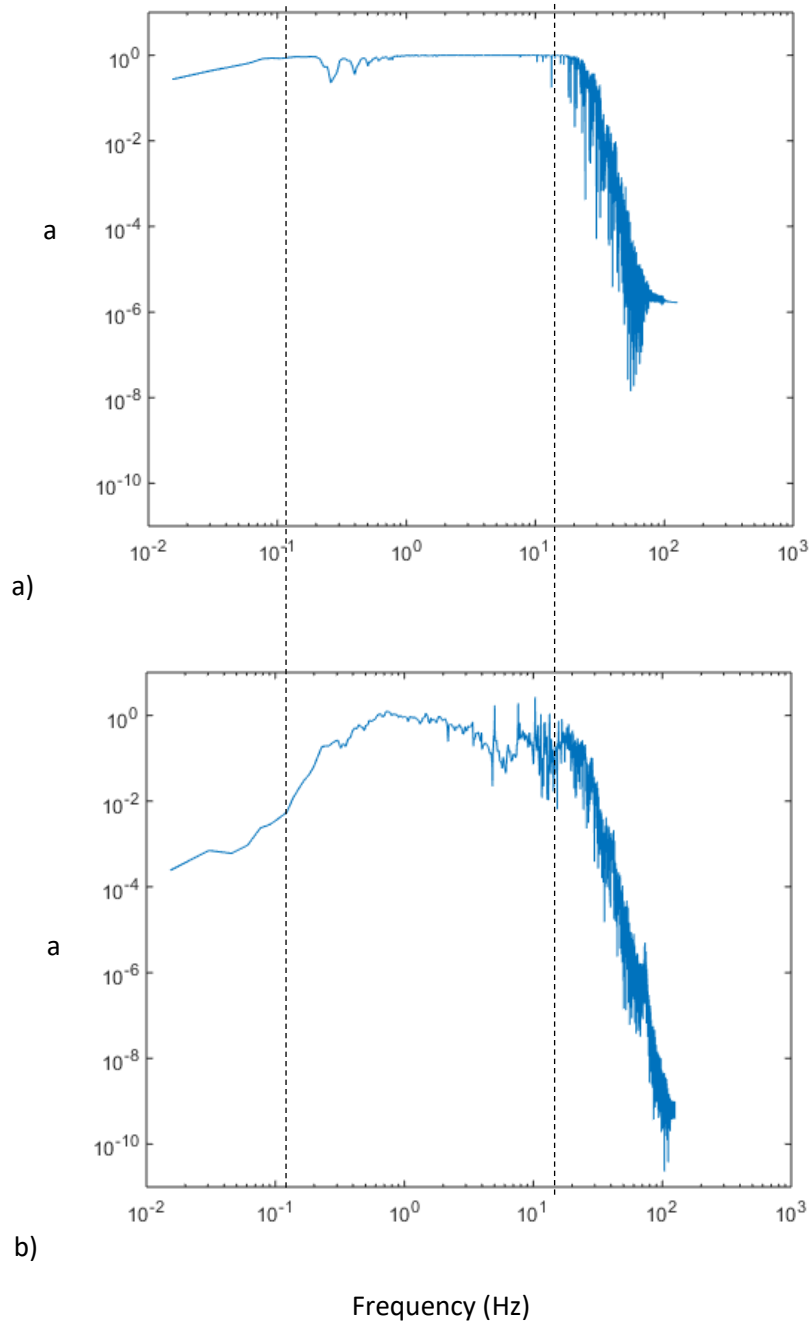


Figure 35 – Deconvolution results: Impulse Response Function (IRF) spectra in the frequency domain, at the centre of the tunnel below the crest (panel a) and at the bottom (panel b), in the North-South direction (upstream-downstream). The crest of the dam was used as reference. The Green function is considered between 0.1 and 15 Hz, because of the filter effect on the signal.

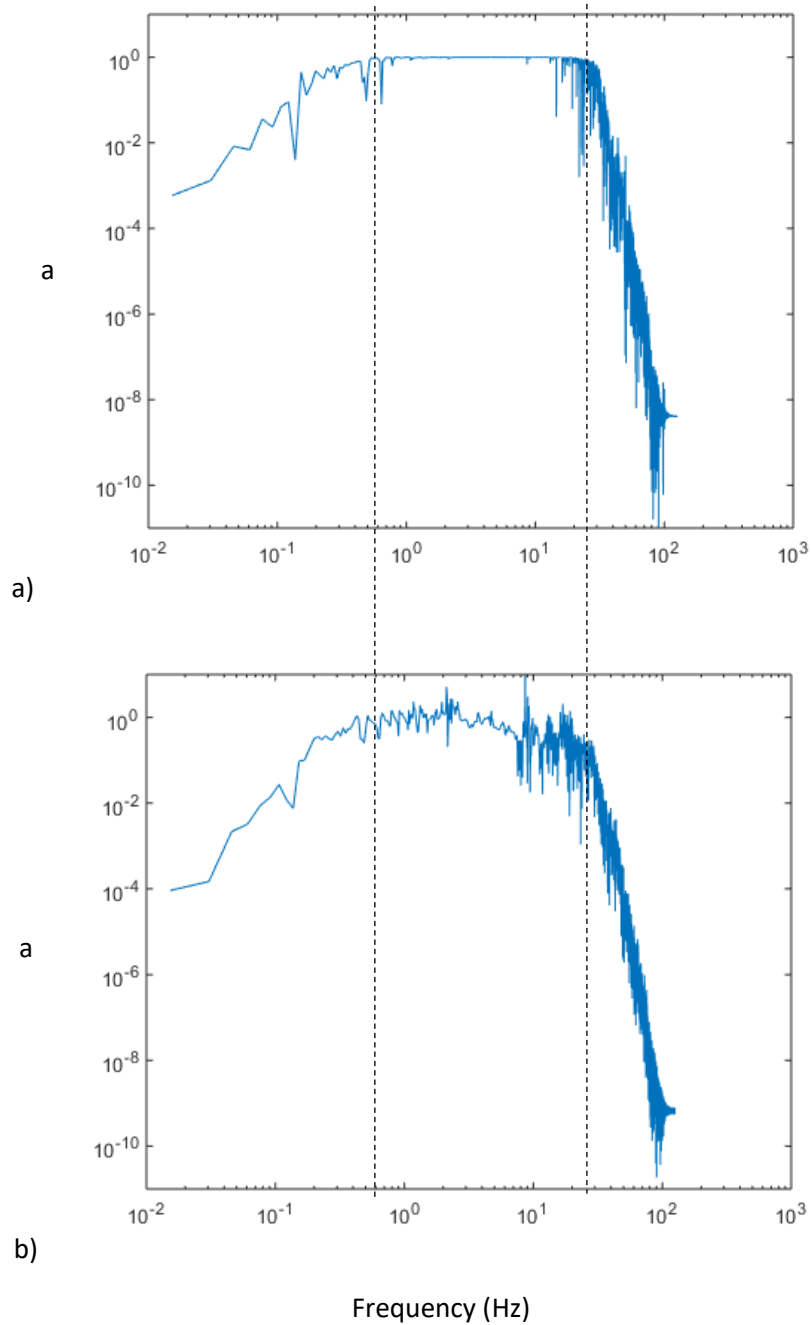


Figure 36 – Deconvolution results: Impulse Response Function (IRF) spectra in the frequency domain, at the centre of the tunnel below the crest (panel a) and at the bottom (panel b), in the Est – West direction (tangent to the crest curvature). The crest of the dam was used as reference. The Green function is considered between 0.7 and 25 Hz, because of the filter effect on the signal.

As we saw in the subchapter 3.5, the result of the deconvolution process is an infinite sum of up-going and down-going waves, that can be described as:

*Equation 10*

$$T(z, \omega) = \frac{u(z, \omega)}{u(z = H, \omega)} = \frac{1}{2} [e^{ik(z-H)} e^{-\gamma|k|(z-H)} + e^{ik(H-z)} e^{-\gamma|k|(H-z)}]$$

Where  $k$  is the wavenumber  $= \omega/c$ ,  $c$  is the shear wave velocity of the building, and  $\gamma$  the viscous damping. In this equation,  $T(z, \omega)$  describes the response of the system when a virtual source is acting at the top of the building at  $t = 0$ .

The deconvolved waves can be used to determine the shear-waves velocity and the attenuation of the structure (Snieder and Şafak, 2006).

To extract the building response, we can deconvolve the recorded waves either referring to the one recorded at the lower tunnel or to the one recorded at the tunnel below the crest of the dam. If we deconvolve a motion with itself, we obtain a bandpass filtered delta-function. That is the reason why in the following figures there will always be a panel in which a spike is displayed. That stands for the self-correlation of the recording taken as reference (for example, Figure 37 panel c).

If we take the record acquired in the tunnel below the crest as a reference, the deconvolved waves at the bottom (as in Figure 38) represents the superposition of two waves: one acausal (up-going) and one causal (down-going). As can be seen in Figure 38, it is quite easy to measure the delay time (the time necessary for them to propagate from the one at the bottom to the one at the top and back), simply by picking the maximum of the picks in the deconvolved waveform diagram. After having measured that time from Figure 38 panel b ( $\tau = 2 \cdot 0.048s = 0.096s$ ), and knowing the distance of the two tunnels in which the sensors are deployed (44 meters), it is possible to determine the shear wave velocity inside the dam:

*Equation 16*

$$c = \frac{2H}{\tau} = \frac{2 \cdot 44m}{0.096s} = 916 \frac{m}{s}$$

Inside regular buildings the shear wave velocity is usually around 300 m/s, but we must consider that the dam is stiff and does not present much empty spaces, other than the tunnels.

The possibility of double checking the consistency of results is given using the expression

*Equation 12*

$$T_0 = \frac{4H}{c}$$

to calculate either the velocity estimated through the periods determined by the experimental tests, or the period estimated through the velocity measured through deconvolution. If significant dissimilarities are found in this consistency check, an internal dispersion in the structure can be hypothesized (Todorovska et al., 2001 a,b).

To check the consistency of the shear wave velocity, we compare it with the fundamental frequency  $f_0$  identified before:

*Equation 17*

$$T_0 = \frac{4H}{c} = \frac{4 \cdot 44m}{916 \text{ m/s}} = 0.19 \text{ s} \rightarrow f_0 = 5.2 \text{ Hz}$$

The result is perfectly matching the fundamental frequency obtained by the forced and ambient vibration tests described in the previous subchapters.

Which is more, if we measure the difference between the amplitude of the causal wave (see Figure 38) and the a-causal wave peaks, we can estimate the intrinsic anelastic attenuation of the structure, the  $\gamma$  factor exponentially damping the wavefield  $T(z, \omega)$  expressed in the previous page:

*Equation 18*

$$\gamma = \frac{\ln(A^-/A^+)}{\omega_{eff} \tau} = \frac{\ln(0.02235/0.02105)}{19 \text{ Hz} \cdot 0.096 \text{ s}} = 0.033 = 3\%$$

Therefore the quality factor is

*Equation 19*

$$\gamma = \frac{1}{2Q} \rightarrow Q = \frac{1}{2\gamma} = \frac{1}{2 \cdot 0.033} = 15$$

On the other way round, if we use the measure at the bottom tunnel as reference, as in Figure 37, we obtain a deconvolved signal that can be described as a superposition of up-going and down-going waves too, or as a sum of normal modes.

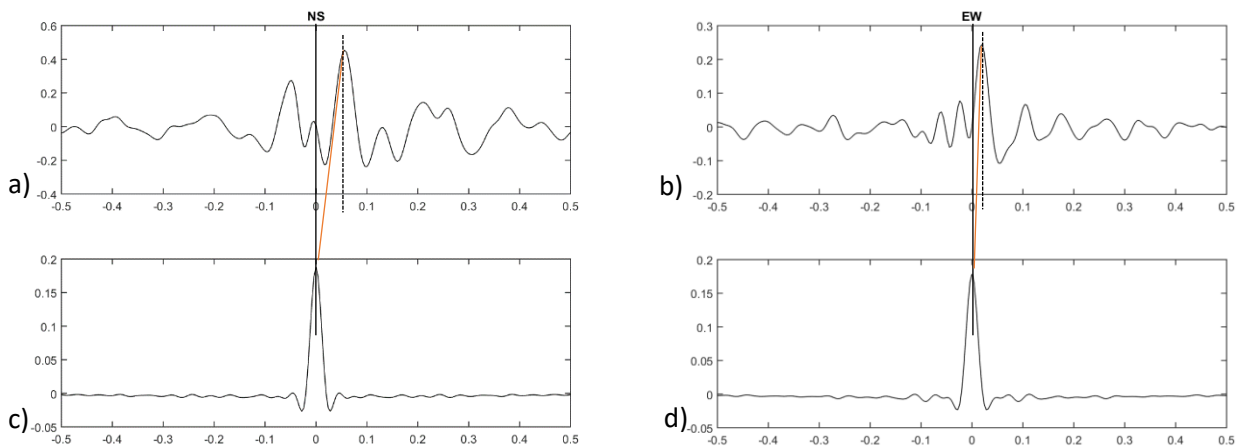


Figure 37 – Impulse Response Function, deconvolved wavefield in the time domain; a) autocorrelation of the signal at the centre of the tunnel below the crest, with the bottom tunnel as reference; b) wavefield at the bottom of the dam. Bandpass filter 1-20 Hz. Please note that the scale is different per each panel.

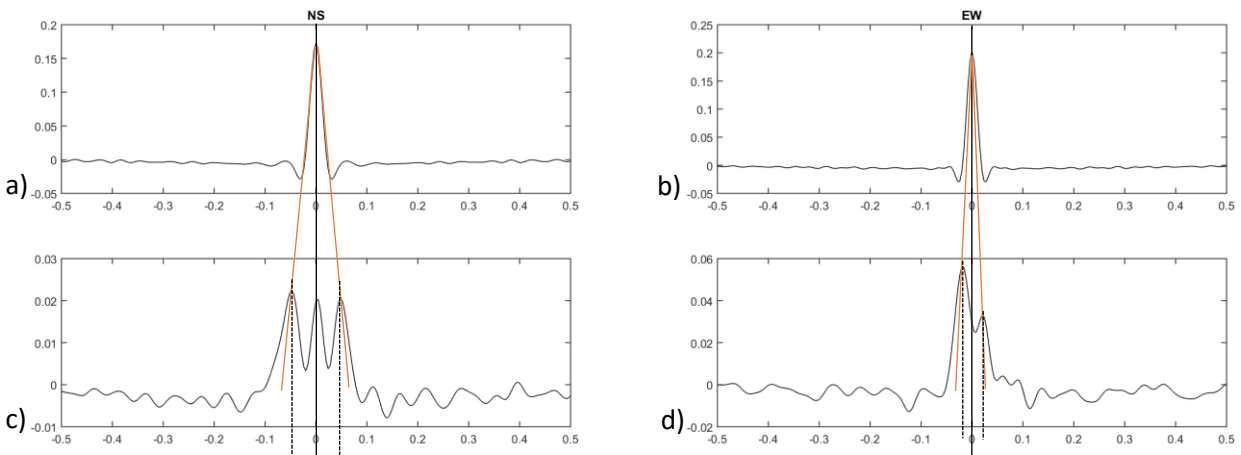


Figure 38 – Deconvolution results: Impulse Response Function, deconvolved wavefield in the time domain for; a) autocorrelation of the signal at the centre of the tunnel below the crest, used as reference; b) wavefield at the bottom of the dam, divided in a causal and a-causal part ( $t < 0$ , left, and  $t > 0$ , right, respectively). Bandpass filter 1-20 Hz. From this plot we can read the time delay between the a-causal and causal peak and the difference in their amplitude, obtaining so shear wave velocity and damping of the structure. Please note that the scale is different per each panel.



Usually, for buildings modelled as cantilevered shear beams, the first mode dominates the dynamic behaviour. For arch dam, instead, it is known that higher modes can be significant in the structural behaviour. In the dam used as a case study, for example, we saw from the experimental tests that the second were characterized by high peaks on the response spectrum. That is the reason why I will proceed in deconvolving the signals with different bandpass filters, in a range of approximately 1 Hz around the frequency of each mode detected with the previous tests. Therefore, Figure 39 and Figure 42 show the deconvolved wavefield for first vibrational mode, with a bandpass filter between 4.5 and 6 Hz, for the two testing point each of which deconvolved using the top and the bottom as a reference. The same for the second vibrational mode, with bandpass filter between 6.5 and 7.5 Hz, shown in Figure 40 and Figure 43. Finally, the results for the third vibrational mode can be seen in Figure 41 and Figure 44, with the bandpass filter between 8.5 and 9.5 We must underline that, using such a narrow filter, in the diagrams some artefacts appear, with the appearance of a sinusoidal pattern. This can be detected also by the fact that the auto-correlated wavefield is not a pure delta-function anymore but shows, instead, two peaks (for example Figure 40 and Figure 41, panel c and d). Obviously, these numerical artefacts should be ignored in the interpretation of results.

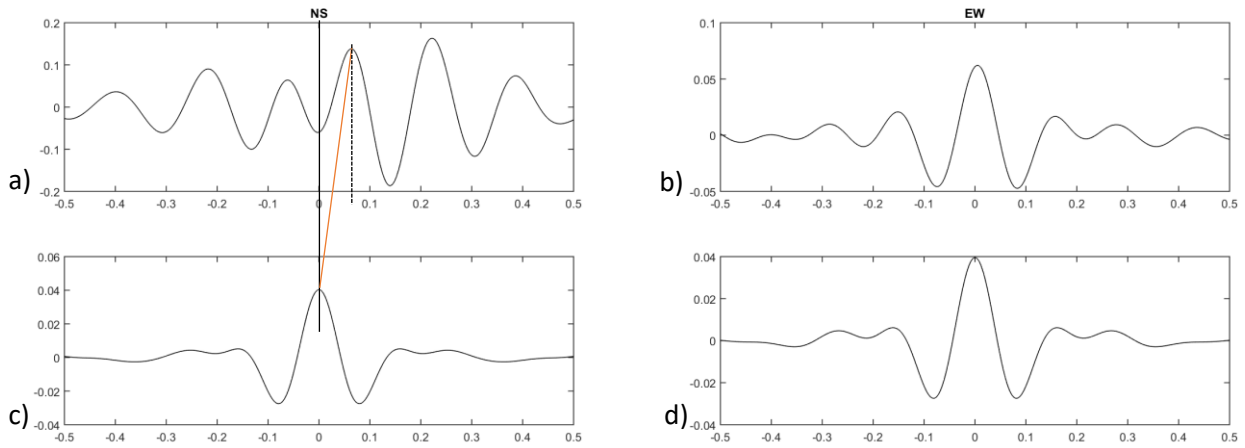


Figure 39 - deconvolved waveform, using the bottom as reference, at the centre of the tunnel below the crest, with bandpass filter between 4.5 and 6 Hz, first mode

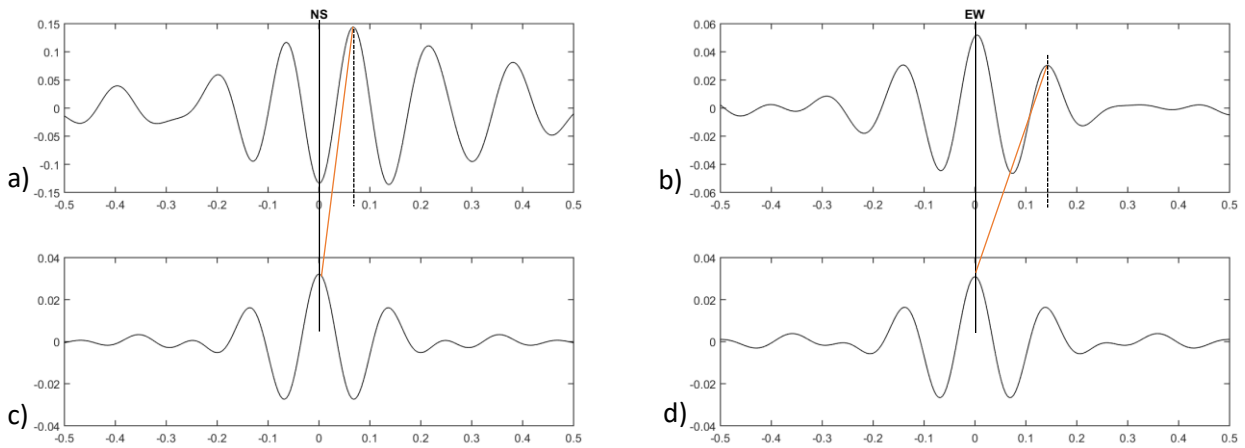


Figure 40 - deconvolved waveform, using the bottom as reference, at the centre of the tunnel below the crest, with bandpass filter between 6.5 and 7.5 Hz, second mode. Please note that the scale is different per each panel.

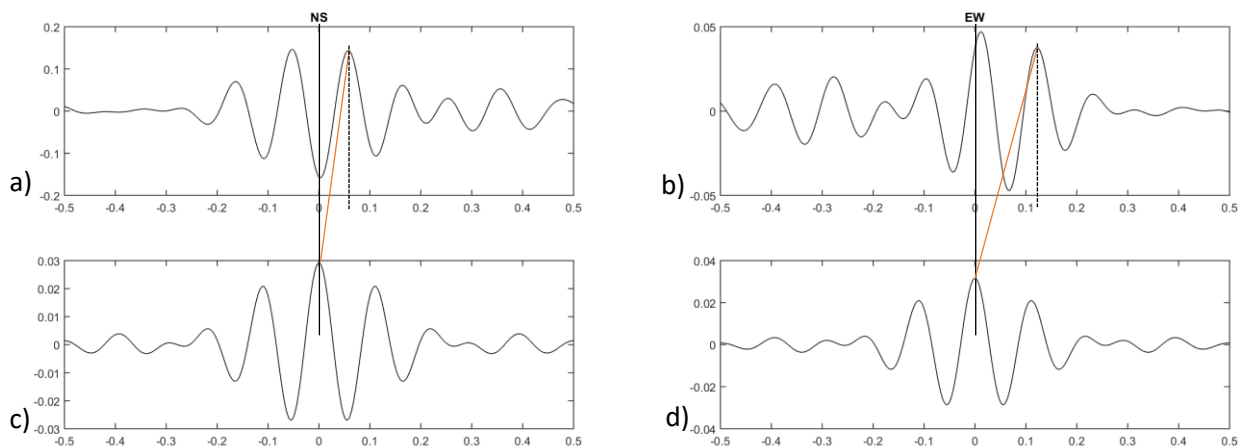


Figure 41 - deconvolved waveform, using the bottom as reference, at the centre of the tunnel below the crest, with bandpass filter between 8.5 and 9.5 Hz, third mode. Please note that the scale is different per each panel.

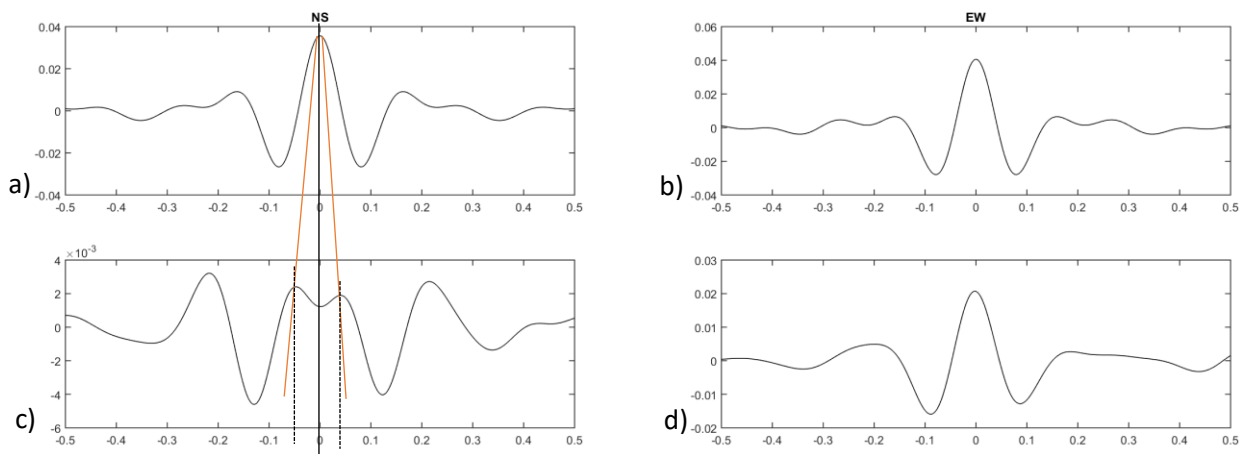


Figure 42 – deconvolved waveform, using the crest as reference, at the centre of the tunnel below the crest, with bandpass filter between 4.5 and 6 Hz, first mode. Please note that the scale is different per each panel.

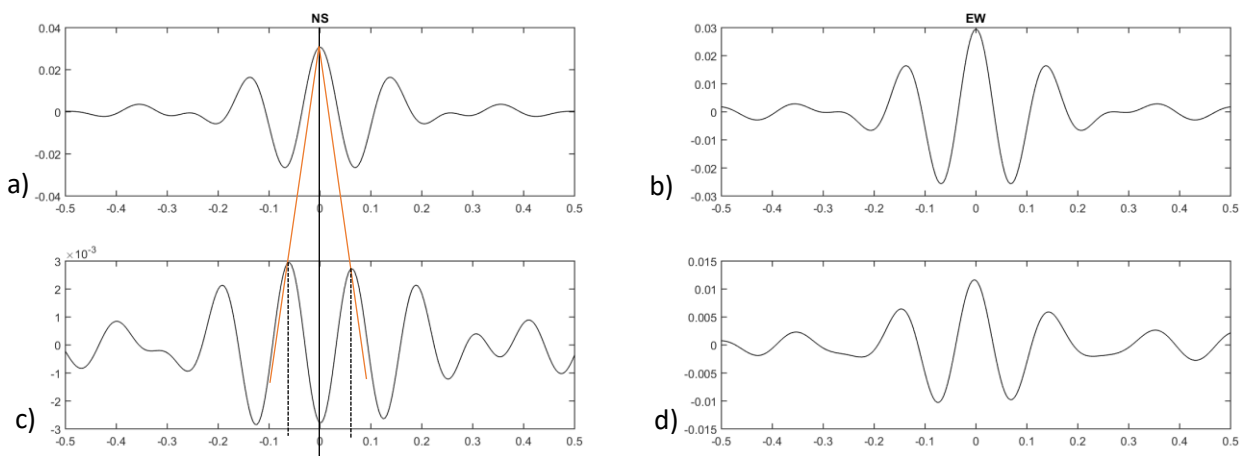


Figure 43 – deconvolved waveform, using the crest as reference, at the centre of the tunnel below the crest, with bandpass filter between 6.5 and 7.5 Hz, second mode. Please note that the scale is different per each panel.

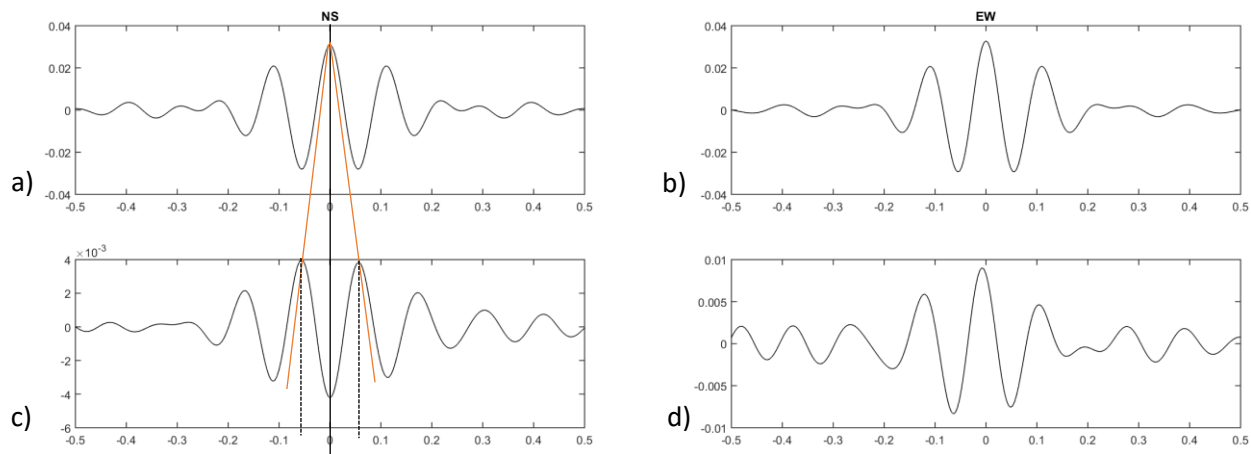


Figure 44 – deconvolved waveform, using the crest as reference, at the centre of the tunnel below the crest, with bandpass filter between 8.5 and 9.5 Hz, third mode. Please note that the scale is different per each panel.

## 4.5.2 Recording at the side of the dam

In this subchapter the results obtained for the recordings of the sensor deployed at the downriver right side of the tunnel are reported. As already explained in the subchapter 4.4, the accelerometer deployed at the downstream right of the dam was installed with the main axis forming a  $19.43^\circ$  angle with the vertical direction. Therefore, the data were rotated before the analysis, so to be with the north axis in the upstream-downstream direction, as for the sensor at the centre of the crest.

As the previous subchapter, in Figure 45 and Figure 46 we can see the range of frequency for which the Green functions are calculated. In the upper panels of these figures, the self correlated signal is shown: the fact that the spectra amplitudes are decreasing before 1 Hz and after 20 Hz indicates the range of frequencies in which the Green Function is calculated. The lower frequency range limit is given mainly by the instrumental noise, that below 1 Hz is dominant, while the upper limit is given by the stabilizing coefficient  $\varepsilon$  in the deconvolution formula.

From Figure 47 to Figure 54 the deconvolved wavefield in the time domain is showed, for the recording at the downriver side of the dam. In the frequency range between 1 and 20 Hz, Figure 47 shows the results with the sensor at the bottom used as reference, in Figure 48 the sensor inside the tunnel below the crest is taken as reference. Figure 49, Figure 50 and Figure 51 show the deconvolved wavefield using the bottom as a reference with a band pass filter around the frequency of the first three vibrational modes: 4.5-6 Hz, 6.5-7.5 Hz and 8.5-9.5 Hz. The same filters are used for the signal deconvolved using the sensor in the tunnel below the crest as reference, showed in Figure 52, Figure 53 and Figure 54.

In Figure 48 panels a and c it can be seen that, on the contrary to what expected and to what happened for the central section described in the previous subchapter, in this case the propagation time of the up-going wave is the double of that of the down-going wave.

It is quite difficult to understand the cause of this delay of the up-going wave. A hypothesis is that the model of wave propagation in a shear-beam model is not valid anymore on this

section because of the interaction with the lateral side of the dam. Moreover, it must be considered that the reference sensor at the bottom of the dam is not in a vertical array with the one at the lateral side of the top tunnel, and this probably has a strong influence on the results.

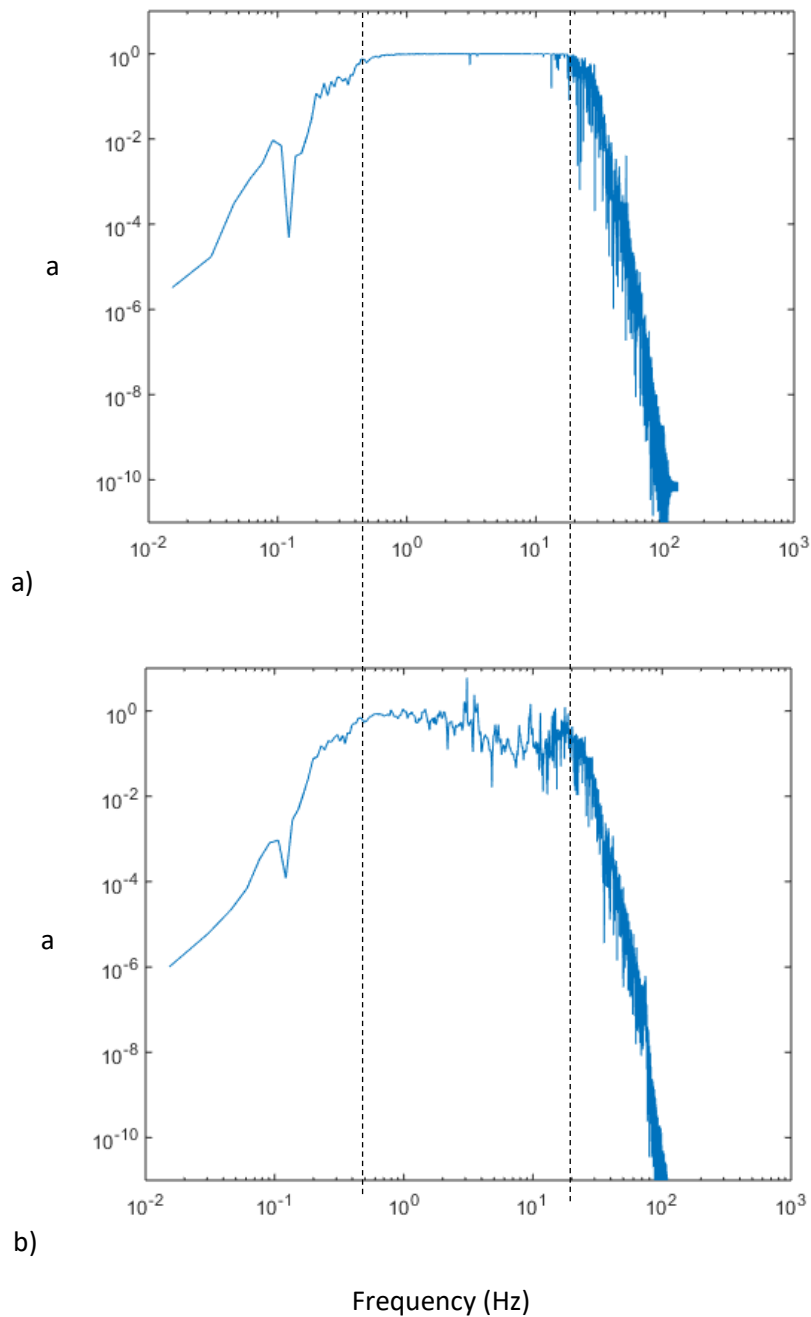


Figure 45 – Deconvolution results: Impulse Response Function (IRF) spectra in the frequency domain, at downriver right side of the tunnel below the crest (panel a) and at the bottom (panel b), in the North-South direction (upstream-downstream direction). The crest of the dam was used as reference. The Green function is considered between 0.5 and 20 Hz, because of the filter effect on the signal.

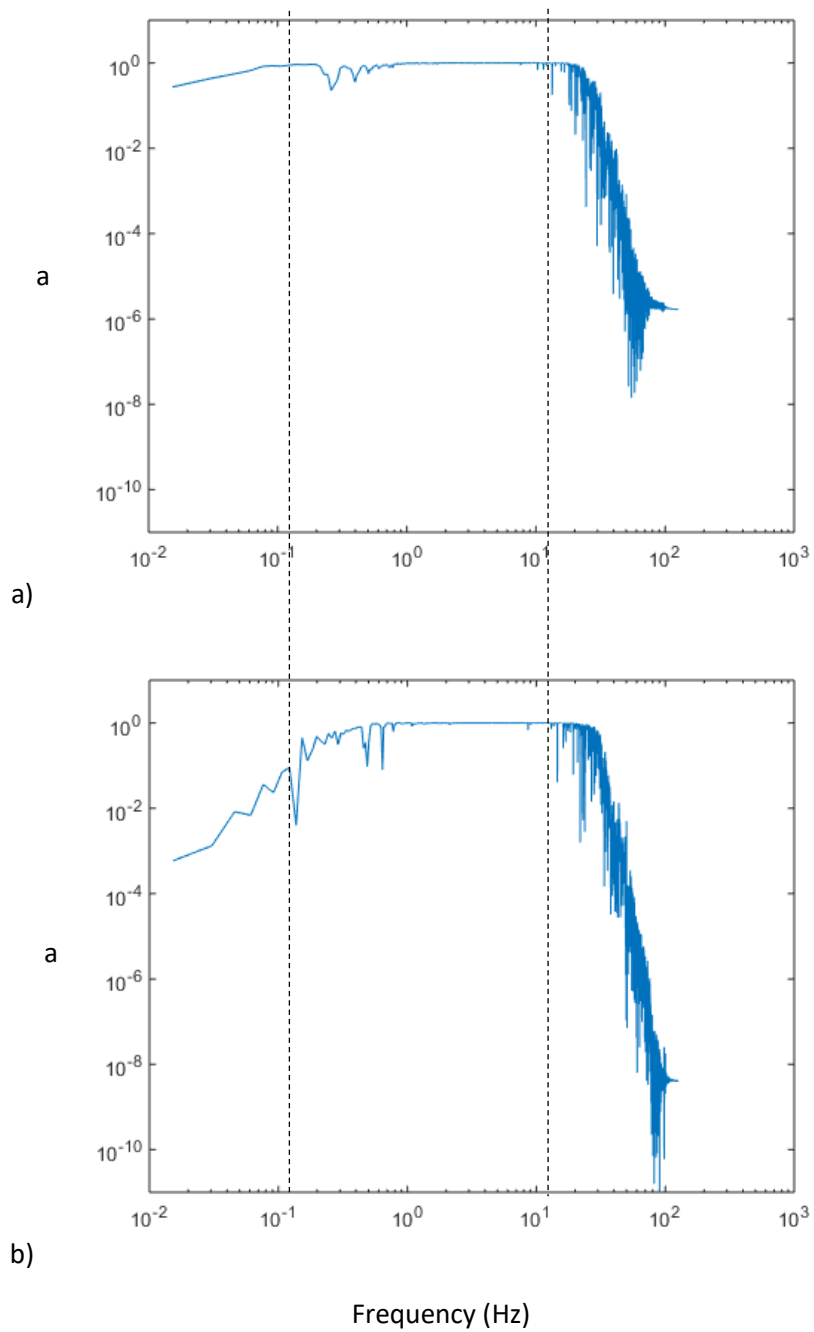


Figure 46 – Deconvolution results: Impulse Response Function (IRF) spectra in the frequency domain, at downriver right side of the tunnel below the crest (panel a) and at the bottom (panel b), in the Est – West direction (tangent to the crest curvature). The crest of the dam was used as reference. The Green function is considered between 0.1 and 12 Hz, because of the filter effect on the signal.

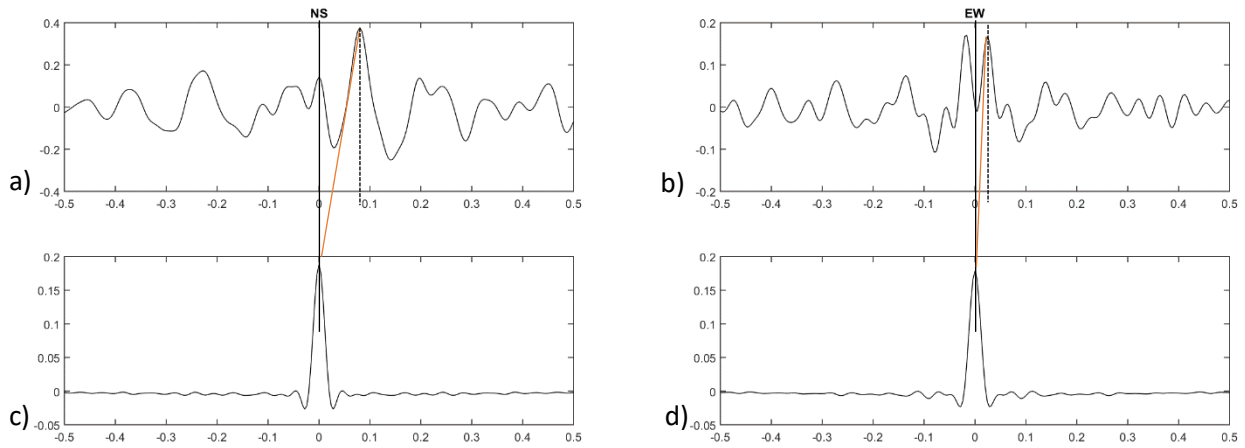


Figure 47 – Deconvolution results: Impulse Response Function, deconvolved wavefield in the time domain; a) autocorrelation of the signal at the downriver right side of the tunnel below the crest, with the bottom tunnel as reference; b) wavefield at the bottom of the dam. Bandpass filter between 1 and 20 Hz. Please note that the scale is different per each panel.

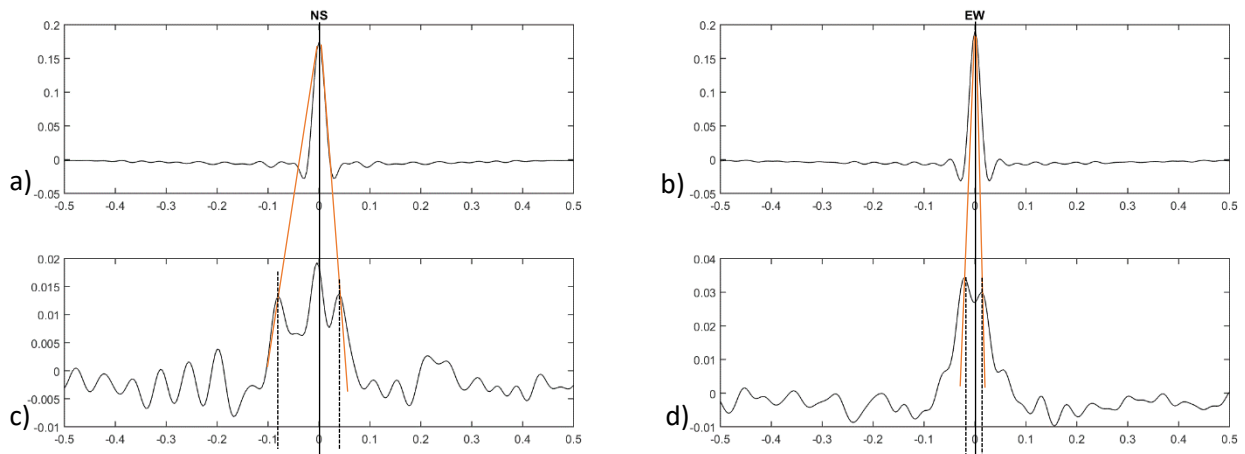


Figure 48 – Deconvolution results: Impulse Response Function, deconvolved wavefield in the time domain; a) autocorrelation of the signal at the downriver right side of the tunnel below the crest, used as reference; b) wavefield at the bottom of the dam, divided in a causal and a-causal part ( $t < 0$ , left, and  $t > 0$ , right, respectively). Bandpass filter between 1 and 20 Hz. Please note that the scale is different per each panel.

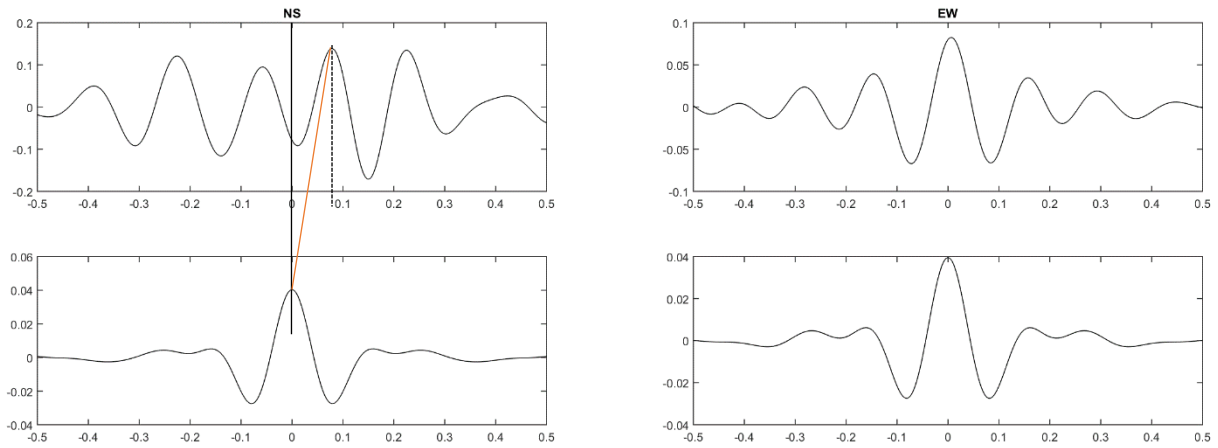


Figure 49 - deconvolved waveform, using the bottom as reference, at the downstream right of the crest tunnel, with bandpass filter between 4.5 and 6 Hz, first mode. Please note that the scale is different per each panel.

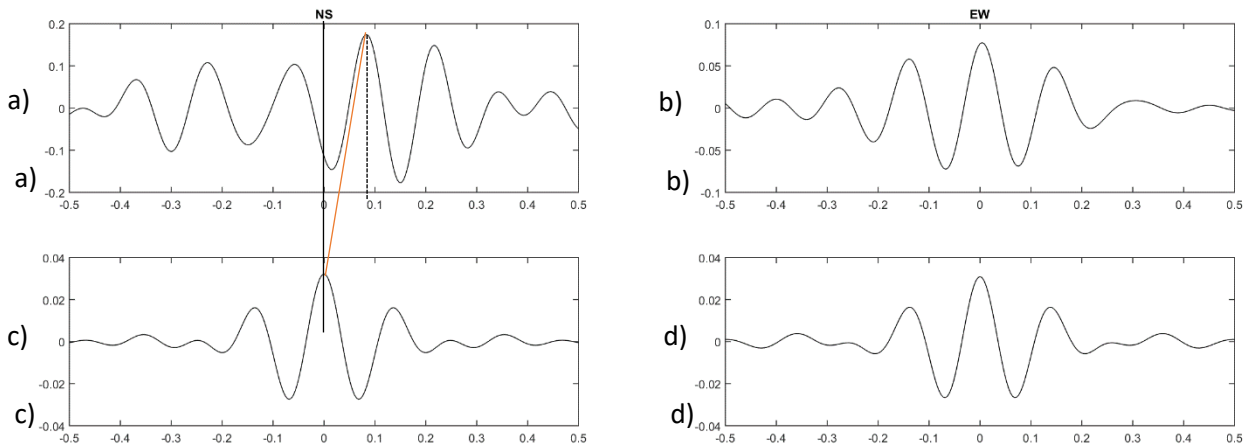


Figure 50 - deconvolved waveform, using the bottom as reference, at the downstream right of the crest tunnel, with bandpass filter between 6.5 and 7.5 Hz, second mode. Please note that the scale is different per each panel.

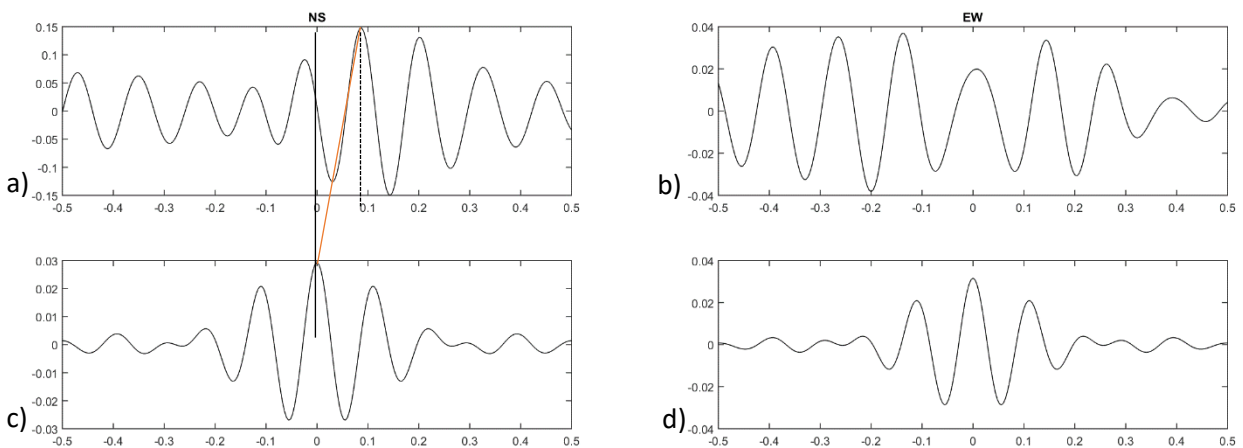


Figure 51 - deconvolved waveform, using the bottom as reference, at the downstream right of the crest tunnel, with bandpass filter between 8.5 and 9.5 Hz, third mode. Please note that the scale is different per each panel.



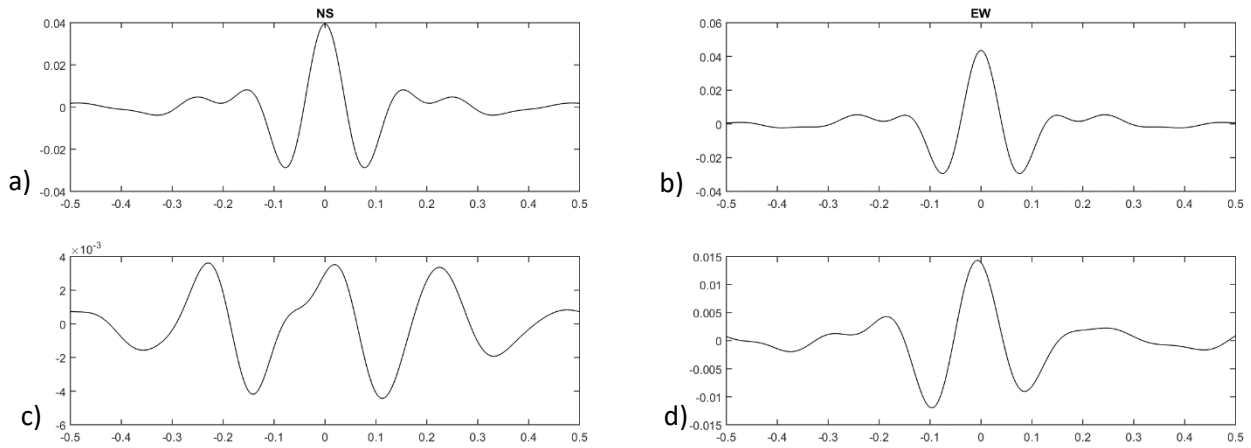


Figure 52 – deconvolved waveform, using the crest as reference, at the downstream right of the crest tunnel, with bandpass filter between 4.5 and 6 Hz, first mode. Please note that the scale is different per each panel.

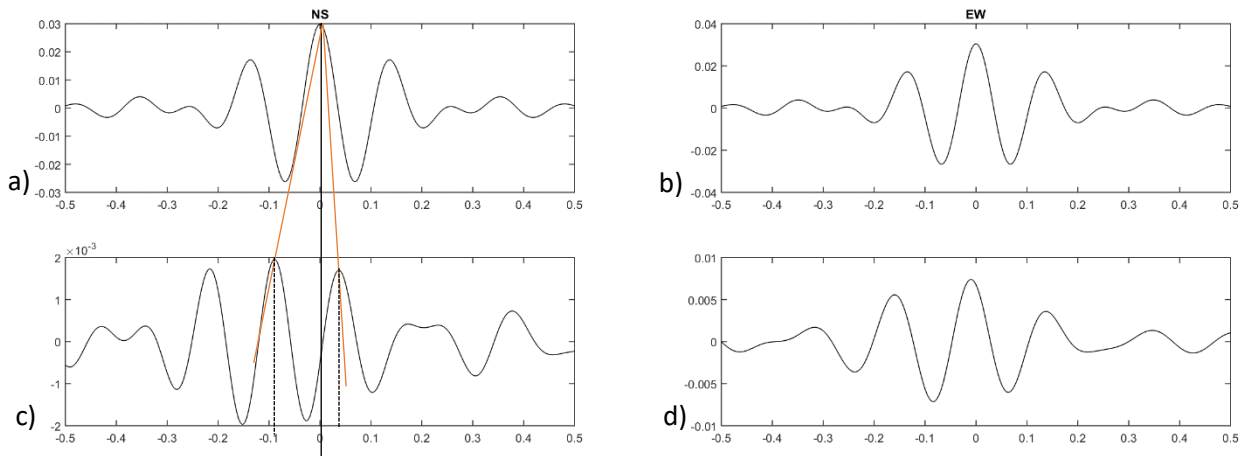


Figure 53 – deconvolved waveform, using the crest as reference, at the downstream right of the crest tunnel, with bandpass filter between 6.5 and 7.5 Hz, second mode. Please note that the scale is different per each panel.

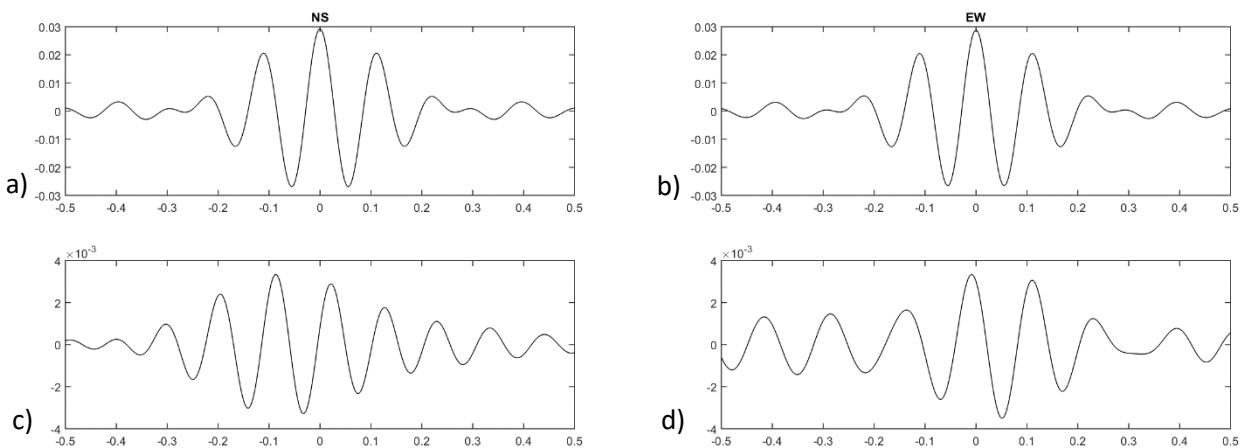


Figure 54 – deconvolved waveform, using the crest as reference, at the downstream right of the crest tunnel, with bandpass filter between 8.5 and 9.5 Hz third mode. Please note that the scale is different per each panel.

## 4.6 Deconvolution applied to ambient vibration recordings

### 4.6.1 Ambient vibration test after the earthquake

As reported in chapter 4, the ambient vibration tests after 2016 earthquake were performed using 15 velocimeters deployed on the crest of the dam (Figure 55), each one oriented with the north axis in the radial direction. This is actually a problem, because the sensors were deployed on the crest (not inside the gallery, as for the earthquakes recordings) and along a curve horizontal line (not in a top-bottom vertical array configuration, as for the earthquakes recordings). With this array configuration, we are not anymore in the conditions of a shear beam as far as the transversal, vertical section is concerned; on the other hand, the crest itself can be modelled as a beam clamped at both ends. Therefore, hereafter I will anyhow apply the deconvolution interferometric approach to the ambient vibration recordings.

To apply the deconvolution interferometry, the first step was to align all the sensors with the north axis in the upstream-downstream direction, as the one at the centre of the crest. To do so, the coordinates of the points of the installed sensors were fitted by a polynomial form. Deriving the analytical equation of the curve of the crest it was possible to estimate the angles formed by each sensor with the downstream direction. All the recorded data were so rotated according to the proper angle.

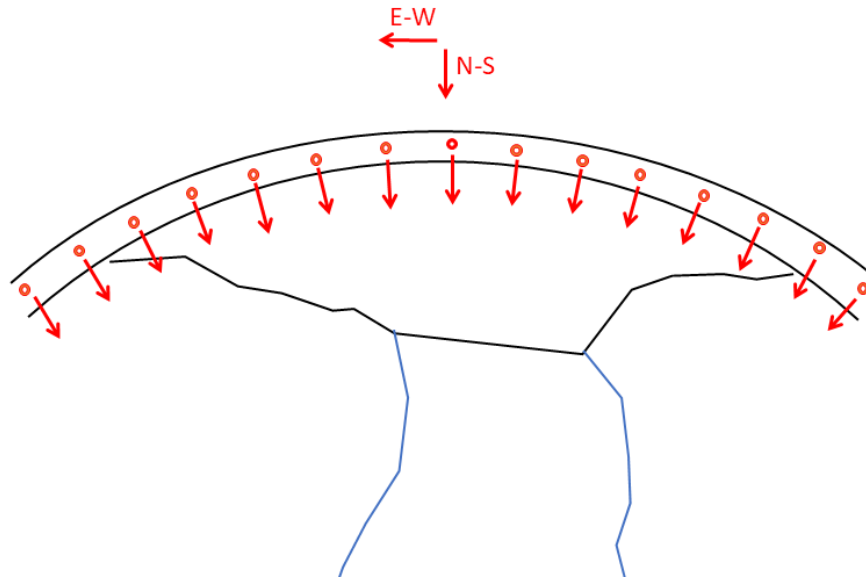


Figure 55 - sensors configuration for the ambient vibration tests performed in 2016, after the earthquake hit the structure. The sensors were deployed with the north axis in the radial direction; before starting the analysis they were rotated with the north axis in the upstream-downstream direction, as the one at the centre of the crest.

The first step was to attempt the elaboration using the recordings of all the sensors, with the sensor at the downriver left side of the dam used as a reference. The results of the deconvolution analysis, in the time domain, are shown in Figure 56. These results are of difficult interpretation, basically for two reasons: the first is that the sensors are deployed only on the crest and there's no reference at the bottom of the dam; the second is that the sensors are not deployed on a straight line, but follow instead the curvature of the crest. Anyhow, we can make few considerations on these results. The first consideration is that, on the contrary to what resulted from the earthquake recordings analysis (with the sensors at the top and bottom of the dam), the direction which shows majors amplifications in the wavefield is the East-West one (Figure 56, panel b) and not the North-South (Figure 56, panel a). In fact, changing the perspective due to the different array configuration, the arrival of the East-West waves should correspond to the arrival of the P-waves coming from the side of the dam; the North-South direction should correspond, instead, to the shear waves.

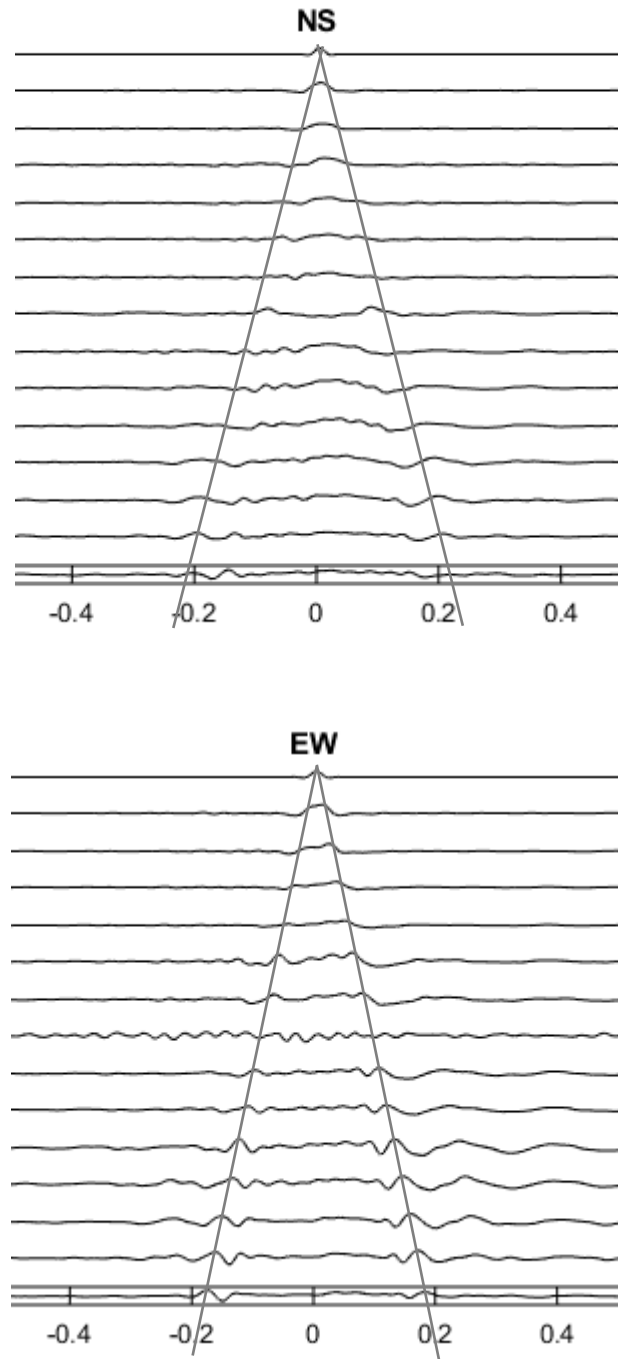


Figure 56 – deconvolved wavefield, using the sensor deployed at the downriver left side as reference, of all the 15 ambient vibration recordings, in the North South (panel a) and East-West directions (panel b)

If we calculate the time needed by the waves to propagate from the left side to the right one and then back, and we divide the distance between the first and the last sensor, we obtain the values of velocity in the two directions. The results per each sensor are listed in Table 10. As can be noticed, the time delay is not reported for all the sensors; in fact, as can be seen in Figure 56, it is not easy to do the picking of the arrival causal and a-causal waves for all the sensor. Those for which the interpretation of the wavefield was unsure were ignored in this analysis. Red circles in Table 10 highlight a slight decrease in the calculated velocity. This decrease can be noticed in the sensors correspondent to the downriver right side of the dam, the side that underwent light damage after the 2016 earthquake. Figure 57 displays the results of Table 10 in a graphic form. It can be noticed how the calculated velocities are well represented by the trend line, which lead to a velocity of 848 m/s in the North-South direction and 1030 m/s in the East-West direction.

Table 10 – sensors used for the ambient vibration tests, their coordinates and the distance of each sensor form the first at the downriver left side of the dam, taken as reference. The orange columns are relative to the North-South (upstream-downstream) direction, while the blue one are relative to the East-West direction (orthogonal to the former). In the first column of each direction, the measured time delay is reported (when the deconvolved wavefield was clear enough for picking), in the second column the calculated velocity is reported. Those data are also reported in the graphic of Figure 57.

Sensor	X	Y	Distance	N-S time delay (s)	N-S velocity (m/s)	E-W time delay (s)	E-W velocity (m/s)
A 112	83.87	25.64	REF.				
A 106	73.04	18.98	12.5				
A 101	61.69	13.27	25.1				
A 108	49.89	8.54	37.9			0.035	1082
A 107	37.73	4.82	50.6			0.045	1125
A 104	25.31	2.15	63.4	0.065	975	0.062	1022
A 114	12.7	0.54	76.1			0.07	1087
A 111	0	0	88.8	0.085	1045		
A 109	-12.7	0.54	101.6	0.12	846	0.1	1016
A 113	-25.31	2.15	114.3			0.115	994
A 103	-37.73	4.82	127.0	0.17	747	0.13	977
A 105	-49.89	8.54	139.8	0.19	736	0.14	999
A 110	-61.69	13.27	152.5	0.195	782	0.15	1017
A 102	-73.04	18.98	165.2	0.205	806	0.165	1001
A 100	-83.87	25.64	177.7			0.175	1015

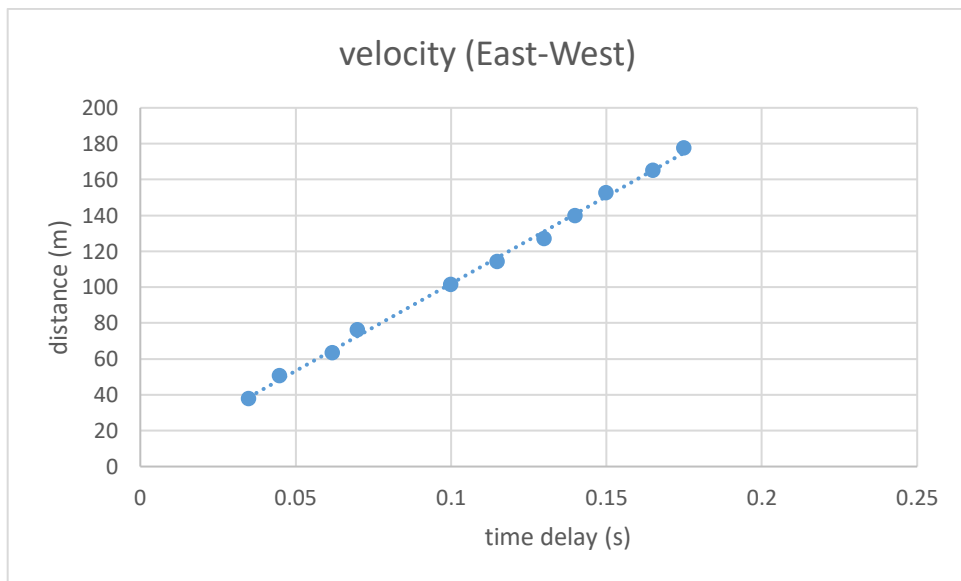
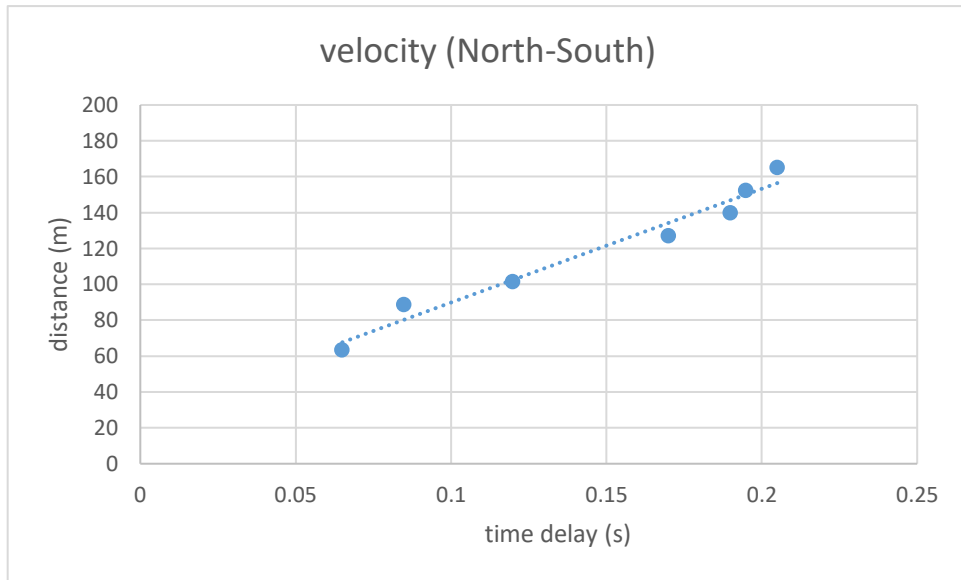


Figure 57 – diagram of the recorded delay time per each sensor and its distance from the first sensor deployed at the downriver left of the dam, in the North-South direction (upstream-downstream direction, panel a) and in the East-West direction (orthogonal to the former, panel b). The dotted line indicates the trend line; the slope of this line is the medium velocity (N-S - 848 m/s ; E-W - 1030 m/s).

To avoid the problem related to the curvature of the vertical array configuration, that could play a certain role in the velocity calculation, an attempt to analyse only the sensors close one to another was performed. The results of this attempt is shown in Figure 58. It can be noticed how this deconvolved wavefield can not be interpreted, since the two sensors are too close on to the other and the signal reached the second sensor substantially at the same time.

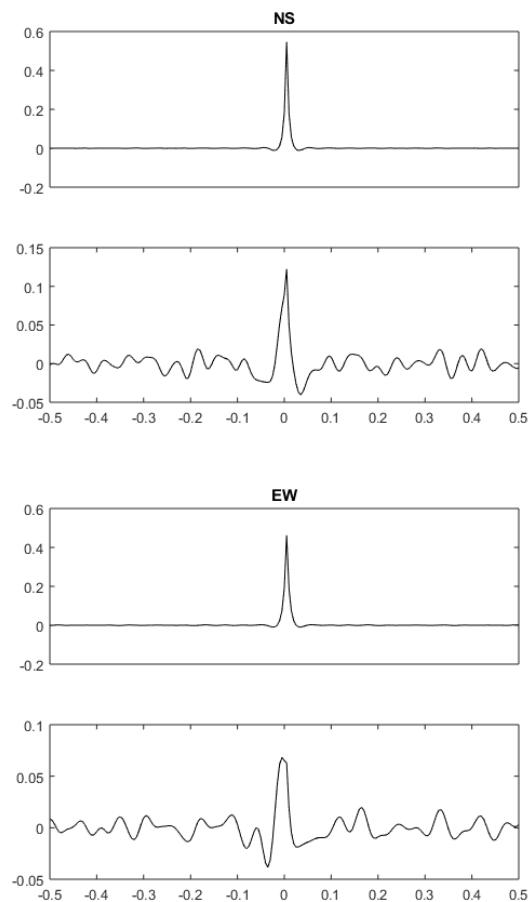


Figure 58 – deconvolved wavefield of ambient vibration recordings between two close receivers on the crest of the dam; after the earthquake, in the upstream-downstream, tangential and vertical directions. It can be seen as it is impossible to separate the two peaks related to the arrival of the causal and a-causal waves. Please note that the scale is different per each panel.

## 4.6.2 Ambient vibration test before the earthquake

Finally, the aim was to do a comparison between the ambient vibration recordings acquired before the earthquake and those acquired after it. The tests before the earthquake were performed using the same configuration of the instrument array as for the seismic events recordings described in the subchapter 4.4, one in the tunnel at the bottom of the dam and one in the tunnel immediately below the crest. The results of the deconvolved wavefield obtained by these recordings are displayed in Figure 59. It can be noticed that the time delay between the peaks, which are easily interpretable only on the North-South (upstream-downstream) direction, is much longer (0.266 s) than the one measured through the seismic events recordings (0.096s). This leads to a velocity which is of 330 m/s, much lower than the one identified through the seismic events recordings and even of that calculated on the ambient vibration recordings on the crest of the dam. Unfortunately, there are many factors that changed in the three different tests (the ambient vibration tests before and after the earthquake – 2015 and 2016 – and the seismic events recordings of 2017). In fact, the array configuration was the same in the 2015 ambient vibration tests and in the 2017 earthquakes recordings, but not in the 2016 ambient vibration tests, when a horizontal array on the crest was used. Also the instruments used in the three tests were different: in 2015 Tromino stations were used; in 2016 velocimeters LE-3Dlite were deployed; in 2017 accelerometers were used for seismic events recordings. Furthermore, in the 2015 campaign, which is the one that gave results significantly different from the other two, the instruments deployed were not synchronized, because the GPS was not available on the instruments. Therefore, I tried to synchronize the data through the autocorrelation analysis. Lastly, the reservoir water level was very different in the 2015 test (867 m.a.s.l.) and in 2016 and 2017 tests (849.6 m.a.s.l.). Given all these factors, it is fairly difficult to identify a unique cause for the different result obtained. In fact, the methods based on shear wave velocity are more sensitive to other methods to variations in the configuration of instruments deployment, and it might be tricky to obtain the real shear velocity instead of the apparent velocity. It would be interesting to investigate more deeply these factors, performing more tests



following a unique operational protocol, in order to exclude the factors that lead to the different results.

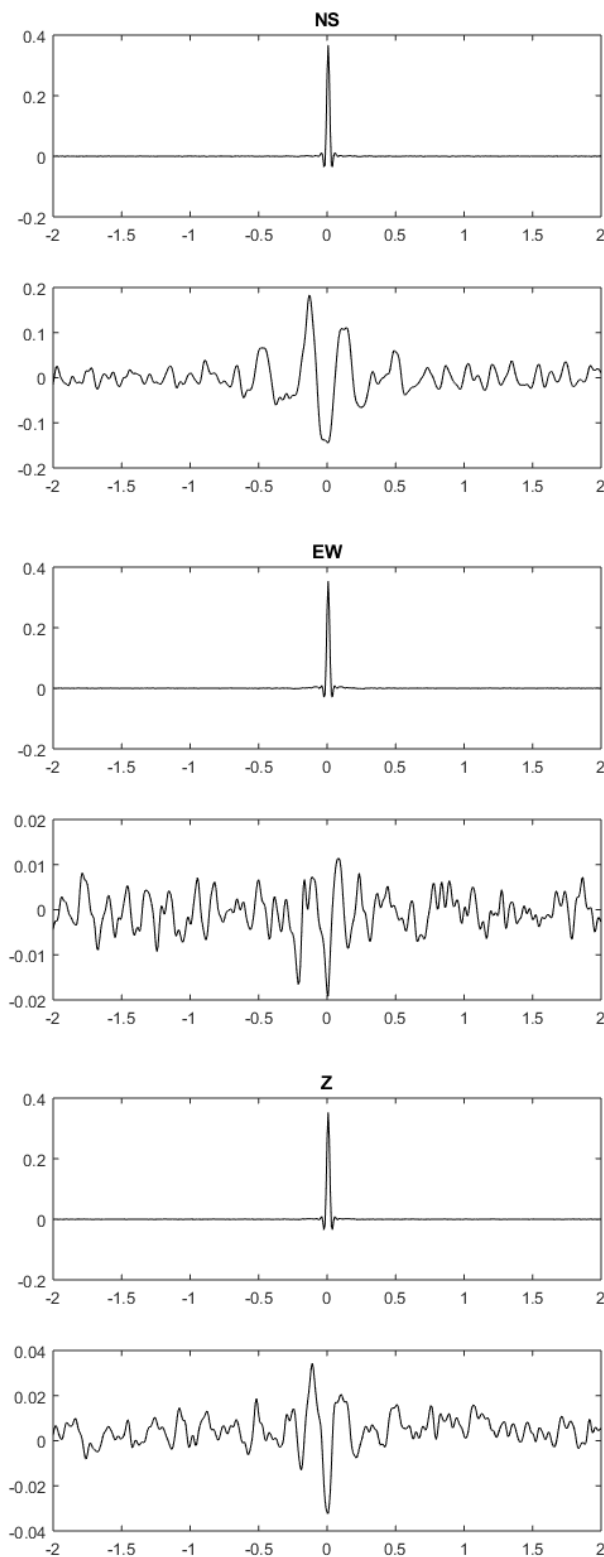


Figure 59 – deconvolved wavefield of ambient vibration recordings before the earthquake, in the upstream-downstream, tangential and vertical directions. Please note that the scale is different per each panel.

## 5 Discussion and comparison

After having exposed the results obtained with the different testing methods in the previous chapter, in this one I compare and discuss them.

### 5.1 Modal frequency and shapes comparison

In Table 11, a comparison between ambient vibration tests performed before and after the Central Italy 2016 earthquake with the results of forced vibration tests is reported. To facilitate the comparison, also Table 12 (copied Table 2), is reported as in the introduction to Chapter 4. As can be seen in these two tables, the first mode is the only one to show dissimilarities in the values identified with the three different techniques. Especially, the first mode is much higher in the ambient vibration test performed in 2016 after the earthquake. Obviously, this must not be interpreted as an index of damage caused by the earthquake, since in that case the frequency would have decreased. The difference in the frequency of the first mode should be imputed to the variation in the reservoir water level between the test performed in 2015 and the one in 2017, that is significant (more than 17 meters). The reason why in the other modes can not be detected any frequency variations attributable to the anti-symmetric deformed shape of these modes. In fact, in this case, the contribution of the water reservoir to the frequency variation is added in half of the structure and subtracted in the other half, becoming zero.

Table 11 – comparison between identified modal frequencies through forced vibration tests, FEM model matched and ambient vibration tests (AVT) before and after the Central Italy earthquake

Frequency 1 <sup>st</sup> mode				Frequency 2 <sup>nd</sup> mode				Frequency 3 <sup>rd</sup> mode			
FVT	FEM	AVT before	AVT after	FVT	FEM	AVT before	AVT after	FVT	FEM	AVT before	AVT after
5.1	5.3	4.8	5.7	6.8	6.4	6.9	6.9	9.1	8.6	8.7	8.9
4.8				6.3				8.8			
5.5				7.3				9.4			

Table 12– reservoir water level at the time of the surveys performed on the dam [meters above sea level]

Tests	Date (DD/MM/YYYY)	Reservoir level [m.a.s.l.]
Forced vibration tests	07/1988	866
Forced vibration tests	05/1993	865.3
Vibration tests (before earthquake)	02/07/2015	867
Vibration tests (after earthquake)	15/12/2016	849.6
Maximum reservoir lever	-	863.3

In the report obtained by the Civil Defence Department it was also available a comparison between the modal shapes obtained in 2016 through ambient vibration tests and those obtained with the two forced vibration surveys (1989 and 1993), shown in Figure 60.

The first mode is symmetric and concordant in the three cases. In the second and third mode, instead, an asymmetry can be noticed, characterized by a higher deformability in the hydraulic right; this difference can not be noticed with the forced vibration tests. The discrepancy is probably due to the different input considered. In the forced vibration tests, the source is applied in a point, in that case was in the centre of the dam and on the left side; whereas, in the ambient vibration tests there is not any specific application point for the source and the boundary condition are crucial for the modal identification.

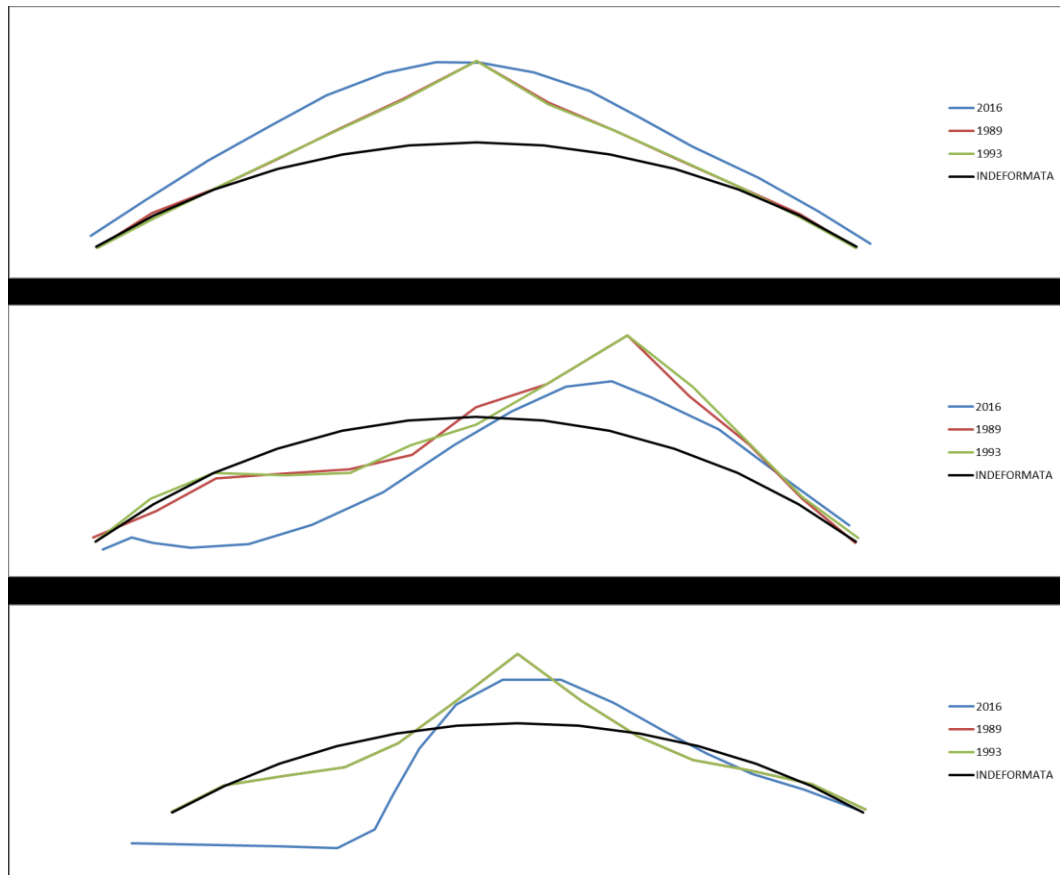


Figure 60 – comparison between the modal shapes obtained through the ambient vibration test after the earthquake (2016) and the forced vibration tests (1989 and 1993), with the un-deformed shape (black line) as reference.

The consultant firm who performed the forced vibration tests also provided a geo-mechanic characterization of the rock mass. The study identified two fundamental rock formations, one mainly marly and one arenaceous (Figure 61, Table 13). There are big differences between the elastic parameters of the two sides, therefore the right side is much more deformable than the other, justifying the asymmetry in the ambient vibration tests results.

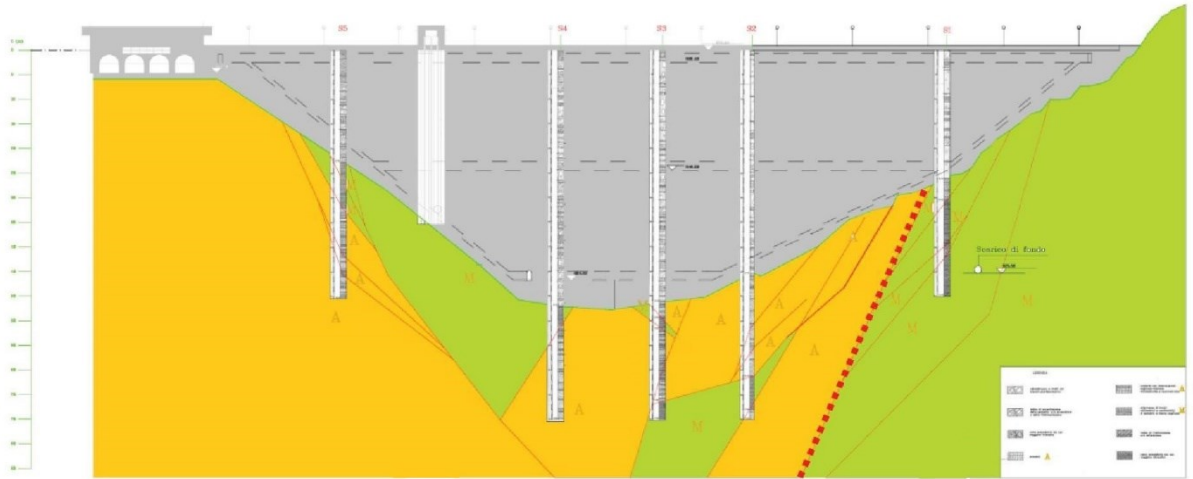


Figure 61 – geo-mechanical characterization provided by the dam’s dealer. Geological section of the rock mass.

Table 13 - geo-mechanical characterization provided by the dam's dealer – estimation of the parameters

	$\Phi$ (°)	C (MPa)	$E_m$ (MPa)
ARENACEE (SX)	30 – 32	5.2 – 7.3	7500 – 12100
MARNE (DX)	20 – 25	0.9 - 3.7	500 - 1830

The dynamic behaviour of the dam was studied through the tri-dimensional finite element model performed by the consultant engineering firm in their seismic assessment of the dam. The model was calibrated considering the experimental frequencies and modal shapes obtained from the forced vibration analysis, considering a coupled behaviour of the fluid-structure system. The frequency obtained by the model matched through the forced vibration tests are also reported in Table 11.

The Civil Defence engineers made a comparison between the modal shapes obtained through the ambient vibration test after the earthquake and those from the FEM model matched with the forced vibration test results. The modal shapes, showed in Figure 62, Figure 63 and Figure 64 for the three vibrational modes identified, are in a perfect agreement one another.

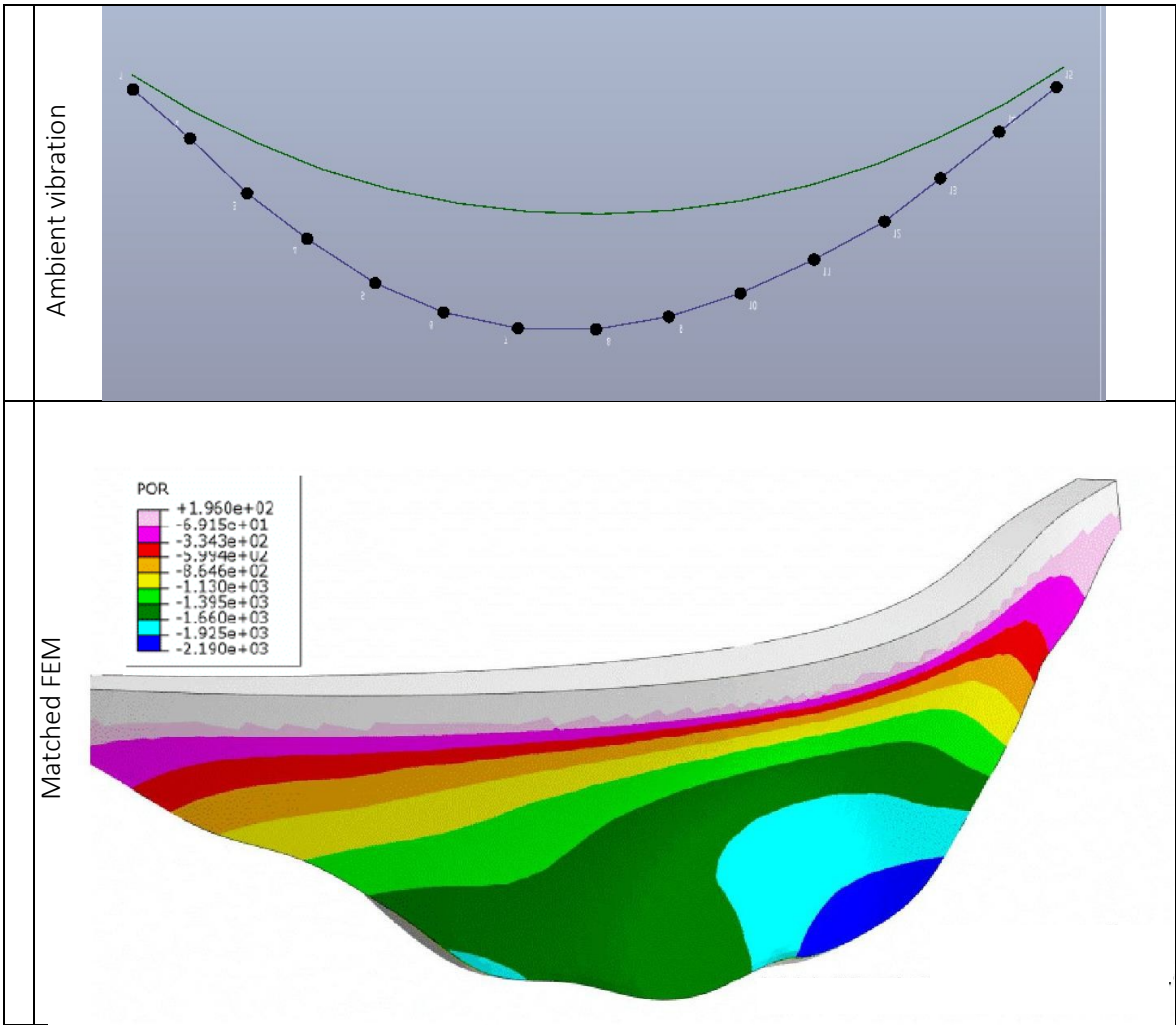


Figure 62 – Comparison between modal shapes identified through ambient vibration test (upper panel) and those calculated by the FEM model matched with the forced vibration test results(lower panel) – 1st vibrational mode

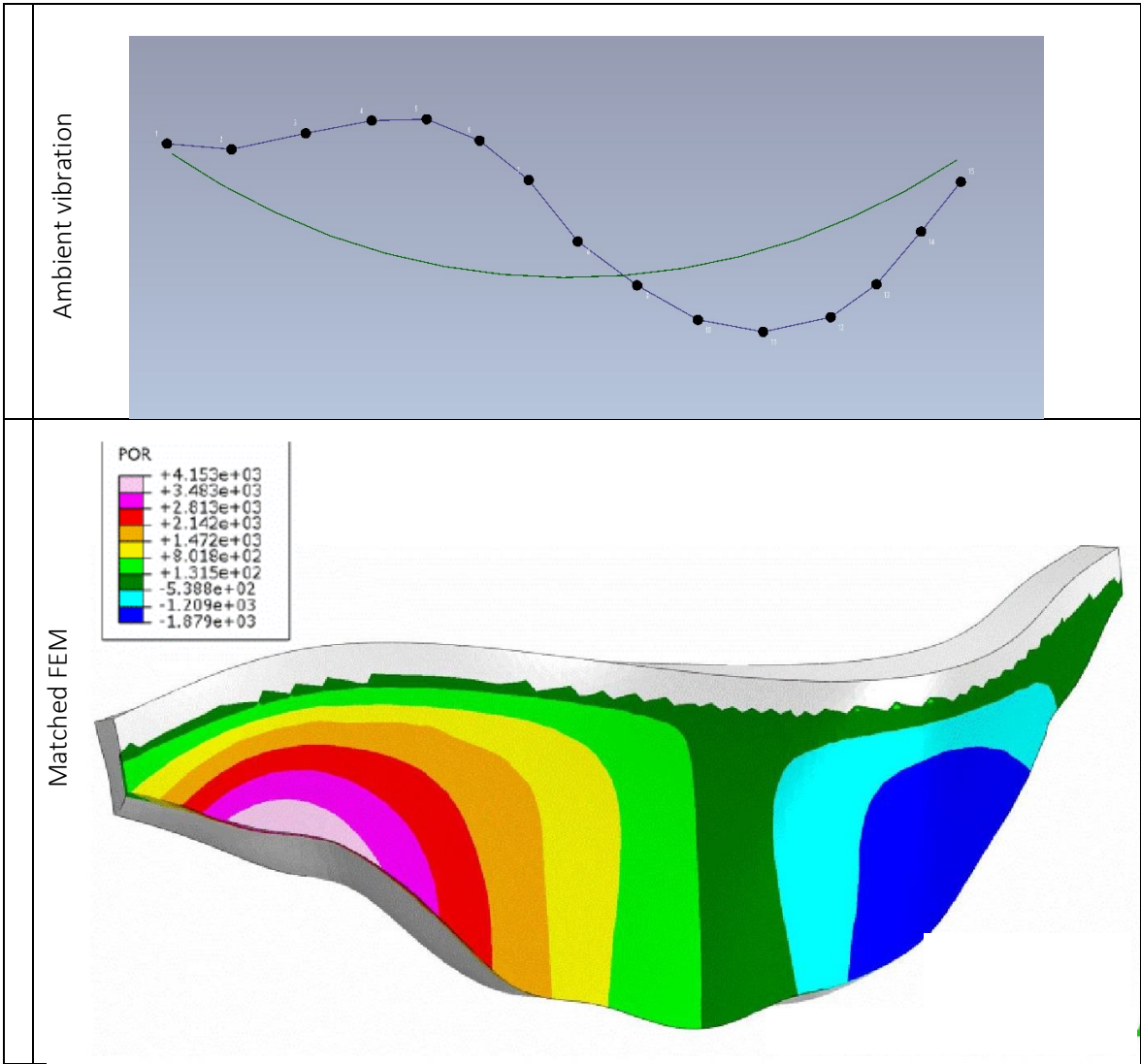


Figure 63 – Comparison between modal shapes identified through ambient vibration test (upper panel) and those calculated by the FEM model matched with the forced vibration test results(lower panel) – 2nd vibrational mode

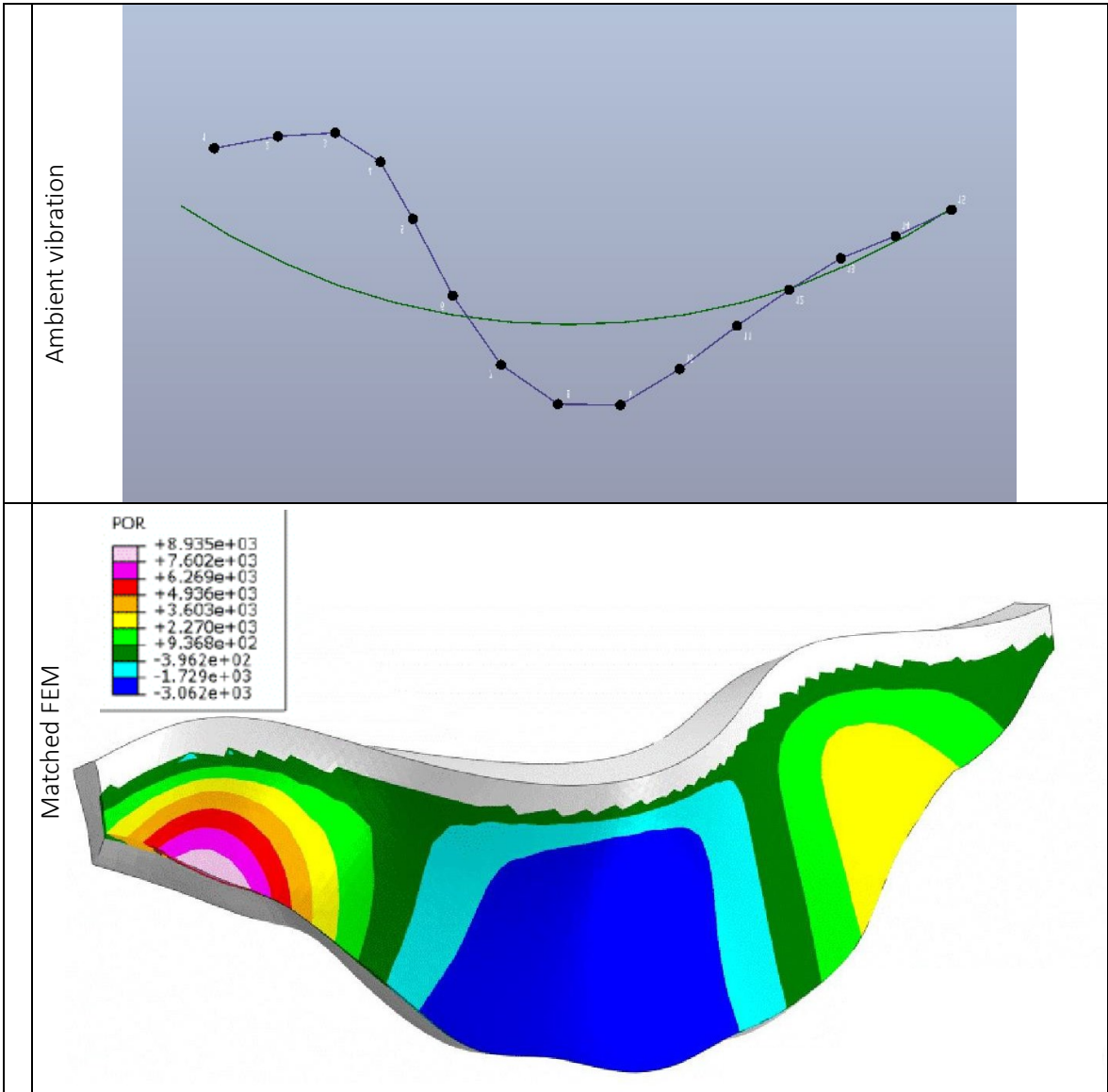


Figure 64 – Comparison between modal shapes identified through ambient vibration test (upper panel) and those calculated by the FEM model matched with the forced vibration test results(lower panel) – 3rd vibrational mode



## 5.2 Seismic deconvolution interferometry – applicability on dams

First of all, it is important to address the problem of the physical applicability of the method to the dam. To define a realistic model for the dam characterization and to theoretically verify all the equations presented in the subchapter 3.5 for that model would be complicated and far beyond the scope of this thesis. The dam in this case study shows a significant gravity behaviour, and that the section of the dam is very large (approximately 40 meters). Hence, just for the interferometric part of this work, it is possible to assume the structural block around the central vertical section of the dam to be representable as a clamped shear beam (see Figure 65), only as far as the upstream-downstream direction is concerned.

This assumption implies to ignore the effect both of bending and of the arch system in the behaviour of the considered section. Anyhow, the results exposed on the previous chapter, in which some comparisons were performed using the formulas valid for shear beams, are consistent with the data from the model and from the other analysis techniques, confirming the hypothesis. Of course, this would be an unjustifiable assumption in the case of a pure arch dam; in that case, the model should be revised and validated.

The model considered above is valid only for the transverse (upstream – downstream) direction, and not for the longitudinal one. The longitudinal direction (East-West axis of the deployed instruments) is actually difficult to address, because of the lateral constraints. Anyway, being the longitudinal direction of the dam extremely stiff (again because of the lateral constraints), we saw in the previous chapter that the wavefields in this direction are of difficult interpretation. Thus, we can consider that the most informative data are those recorded in the North-South direction (upstream-downstream) for the central transversal section of the dam, for which the clamped shear beam model is not that far from reality.

Furthermore, this assumption implies that the data acquired by the sensor deployed on the downstream right side of the tunnel below the crest are not suitable to be taken into

consideration. The resulting data in this case were in any case of difficult interpretation. Further studies would be needed to address this issue in order to be able to apply the interferometric approach based on seismic waves deconvolution also for different spatial configuration of sensors arrays.

Sensors arrays configuration affects and is affected by the possibility of having a lateral excitation. We saw in subchapter 3.5 that seismic deconvolution interferometry is used to separate the response of a building from that of the soil behind it, becoming independent from the excitation applied to the building. This is valid as long as there is not any source internal to the building, assumption that is actually reasonable in regular civil structures. On the contrary, in this case it should be considered that seismic sources are acting also (or even mostly) from the lateral constraints. The contribution of lateral excitation can be negligible in the central transverse section, but should be addressed if the array configuration includes sensors deployed on the sides of the dam.

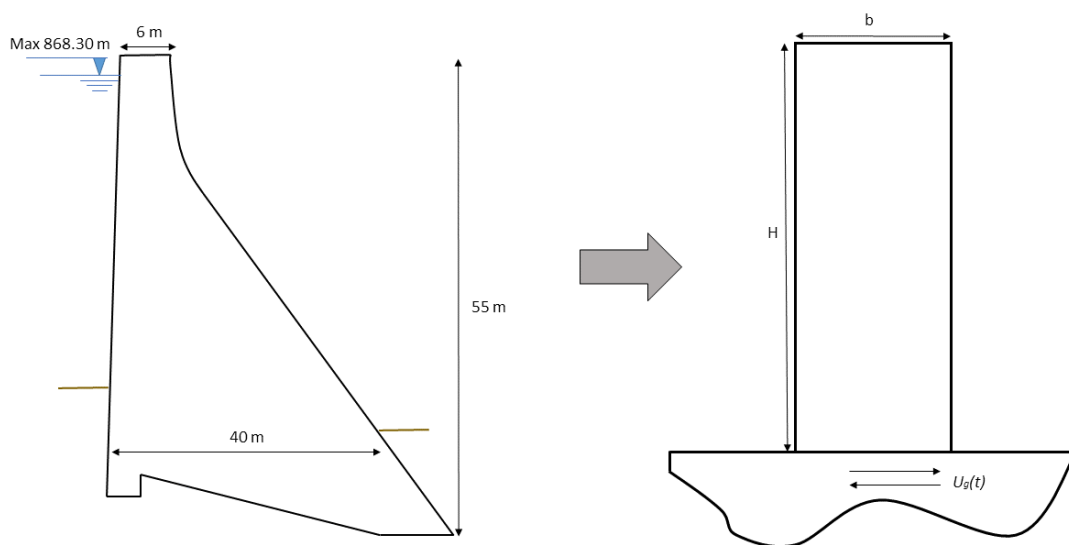


Figure 65 – Central transversal section of the case study dam (left); clamped shear beam model (right)

## 5.3 Seismic deconvolution interferometry – results discussion

In the subchapter 3.5 we saw that seismic deconvolution interferometry is used to separate the response of a building from that of the soil behind it, and in the subchapter 5.2 we discussed how it is possible to do the same for dams. It is anyhow important to specify that, in the case of dam, it is impossible to separate the behaviour of the structure from that of the water reservoir, acting on the structure throughout its height. Anyhow, also the numerical models of dams take into account a coupled soil-water behaviour.

The main results obtained through the tool of deconvolution are:

- Shear waves velocity:  $c = 916$  m/s
- Intrinsic attenuation damping: 3%

The damping calculated through the interferometric approach is much lower than the one calculated by forced vibration tests (3% instead of 8-10%), since in the latter case the radiation damping at the base of the structure is also considered. The damping calculated through deconvolution, instead, is only related to the structural attenuation. Anyhow, it must be considered that the damping parameter is complicated to be determined from experimental tests. Damping values increase with shaking amplitude and are frequency dependant. (Mikael et al., 2013). As in tall buildings aerodynamic effects may also contribute to damping, for dams a significant role is played by the water reservoir.

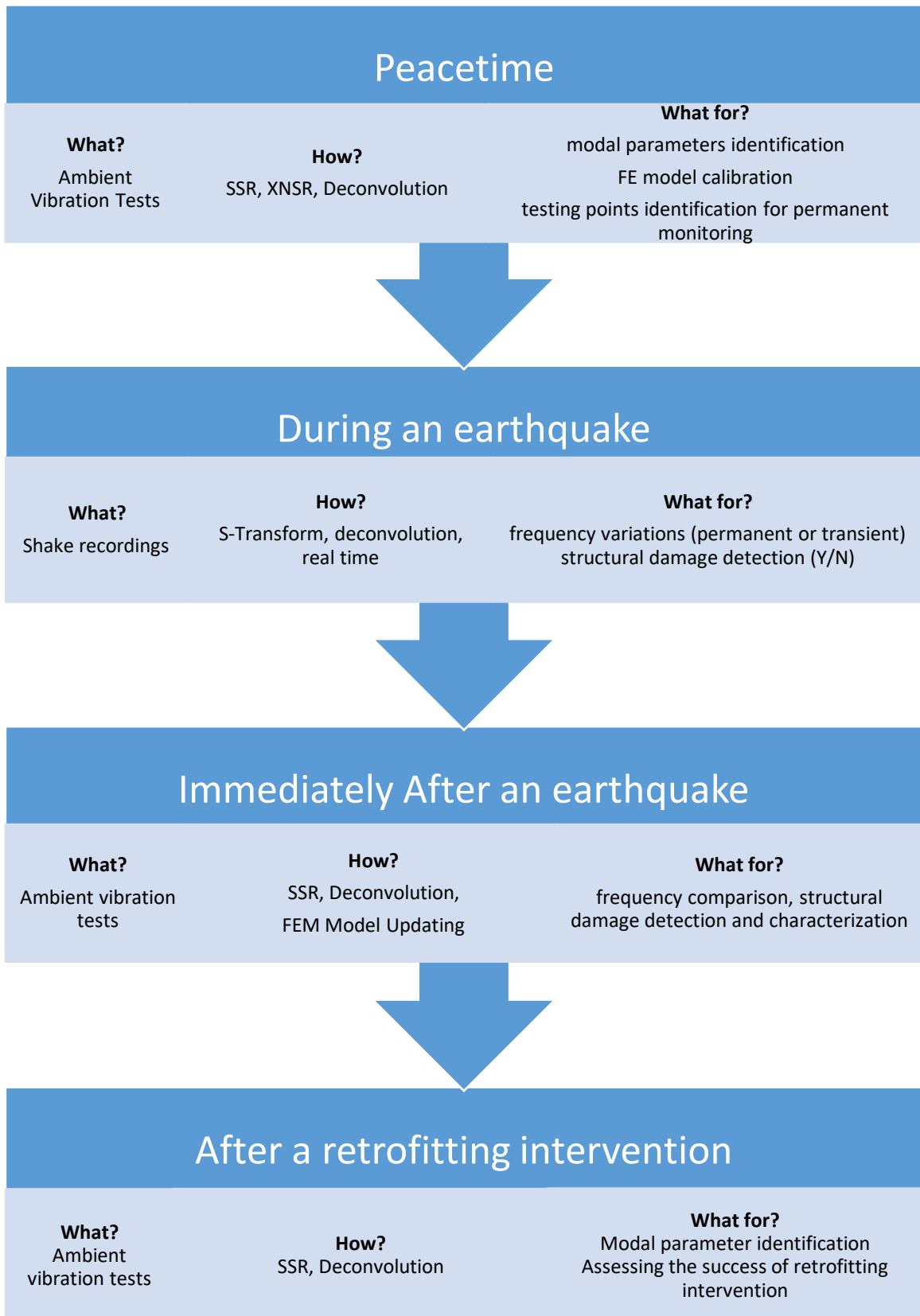
Unfortunately, the instruments array configuration in the three kind of passive tests performed (two ambient vibration tests – before and after the earthquake – and the seismic event recording) was different, hence the comparison between before and after the earthquake and between interferometry applied on seismic events or ambient vibrations was complex. Actually, there are actually many factors that changed in the three different tests (the ambient vibration tests before and after the earthquake – 2015 and 2016 – and

the seismic events recordings of 2017). In fact, the array configuration was the same in the 2015 ambient vibration tests and in the 2017 earthquakes recordings, but not in the 2016 ambient vibration tests, when a horizontal array on the crest was used. Also the instruments used in the three tests were different: in 2015 Tromino stations were used; in 2016 velocimeters LE-3Dlite were deployed; in 2017 accelerometers were used for seismic events recordings. Furthermore, in the 2015 campaign, which is the one that gave results significantly different from the other two, the instruments deployed were not synchronized, because the GPS was not available on the instruments. Therefore, I tried to synchronize the data through the autocorrelation analysis. Lastly, the reservoir water level was very different in the 2015 test (867 m.a.s.l.) and in 2016 and 2017 tests (849.6 m.a.s.l.). Given all these factors, it is fairly difficult to identify a unique cause for the different result obtained. It would be interesting to investigate more deeply these factors, performing more tests following a unique operational protocol, in order to exclude the factors that lead to the different results.

## 5.4 Use of ambient vibration tests for dam damage detection

For regular buildings, ambient vibration tests results can also be used as a reference to be compared with new data acquired after an earthquake occurs. In fact, a change in the dynamic properties of a building is usually a symptom of the presence of structural damage. It is, therefore, very easy to proceed with a Y/N classification of possible damage in a specific area. In the case of dams, instead, this comparison is not easy to perform, since a change in modal frequency can also be attributable to a variation in the reservoir water level or temperature. Therefore, the only way to perform a significant analysis on frequency variation due to a seismic event would be to analyse those frequency during the shaking. This can be done applying the Stockwell Transform to the earthquake recording. Of course, this could be implemented as a real time procedure of the structural monitoring system. A change in the frequency response of the structure is perfectly normal during the shock, since the structure undergoes non-linear behaviour; if the frequency drop does not recover after the shake, this should be considered as an indicator of structural damage. In this way, the dam's dealer or the Civil Defence Authority could immediately have a raw indicator of the structural integrity of the structure, detecting even hidden damage. Obviously, the damage assessment should be performed in a second step.

Ambient vibration tests could be used also as a preliminary, raw, indicator of the characteristics of possible damage. The results of the ambient vibration tests after the seismic event should be compared with the results of previous surveys campaign, of course considering also differences in boundary conditions (temperature, water level, etc.). The outcomes of the comparison can be an useful tool for the planning of the in-depth damage assessment and retrofitting intervention.



## 6. Conclusion

The aim of this work was to explore the possibility of using preliminary parameters from geophysical tests as a level zero of a multi-level approach to existing dams structural integrity monitoring.

In chapter 2, I discussed the issues related to the state of the art of dam monitoring. We saw that experimental tests are essential for the dynamic analysis of dams, but can often present several disadvantages. In fact, sometimes they could be very expensive, as happens for forced vibration tests. Moreover, they can be not representative of the general behaviour of the structure, as is for laboratory tests on material samples or tomography on a single section of the dam. They could even be strongly dependent on how the test was performed: for example, the vibrodyne test in this case study could not detect the major deformability of one of the two sides of the dam because the source was by chance applied to the other side. Which is more, they are usually significantly affected by the boundary conditions of the structure at the moment of the testing.

In chapter 3, the evolution of experimental modal testing on buildings is exposed, in order to find out which of the structural parameters provided by experimental tests could be suitable to be used as an index of structural integrity. That chapter ends with a review on the seismic deconvolution interferometry applied on buildings for the determination of shear wave velocity and damping factor. The technique can be applied both on seismic events recordings that on ambient vibration recordings, and is therefore suitable to be used to obtain the researched parameters from a continuous monitoring. These tests have been demonstrated to provide consistent results, easy to relate to the structural properties of engineering interest, as stiffness, frequency and damping. The parameters obtained by this technique are only related to the structure investigated and are completely independent from the characteristics of ground coupling and from the effects of the source.

To verify the applicability of the deconvolution interferometry approach on dams, a case study is analysed in chapter 4. A concrete arch-gravity dam located in Central Italy is assessed using different techniques. On the dam several survey campaigns were performed in different time periods (see Table 2). Two dynamic forced vibrations tests were performed in the past (July 1988 and May 1993), on the basis of which a finite element model was developed. In 2015 I performed an ambient vibration survey, together with an OGS team, with tri-axial digital high resolution tomographs (Tromino, Moho®). After this field campaign, one year later, the Central Italy earthquake of the 24<sup>th</sup> August 2016 happened and hit the structure, causing non-structural damage. Soon after, in December 2016, the Civil Defence Department repeated the ambient vibration tests on the dam. These test preceded the installation of a permanent dynamic monitoring system (installed in February 2017), belonging to the Seismic Observatory for Structures (*OSS – Osservatorio Sismico delle Strutture*). The monitoring system recorded five seismic events (listed in Table 3), which are analysed in this thesis using deconvolution interferometry.

The accurate modelling of the dam, beside being not innovative, is far beyond the aim of this thesis. In fact, accurate dam numeric modelling are already widely used for dam design and verification, and a FEM model was built several years ago also for the dam of this case study. On the other hand, as previously discussed in this thesis, numerical model can be very far from real and actual condition of a dam, because of changes in the boundary conditions (water level, water and air temperature, ...) or changes in the structure itself, due to long term deterioration (aging or intrinsic defects) or due to shocks (seismic events or accidents). Therefore, it is always unavoidable to use both methods (numerical model and experimental testing) when verifying an existing dam. On the other hand, the organization of the necessary survey campaigns on dams is a delicate issue.

The aim of the thesis was to test the possibility of using a set of preliminary parameters to decide when and how to organize further structural investigations, optimizing their cost and accuracy. The parameters researched should be the outcome of a method that must be cost effective and therefore simplified. The identification of a set of parameter related to the structural characteristic of the dam, as stiffness, damping and frequency, could give earliest evidences in order to optimize the planning of detailed surveys. The large amount of data recorded on this specific dam was used in order to compare the results obtained with the



different techniques, working as a consistency check on the outcomes of the interferometric approach based on deconvolution.

Obviously, the physical model of the dam is highly complicated, because of the curvature of the structural elements, the lateral constraints, the stress distribution, the variations in the section thickness, not to mention the interaction with the foundation soil and with the water reservoir. Though, the aim of this thesis was to propose a cost effective and easy to apply experimental method for a preliminary assessment of the structural integrity of the dam. To do so, an extremely simplified structural model was considered. Specifically, only as far as seismic waves propagation inside the structure is concerned, a clamped shear beam was assumed to be representative of the central section of the dam, where the instruments were deployed. It would be interesting to further theoretically investigate this assumption, in order to build a model valid also for sensors configuration far from the centre of the crest, so to address the issue of sensors array configuration. It is, indeed, quite a thorny problem to identify the optimal locations for the installation of sensors on a dam. As already discussed, dams' structural behaviour is defined not only and not mainly by the first vibrational mode: superior modes play a key role. Moreover, as was shown for the dam taken as a case study, the dam could present some kind of asymmetric behaviour, which can be highlighted by ambient vibration tests, and that should lead to more in-depth surveys. Therefore, if the instruments are installed only in one point (at the centre of the crest), one may lose crucial information about its dynamic behaviour. On the other hand, one of the mandatory characteristics of this system, to be affordable on a large number of dams, is to be cost effective. Therefore, low cost instruments should be used and on a reasonably little number of testing points. Hence, ambient vibration tests can be a useful tool for planning the installation of a permanent monitoring system, identifying the best installation points to optimize provided information.

The results obtained by the seismic deconvolution interferometry are actually promising. The identification of structural frequency was quite accurate for all the tests performed and for all the structural modes. The shear wave velocity inside the structure, in the central section of the dam, was estimated to be around 900 m/s. This value of velocity could be expected, since shear wave velocity inside regular buildings is usually around 300 m/s, but the investigated dam is much stiffer and does not present any empty spaces except the

tunnels, which are negligible in comparison to the geometric dimensions of the dam. The consistency of this velocity value was also checked through the formula, valid for the shear beam model, which relates the fundamental frequency to the measured velocity, obtaining a value of frequency very close to the one determined by forced and ambient vibration tests, although the excessively simplification assumed to apply this formula. The damping was calculated too, using the attenuation of the recorded wavefield. We must recall that this results only concerns the intrinsic structural attenuation and does not include the radiation damping at the base of the dam. Thus, the value obtained with this analysis is much lower than the one obtained by the forced testing (3% instead of 8%).

The several experimental tests on the dam whose results have been analysed in this thesis were not planned in a systematic way. Tests were performed by several actors in various time periods, using disparate instruments, with different array configurations, for different purposes and – especially – with variations in reservoir water level. Hence, it was not easy to compare the results obtained, except for structural frequency identification that gave satisfactory results. Considering the promising outcomes of this first explorative study, it would be interesting to apply the seismic deconvolution interferometry approach on a significant sample of existing dam, following a common a-priori *operational protocol* to perform the tests, in order to be able to easily compare the results.

If deconvolution interferometry will be proven to be efficient on a larger scale test, it would be interesting to define an operational protocol for structural testing using geophysical techniques. This protocol should include instructions to successfully undertake a first approach based on ambient vibration tests, including the description of the methods for the analysis of data. Seismic deconvolution can be used also in this phase. Then, the protocol should include the instructions to plan (if it is considered necessary) the permanent monitoring system: how many instruments, how and where they should be deployed, on the basis of the results of the preliminary ambient vibration tests. In the case any seismic event is recorded during the permanent monitoring campaign, the deconvolution interferometry approach can be instantly applied both on the seismic recordings that on the ambient recording obtained immediately before the event. In this case, we can assume that the boundary conditions (i.e. the reservoir water level, since the source and the soil influences are already excluded in the approach) does not undergo any variation. Therefore,

if the results of the deconvolution approach highlight some variations, they can be attributed to a change in the structural parameters of the dam. In this case, further investigation should be planned taking into consideration the *ensemble* of the results from deconvolution on seismic events and on ambient vibrations. Finally, deconvolution interferometry can be used also for periodic verifications of dams structural conditions, being careful on repeating the test with comparable boundary conditions (for example, to plan the periodic tests always in the same period of the year, with a certain reservoir water level and temperature).

In conclusion, in the framework of a multi-level approach to dam dynamical characterization, structural parameters (frequency, shear wave velocity and structural damping) are able to provide useful preliminary information – although raw and incomplete – in order to address further levels of investigation. The advantage of using these parameters is that they can be obtained through non-invasive cost-effective techniques. Among these techniques, deconvolution interferometry has the benefit to be able to separate the structural answer from the influence of the source and of the soil. Far from being exhaustively representative of the complex structural behaviour of the dam, structural parameters obtained in this way could be used as a preliminary explorative indication on structural integrity condition, to address conventional ordinary and extraordinary monitoring methods.

# References

- Abdulmit A., Demetriu S., Aldea A., Neagu C. and Gaftoi D.; 2017: *Ambient Vibration Tests at Some Buttress Dams in Romania*. X International Conference on Structural Dynamics, EURODYN 2017.
- Acikgoz S. and DeJong M.J.; 2017: *Vibration modes and equivalent models for flexible rocking structures*. Bulletin of Earthquake Engineering (2017) 15:4427–4452 DOI 10.1007/s10518-017-0128-4
- Allemang R.J.; 2003: *The Modal Assurance Criterion – Twenty Years of Use and Abuse*. Sound and vibration, August 2003.
- Allemang R.J. and Brown D.L.; 1982: *A correlation coefficient for modal vector analysis*. First International Modal Analysis Conference (IMAC), Orlando, FL, 1982.
- Antonovskaya G.N, Kapustian N.K., Moshkunov A.I., Danilov A.V. and Moshkunov K.A.; 2017: *New seismic array solution for earthquake observations and hydropower plant health monitoring*. Journal of Seismology (2017) 21:1039–1053 DOI 10.1007/s10950-017-9650-8.
- Barazza F., Grimaz S., Malisan P.; 2009. *Individuation of vulnerability parameters by passive tremor measurements*. Atti del 28 Convegno Nazionale Gruppo Nazionale di Geofisica della Terra Solida. :430-433.
- Bard P.Y., Guéguen P. and A.Wirgin; 1996: *A note on the seismic wavefield radiated from large building structures into soft soil*, Proceedings of the 11th World Conference on Earthquake Engineering, Acapulco, 23-28 June, paper n.1838
- Bindi, D., Petrovic, B., Karapetrou, S., Manakou, M., Boxberger, T., Raptakis, D., Pitilakis, K. D., Parolai, S.; 2015: *Seismic response of an 8-story RC-building from ambient vibration analysis*. Bulletin of Earthquake Engineering, 13, 7, p. 2095-2120.
- Bonnefoy-Claudet S., Cotton F., Bard P.-Y.; 2006: *The nature of noise wavefield and its applications for site effects studies. A literature review*. Earth-Science Reviews 79 (2006) 205–227
- Borcherdt R.D.; 1970. *Effects of local geology on ground motion near San Francisco Bay*. Bull Seism. Soc. Am., 60:29–61.
- Bolisetti C. and Whittaker A. S.; 2015: *Site Response, Soil-Structure Interaction and Structure-Soil-Structure Interaction for Performance Assessment of Buildings and Nuclear Structures*. Technical Report CEER-15-0002 June 15, 2015.

- Boutin C. and Hans S.; 2009 : *How Far Ambient Noise Measurement May Help to Assess Building Vulnerability?* In *Increasing Seismic Safety by Combining Engineering Technologies and Seismological Data*, NATO Science for Peace and Security Series C: Environmental Security, 2009, XVII, pp. 151-180.
- Brincker R, Ventura C and Andersen P; 2003: *Why output-only modal testing is a desirable tool for a wide range of practical applications*. Twenty-first International Modal Analysis Conference (IMAC), Kissimmee, FL, 2003.
- Brincker R., Zhang L. and Andersen P.;2001: *Modal identification of output only systems using frequency domain decomposition*. Smart Materials and Structures 2001;10:441–5.
- Bukenya P., Moyo P. and Oosthuizen C.; 2012: *Comparative study of operational modal analysis techniques using ambient vibration measurements of a concrete dam*. Proceedings of ISMA2012-USD2012.
- Calcina S. V., Eltrudis L., Piroddi L. and Ranieri G.; 2014: *Ambient Vibration Tests of an Arch Dam with Different Reservoir Water Levels: Experimental Results and Comparison with Finite Element Modelling*. Hindawi Publishing Corporation, The Scientific World Journal, Volume 2014, Article ID 692709, 12 pages – <http://dx.doi.org/10.1155/2014/692709>
- Cao Haitao; 2016: *Comparison of seismic interferometry by cross correlation, deconvolution and cross coherence*. MS thesis, Michigan Technological University.
- Capizzi P., Martorana R., Pirrera C. and D'Alessandro A.; 2016: *Seismic Investigation for the Characterization of a Gravity Concrete Dam*. Near Surface Geoscience 4-8 September 2016, Barcelona, Spain.
- Castro R.R., Mucciarelli M., Pacor F., Federici P., Zaninetti A.; 1998: *Determination of the characteristic frequency of two dams located in the region of Calabria, Italy*. Bulletin of Seismological Society of America, 88(2):503–511.
- Chen X., Omenzetter P. and Beskhyroun S.; 2014: *Ambient vibration testing, system identification and model updating of a multiple-span elevated bridge*. Proceedings of the 9th International Conference on Structural Dynamics, EURO-DYN 2014 Porto, Portugal, 30 June - 2 July 2014 A. Cunha, E. Caetano, P. Ribeiro, G. Müller (eds.) ISSN: 2311-9020; ISBN: 978-972-752-165-4
- Chiauzzi Chiauzzi L., Masi A. and Mucciarelli M. Cassidy J. F. Kutyn K., Traber J., Ventura C. & Yao F; 2012: *Estimate of fundamental period of reinforced concrete buildings: code provisions vs. experimental measures in Victoria and Vancouver (BC, Canada)*. 15 WCEE Lisboa 2012

- Clinton J.F., Bradford S. C., Heaton T.H., Favela J.; 2006: *The Observed Wander of the Natural Frequencies in a Structure*. Bulletin of the Seismological Society of America 96, no. 1, 237–257.
- De Sortis A. and Paoliani P.; 2005: *Statistical and Structural Identification Techniques in Structural Monitoring of Concrete Dams*. Paper No.: 216-S6, 73<sup>rd</sup> Annual Meeting of ICOLD, Teheran, Iran, May 1-6 2005.
- Del Gaudio V., Coccia S., Wasowski J., Gallipoli M.R. and Mucciarelli M.; 2008: *Detection of directivity in seismic site response from microtremor spectral analysis*. Nat. Hazards Earth Syst. Sci., 8, 751-762. [www.nat-hazards-earth-syst-sci.net/8/751/2008](http://www.nat-hazards-earth-syst-sci.net/8/751/2008)
- Di Giulio G., Azzara R.M., Cultrera G., Giammarinaro M.S., Vallone P., Rovelli A.; 2005: *Effect of local geology on ground motion in the city of Palermo, Italy, as inferred from aftershocks of the 6 September 2002 MW 5.9 earthquake*. Bulletin of Seismological Society of America, 95:2328–2341.
- Di Marcantonio P. and Ditommaso R.; 2012: *Effetti dell'irregolarità strutturale e dell'interazione dinamica terreno-struttura: tre casi studio*. Tecniche speditive per la stima dell'amplificazione sismica locale, Aracne Editrice, January 2012. [in Italian]
- Ditommaso R., Vona M., Gallipoli M.R. and Mucciarelli M.; 2013: *Evaluation and considerations about fundamental periods of damaged reinforced concrete buildings*. Natural Hazards and Earth System Sciences, 13, 7, 1903-1912.
- Ditommaso R., Mucciarelli M., Parolai S., Picozzi M.; (2012). *Monitoring the structural dynamic response of a masonry tower: comparing classical and time-frequency analyses*. Bulletin of Earthquake Engineering, 10, 4, 1221-1235. Doi: 10.1007/s10518-012-9347-x.
- Dunben S. and Qingwen R.; 2016: *Seismic Damage Analysis of Concrete Gravity Dam Based on Wavelet Transform*. Hindawi Publishing Corporation - Shock and Vibration. Volume 2016, Article ID 6841836, <http://dx.doi.org/10.1155/2016/6841836>.
- EN 1998-1 (2004) (English): *Eurocode 8: Design of structures for earthquake resistance – Part 1: General rules, seismic actions and rules for buildings*. Authority: The European Union Per Regulation 305/2011, Directive 98/34/EC, Directive 2004/18/EC.
- Farrar C.R. and James III G.H.; 1997: *System identification from ambient vibration measurements on a bridge*. Journal of Sound and Vibration, Volume 205, Issue 1, 7<sup>th</sup> August 1997, pages 1-18 <http://doi.org/10.1006/jsvi.1997.0977>
- Fornari F.; 2013: *Gli interventi riabilitativi delle dighe in Italia*. Presentazione ITCOLD – Osservatorio permanente sulla Riabilitazione delle dighe – Giornata mondiale dell'acqua 20 marzo 2013. [in Italian]

- Fujino Y. and Abe M.; 2002: *Vibration – based health monitoring of bridges using ambient motion*. Structural Dynamics, EURO-DYN2002, Grunfmann&Schuëller ISBN 90 5809510 X
- Gallipoli M.R., Stabile T.A., Guéguen P., Mucciarelli M., Comelli P. and Bertoni M.; 2016: *Fundamental period elongation of a RC building during the Pollino seismic swarm sequence*. Case Studies in Structural Engineering 6 (2016) 45–52.
- Gallipoli M.R., Mucciarelli M., Šket-Motnikar B., Zupančić P., Gosar A., Prevolnik S., Herak M., Stipcević J., Herak D., Milutinović Z. and Olumčeva T.; 2010: *Empirical estimates of dynamic parameters on a large set of European buildings*. Bulletin of Earthquake Engineering, 8, 593–607.
- Gallipoli M.R.; 2004: *Tecniche geofisiche integrate*. [in Italian]
- Gallipoli M.R., Mucciarelli M., Castro R.R., Monachesi G. and Contri P.; 2004: *Structure, soil–structure response and effects of damage based on observations of horizontal-to-vertical spectral ratio of microtremors*. Soil Dynamics and Earthquake Engineering, 24(6):487–495.
- Gallipoli M.R., Mucciarelli M. and Vona M.; 2008. *Empirical estimate of fundamental frequencies and damping for Italian buildings*. Earthquake Engineering & Structural Dynamics, 18 December 2008. Doi: 10.1002/eqe.878.
- Gaohui W., Yongxiang W., Wenbo L., Mao Y., Chao W.; 2017: *Deterministic 3D seismic damage analysis of Guandi concrete gravity dam: A case study*. Engineering Structures 148 (2017) 263–276
- Grimaz S., Barazza F. and Malisan P.; 2012. *Misure all'interno degli edifici. Tecniche speditive per la stima dell'amplificazione sismica e della dinamica degli edifici. Studi teorici ed applicazioni professionali*.:195-209.
- Guéguen P., Gallipoli M.R., Navarro M., Masi A., Michel C., Guillier B., Karakostas C., Lekidis V., Mucciarelli M., Ponzio F. and Spina D.; 2014. *Testing Buildings Using Ambient Vibrations for Earthquake Engineering: a European Review*. Second European Conference on Earthquake Engineering, Istanbul, Aug. 25-29, 2014.
- Guéguen P., Bard P. Y. and Chavez-Garcia F.J.; 2002: *Site-City Seismic interaction in Mexico City-Like Environments: An Analytical Study*. Bull. Seism. Soc. Am., 92, 2, 794-811.
- Hans S., Boutin C., Ibrahim E. and Roussillon P; 2005: *In situ experiments and seismic analysis of existing buildings. Part I: experimental investigations*. Earthquake Engineering and Structural Dynamics, 34, 1513–1529.
- Huang C.S. and Lin H.L.; 2010: *Modal identification of structures from ambient vibration, free vibration, and seismic response data via a subspace approach*. Earthquake Engineering and Structural Dynamics 2001; 30:1857–1878. DOI: 10.1002/eqe.98.

- ICOLD International Commission on Large Dams; 2000: *Automated Dam Monitoring Systems: Guidelines and Case Histories*, Volume 118 of Bulletin (International Commission on Large Dams)
- ITCOLD a) Comitato Nazionale Italiano delle Grandi Dighe; 2012: *Dighe ed energia elettrica*. [in Italian]
- ITCOLD b) Comitato Nazionale Italiano delle Grandi Dighe; 2012: *Riabilitazione delle dighe. Roma 2012*. [in Italian]
- ITCOLD c) Comitato Nazionale Italiano delle Grandi Dighe; 2012: *Potenzialità, limiti e possibili sviluppi delle tecniche di identificazione strutturale per la diagnostica delle dighe* [in Italian]
- ITCOLD Comitato Nazionale Italiano delle Grandi Dighe; 2014: *Riabilitazione delle dighe, osservatorio permanente – rapporto maggio 2014*. [in Italian]
- ITCOLD Comitato Nazionale Italiano delle Grandi Dighe; 2012. *Potenzialità, limiti e possibili sviluppi delle tecniche di identificazione strutturale per la diagnostica delle dighe*. [in Italian]
- ITCOLD Comitato Nazionale Italiano delle Grandi Dighe; 1998. *La verifica sismica delle normative – Criteri generali e confronto con le normative*. [in Italian]
- ITCOLD; 1988: *Tecniche e realizzazioni italiane per il monitoraggio delle dighe e delle fondazioni*. *Bollettino* n.1, 1988 [In Italian]
- Ivanović S.S., Trifunac M.D. and Todorovska M.I.; 2000: *Ambient vibration tests of structures – a review*. ISET Journal of Earthquake Technology, Paper NO. 407, Vol. 37, No. 4, December 2000, pp. 165-197.
- Jian Y., Feng J., Jin-Ting W. and Li-Hang K.; 2017: *System identification and modal analysis of an arch dam based on earthquake response records*. *Soil Dynamics and Earthquake Engineering* 92 (2017) 109–121.
- Jacobsen N. J., Andersen P., Brinker R.; 2008: *Applications of Frequency Domain Curve-fitting in the EFDD Technique*. Conference Proceedings : Imac-XXVI : a Conference & Exposition on Structural Dynamics, 2008.
- Jennings P. C.; 1970: *Distant motion from a building vibration test*. *Bull.Seism.Soc.Am.*, 60, 2037-2043.
- Kanamori H., Mori J., Anderson D. L. and T.H. Heaton; 1991: *Seismic excitation by the space shuttle Columbia*, *Nature*, 349, 781-782.
- Karapetrou S., Manakou M., Bindi D., Petrovic B., Potilakis K.; 2016: “Time-building specific” seismic vulnerability assessment of a hospital PC building using field monitoring data.



- Karastathis V.K., Karmis P.N., Drakatos G. and Stavrakakis G.; 2002: *Geophysical methods contributing to the testing of concrete dams. Application at the Marathon Dam*. Journal of Applied Geophysics, vol. 50, no. 3, 247- 260
- Kotkar R.K. and Patankar J. P.; 2017: *Effect of Soil Structure Interaction on Buildings with Stiffness Irregularity under Seismic Load*. International Research Journal of Engineering and Technology (IRJET) Volume: 04 Issue: 07 | July -2017 e-ISSN: 2395-0056
- Kumar R., Sumathi P. and Kumar A.; 2015: *Analysis of frequency shifting in seismic signals using Gabor-Wigner transform*. Earthquake Engineering and Engineering Vibration (2015) 14: 715-724. DOI: 10.1007/s11803-015-0056-8.
- Lobkis O.I. and Weaver R.L.; 2001: *On the emergence of the Green's function in the correlations of a diffuse field*. Acoustical Society of America. DOI: 10.1121/1.1417528
- Loddo G. and Komin A.; 2015. *Controllo con metodi geodetici e geofisici di grandi dighe*. Il Nuovo Cantiere, 10 ottobre 2015.
- Malisan P., Grimaz S., Riuscetti M., Barazza F., Puntel E., Carniel R, Del Pin E., Di Cecca M.; 2008: *Utilization of passive seismic methods for a rapid dynamical characterization of structures: the Salt bridge case study*. Atti 27 Convegno Nazionale Gruppo Nazionale di Geofisica della Terra Solida. :355-360.
- Masi A.; 2009: *Role of Dynamic Properties on Building Vulnerability*. In *Increasing Seismic Safety by Combining Engineering Technologies and Seismological Data*. NATO Science for Peace and Security Series C: Environmental Security, 2009, XVII, p. 147-148.
- McCann D.M. and Forde M.C.; 2001: *Review of NDT methods in the assessment of concrete and masonry structures*. NDT&E International 34 (2001) 71–84.
- Michel C., Guéguen P., El Arem S., Mazars J. and Kotronis P.; 2010: *Full-scale dynamic response of an RC building under weak seismic motions using earthquake recordings, ambient vibrations and modelling*. Earthquake Engineering and Structural Dynamics 2010; 39:419–441. DOI: 10.1002/eqe.948
- Michel C. and Guéguen P.; 2009: *Time-Frequency Analysis of Small Frequency Variations in Civil Engineering Structures Under Weak and Strong Motions Using a Reassignment Method*. Structural Health Monitoring 2010 9: 159 originally published online 4 December 2009 DOI: 10.1177/1475921709352146
- Michel C., Guéguen P. and Bard P.-Y.; 2008: *Dynamic parameters of structures extracted from ambient vibration measurements: An aid for the seismic vulnerability assessment of existing buildings in moderate seismic hazard regions*. Soil Dynamics and Earthquake Engineering 28 (2008) 593–604.

- Ministero delle Infrastrutture e dei Trasporti, Direzione Generale per le Dighe e le infrastrutture Idriche ed Elettriche; 2017. <http://www.registroitalianodighe.it/>
- Ministero delle Infrastrutture e dei Trasporti; 2014: *Decreto del Ministro delle Infrastrutture e dei Trasporti 26 giugno 2014 - Norme tecniche per la progettazione e la costruzione degli sbarramenti di ritenuta (dighe e traverse)*. Pubblicato sulla Gazzetta Ufficiale della Repubblica Italiana, Serie generale - n. 156 del 7-8-2014. [in Italian]
- Mikael A., Guéguen P., Bard P.-Y., Roux P. and Langlais M.; 2013: *The Analysis of Long-Term Frequency and Damping Wandering in Buildings Using the Random Decrement Technique*. Bulletin of the Seismological Society of America, Vol. 103, No. 1, pp. 236–246, February 2013, doi: 10.1785/0120120048
- Mucciarelli M.; 2011: *Tecniche speditive per la stima dell'amplificazione sismica e della dinamica degli edifici*. Studi teorici ed applicazioni professionali. ARACNE editrice S.r.l.
- Mucciarelli M., Herak M. and Cassidy J.; 2009: *Increasing Seismic Safety by Combining Engineering Technologies and Seismological Data*. NATO Science for Peace and Security Series C: Environmental Security, 2009, XVII, 382 p.
- Mucciarelli M. and Gallipoli M.R.; 2007: *Damping estimate for simple buildings through non-parametric analysis of a single ambient vibration recording*. Annals of Geophysics, 50, 259–266.
- Mucciarelli M., Gallipoli M.R., Masi A., Vona M., Ponso F. and M. Dolce; 2004: *Analysis of RC building dynamic response and soil-building resonance based on data recorded during a damaging earthquake (Molise, Italy 2002)*. Bulletin of the Seismological Society of America, 94, 5, 1943-1953.
- Mucciarelli M., Gallipoli M.R., Ponso F. and Dolce M.; 2002: *Seismic waves generated by oscillating buildings: analysis of release test*. Soil Dynamic and Earthquake Engineering, 21, 255-262.
- Nakamura Y.; 1989: *A method for dynamic characteristics estimation of subsurface using microtremor on the ground surface*. Q.R. of RTRI, 30, 1, 25-33 2.
- Nakamura Y.; 2000: *Clear identification of fundamental idea of Nakamura's technique and its applications*. Proceedings of 12th World Conference on Earthquake Engineering, New Zeland.
- Nakata N., Snieder R., Kuroda S., Ito S., Aizawa T. and Kumini T.; 2013: *Monitoring a Building Using Deconvolution Interferometry. I: Earthquake-Data Analysis*. Bulletin of the Seismological Society of America, Vol. 103, No. 3, pp. 1662–1678, June 2013, doi: 10.1785/0120120291.

- Nakata N. and Snieder R.; 2014: *Monitoring a Building Using Deconvolution Interferometry. II: Ambient-Vibration Analysis*. Bulletin of the Seismological Society of America, Vol. 104, No. 1, pp. 204–213, February 2014, doi: 10.1785/0120130050.
- Navarro M. and Oliveira C.S.; 2006: *Experimental techniques for assessment of dynamic behaviour of buildings*. In: Oliveira CS, Roca A, Goula X. Assessing and managing earthquake risk. Volume 2, part II, chapter 8. Springer, pp 159–183.
- Newton C. and Snieder R.; 2012. *Estimating intrinsic attenuation of a building using deconvolution interferometry and time reversal*. Bulletin of the Seismological Society of America; 5; 2200-2208.
- O.P.C.M. n. 3274; 2003. *Primi elementi in materia di criteri generali per la classificazione sismica del territorio nazionale e di normative tecniche per le costruzioni in zona sismica*. Gazz. Uff. 8 maggio 2003, n. 108 [in Italian]
- Parolai S., Ansal A., Kurtulus A., Strollo A., Wang R. and Zschau J.; 2009: *The Ataköy vertical array (Turkey): Insights into seismic wave propagation in the shallow-most crustal layers by waveform*. Geophysical Journal International, 178, 1649–1662.
- Parolai S., Facke A., Richwalski S.M. and Stempniewski L.; 2005: *Assessing the vibrational frequencies of the Holweide hospital in the city of Cologne (Germany) by means of ambient seismic noise analysis and FE modelling*. Natural Hazard, 34:217–230.
- Pascucci V. and Tamponi G.; 2013: *Le grandi dighe italiane: quadro normativo e attività di vigilanza e controllo*. Direzione generale per le dighe e le infrastrutture idriche ed elettriche, Ministero delle Infrastrutture e dei Trasporti, Presentazione a Longarone, discussione ed analisi a 50 anni dalla grande frana, 6-7 ottobre 2013 [in Italian]
- Perez-Ramirez C. A., Amezcua-Sanchez J. P., Adeli H., Valtierra-Rodriguez M., Romero-Troncoso R. J., Dominguez-Gonzalez A. and Osornio-Rios R. A.; 2016: *Time-frequency techniques for modal parameters identification of civil structures from acquired dynamic signals*. Journal of Vibroengineering, Vol.18, Issue 5, 2016, p. 3164-3185.
- Petrovic B. and Parolai S.; 2016: *Joint Deconvolution of Building and Downhole Strong-Motion Recordings: Evidence for the Seismic Wavefield Being Radiated Back into the Shallow Geological Layers*. Bulletin of the Seismological Society of America, Vol. 106, No. 4, pp. 1720–1732, August 2016, doi: 10.1785/0120150326
- Ponzo F.C., Ditommaso R. and Auletta G.; 2012: *Structural Health Monitoring of Reinforced Concrete Structures using Nonlinear Interferometric Analysis*. 15 WCEE, Lisboa 2012.
- Ponzo F.C., Auletta G., Ditommaso R.; 2010 a): *A Fast Method for Structural Health Monitoring of Strategic Buildings*. 5th World Conference on Structural Control and Monitoring.

- Ponzo F.C., Ditommaso R., Auletta G. and Mossucca A.; 2010 b): *A fast method for structural health monitoring of Italian reinforced concrete strategic buildings*. Bulletin of Earthquake Engineering (2010) 8:1421–1434 DOI 10.1007/s10518-010-9194-6.
- Direttiva del Presidente del Consiglio dei Ministri 27 febbraio 2004: *Indirizzi operativi per la gestione organizzativa e funzionale del sistema di allertamento nazionale e regionale per il rischio idrogeologico ed idraulico ai fini di protezione civile*. Pubblicato nella Gazzetta Ufficiale n. 59 del 11 marzo 2004 - Supplemento Ordinario n. 39 [in Italian]
- Priscu R., Popovici A., Stematiu D. and Stere C.; 1985: *Earthquake Engineering for Large Dams*. John and Wiley Sons, Romania.
- Reynders E.; 2012: *System identification methods for (operational) modal analysis: review and comparison*. Archives of Computational Methods in Engineering, 19(1):51-124, 2012. <http://dx.doi.org/10.1007/s11831-012-9069-x>
- Reynders E., Teughelsb A. and De Roeck G.; 2010: *Finite element model updating and structural damage identification using OMAX Data Mechanical Systems and Signal Processing*. 24(5) 1306-1323, <http://dx.doi.org/10.1016/j.ymsp.2010.03.014>
- Şafak, E.; 1995: *Detection and identification of soil-structure interaction in buildings from vibration recordings*. Journal of Structural Engineering 121, 899–906.
- Sevim B., Altunisik A.C., Bayraktar A. and Abrahamson N. A.; 2013: *Structural identification of concrete arch dams by ambient vibration tests*. In: Advances in Concrete Construction, Vol. 1, No.3 (2013) 227-237. DOI: <http://dx.doi.org/10.12989/acc2013.1.3.227>.
- Sinou J.J.; 2009. *A review of damage detection and health monitoring of mechanical systems from changes in the measurement of linear and non-linear vibrations*. Robert C. Sapri. Mechanical Vibrations: Measurement, Effects and Control, Nova Science Publishers, Inc., pp.643-702, 2009, 978-1-60692-037-4.
- Snieder R. and Şafak E.; 2006: *Extracting the Building Response Using Seismic Interferometry: Theory and Application to the Millikan Library in Pasadena, California*. Bulletin of the Seismological Society of America, Vol. 96, No. 2, pp. 586–598, April 2006, doi: 10.1785/0120050109.
- Stabile T.A., Perrone A., Gallipoli M.R., Ditommaso R. and Ponzo F.C.; 2013: *Dynamic Survey of the Musmeci Bridge by Joint Application of Ground-Based Microwave Radar Interferometry and Ambient Noise Standard Spectral Ratio Techniques*. IEEE Geoscience And Remote Sensing Letters, Vol. 10, No. 4, July 2013.
- Stockwell R.G., Mansinha L. and Lowe R.P.; 1996. *Localization of the complex spectrum: the S transform*. IEEE Trans. Signal Process., Vol.44, pp.998-1001.

- Stubbs N., Perk S., Sikorsky C. and Choi S.; 2000: A global non-destructive damage assessment methodology for civil engineering structures. *International Journal of Systems Science*, 31:11, 1361-1373, DOI: 10.1080/00207720050197758.
- Todorovska M.I. and Rahmani M.T.; 2013: *System identification of buildings by wave travel time analysis and layered shear beam models—Spatial resolution and accuracy*. *Structural Control and Health Monitoring*. 2013; 20-686-702. DOI: 10.1002/stc.1484
- Todorovska M. I., Ivanović S.S. and Trifunac M.D.; 2001 (a): *Wave propagation in a seven-story reinforced concrete building. I. Theoretical models*. *Soil Dynamics and Earthquake Engineering* 21, 211–223.
- Todorovska M. I., Ivanović S.S. and Trifunac M. D.; 2001 (b). *Wave propagation in a seven-story reinforced concrete building. II. Observed wavenumbers*. *Soil Dynamics and Earthquake Engineering* 21, 225–236.
- Trifunac M. D., Ivanović S. S. and Todorovska M. I.; 2001: *Apparent periods of a building. I: Fourier analysis*. *Journal of Structural Engineering* 127, 517–526.
- Trifunac, M. D.;1999: *Period formulas for concrete shear wall buildings—discussion*. *Journal of Structural Engineering*, ASCE 125, no. 7, 797–798.
- Trifunac, M. D.; 1972: *Comparisons between ambient and forced vibration experiments*. *Earthquake Engineering and Structural Dynamics*, 1: 133–150. doi: 10.1002/eqe.4290010203.
- Ventura C.E., Lord J.F., Turek M., Brincker R., Andersen P. and Dascotte E.; 2005: *FEM Updating of Tall Building using Ambient Vibration Data*. In C. Soize & G.I. Schuëller (Eds.), *Structural Dynamics EURO-DYN 2005: Proceedings of 6th International Conference on Structural Dynamics*, Paris, France, 4-7 September 2005 (pp. 237 – 242). Millpress.
- Vidal F., Navarro M., Aranda C., Enomoto T.; 2013: *Changes in dynamic characteristics of Lorca RC buildings from pre- and post-earthquake ambient vibration data*. *Bulletin of Earthquake Engineering*. DOI 10.1007/s10518-013-9489-5
- Wapenaar, K., Slob, E. and Snieder, R.; 2008: *Seismic and electromagnetic controlled source interferometry in dissipative media*. *Geophysical Prospecting*, 56: 419–434. doi: 10.1111/j.1365-2478.2007.00686.x
- Wolf J.P. and C. Song; 2002: *Some cornerstones of dynamic soil–structure interaction*, *Engineering Structures*, 24, 13–28
- Wong H.L. and Trifunac M.D.; 1975: *Two dimensional antiplane building-soil-building interaction for two or more buildings and for incident plane SH waves*, *Bull. Seism. Soc. Am.*, 65, 1863-1885